UNIVERSIDADE ESTADUAL DE MARINGÁ
CENTRO DE CIÊNCIAS BIOLÓGICAS
DEPARTAMENTO DE BIOLOGIA
PROGRAMA DE PÓS-GRADUAÇÃO EM ECOLOGIA DE AMBIENTES AQUÁTICOS CONTINENTAIS

GILIANE GESSICA RASBOLD

Paleoecology of Pantanal lakes via multiproxy analysis

Maringá
2020

GILIANE GESSICA RASBOLD

Paleoecology of Pantanal lakes via multiproxy analysis

Tese apresentada ao Programa de Pós-Graduação em Ecologia de Ambientes Aquáticos Continentais do Departamento de Biologia, Centro de Ciências Biológicas da Universidade Estadual de Maringá, como requisito parcial para obtenção do título de Doutora em Ecologia e Limnologia.
Área de concentração: Ecologia e Limnologia

Orientador: Prof. Dr. José Cândido Stevaux
Coorientador: Prof. Dr. Aguinaldo Silva
Prof. Dr. Mauro Parolin
Prof. Dr. Michael M. McGlue

Maringá
2020

"Dados Internacionais de Catalogação-na-Publicação (CIP)"
(Biblioteca Setorial - UEM. Nupélia, Maringá, PR, Brasil)

Rasbold, Giliane Gessica, 1991-
R222p Paleoecology of Pantanal lakes via multiproxy analysis / Giliane Gessica Rasbold. -- Maringá, 2020.
109 f. : il. (algumas color.).

Tese (doutorado em Ecologia de Ambientes Aquáticos Continentais)--Universidade Estadual de Maringá, Dep. de Biologia, 2020.
Orientador: Prof. Dr. José Cândido Stevaux.
Coorientador: Prof. Dr. Aguinaldo Silva.
Coorientador: Prof. Dr. Mauro Parolin.
Coorientador: Prof. Dr. Michael M. McGlue.

1. Paleoecologia - Quaternário Tardio - Lagoas - Planície de inundação - Pantanal – Mato Grosso do Sul - Brasil. 2. Microfósseis de água doce - Espículas de esponjas - Quaternário Tardio - Lagoas - Planície de inundação - Pantanal – Mato Grosso do Sul - Brasil. 3. Microfósseis de plantas - Fitólitos - Quaternário Tardio - Lagoas - Planície de inundação - Pantanal - Mato Grosso do Sul - Brasil. 4. Geomorfologia fluvial - Quaternário Tardio - Lagoas - Planície de inundação - Pantanal - Mato Grosso do Sul - Brasil. 5. Mudanças climáticas - Quaternário Tardio - Lagoas - Planície de inundação - Pantanal - Mato Grosso do Sul - Brasil. I. Universidade Estadual de Maringá. Departamento de Biologia. Programa de Pós-Graduação em Ecologia de Ambientes Aquáticos Continentais.

CDD 23. ed. -560.4564098171

Maria Salete Ribelatto Arita CRB 9/858
João Fábio Hildebrandt CRB 9/1140

GILIANE GESSICA RASBOLD

Paleoecology of Pantanal lakes via multiproxy analysis

Tese apresentada ao Programa de Pós-Graduação em Ecologia de Ambientes Aquáticos Continentais do Departamento de Biologia, Centro de Ciências Biológicas da Universidade Estadual de Maringá, como requisito parcial para obtenção do título de Doutor em Ecologia e Limnologia e aprovada pela Comissão Julgadora composta pelos membros:

COMISSÃO JULGADORA

Prof.ª Dr. José Cândido Stevaux
Universidade Estadual de Maringá (Presidente)

Prof. Dr. Sidney Kuerten
Universidade Estadual do Mato Grosso do Sul (UEMS)

Prof. Dr. Ulisses Pinheiro
Universidade Federal do Pernambuco (UFPE)

Prof.ª Dr.ª Liliana Rodrigues
Nupélia/Universidade Estadual de Maringá (UEM)

Prof.ª Dr.ª Evanilde Benedito
Nupélia/Universidade Estadual de Maringá (UEM)

Aprovada em: 20 de março de 2020.
Local de defesa: Auditório do Nupélia, Bloco H-90, *campus* da Universidade Estadual de Maringá.

Dedico este trabalho à minha base, minha mãe Oresta Rasbold e meu pai Gilberto Rasbold (*in memoriam*).

AGRADECIMENTOS

Ao meu orientador Dr. José Cândido Stevaux, por toda generosidade, confiança e incentivo. A liberdade durante todo o processo, bem como os conselhos e orientações foram primordiais para desenvolver a minha autonomia como pesquisadora, sou muito grata por cada ensinamento!

Ao meu coorientador Dr. Michael McGlue. Mike, não tenho palavras para agradecer a ajuda e paciência que teve ao me orientar. Só posso dizer que seu "*don't worry*" e "*why not?*" foram fundamentais para minimizar os medos e principalmente por me encorajar a me arriscar. Seu exemplo de profissionalismo, ética e empatia serão levados para toda minha vida. Obrigada por me fazer ficar confortável, mesmo fora da minha zona de conforto.

Ao meu coorientador Dr. Mauro Parolin, por ser meu primeiro mentor e ter me entusiasmado com a pesquisa paleoambiental. Obrigada por todas as portas abertas, todas as pessoas e laboratórios que me ajudaram a conhecer.

Ao meu coorientador Dr. Aguinaldo Silva, por toda a ajuda logística, planejamento e execução dos trabalhos de campo. Seu auxílio e confiança desde o primeiro momento foram fundamentais para a finalização desta pesquisa.

Ao Dr. Ivan Bergier, que sempre esteve disposto a me auxiliar nas discussões e hipóteses do trabalho, com respostas imediatas e sempre muito prestativo. Obrigada também pelas análises laboratoriais realizadas e todo o ensinamento na utilização do MEV.

Ao curso de Pós-graduação em Ecologia de Ambientes Aquáticos Continentais (PEA), por proporcionar a realização desta pesquisa, pelo excelente corpo docente, equipe técnica e instalações.

Aos professores do PEA, por todo ensinamento repassado, ampliação das áreas de conhecimentos e pelos exemplos de pesquisadores.

À CAPES, pela bolsa de doutorado que possibilitou a dedicação integral.

Ao CNPq pela bolsa de doutorado sanduíche (processo - 204880/2018-1), os recursos financeiros foram fundamentais para o aperfeiçoamento e internacionalização da pesquisa.

À University of Kentucky e ao Department of Earth and Environmental Sciences (DEES) por toda a estrutura disponibilizada ao decorrer do período Sanduíche.

Ao CNPq pelo recurso financeiro referente ao projeto de pesquisa “Sistemas fluviais avulsivos e sua relação com as inundações e dinâmica hídrica do pantanal Sulmatogrossense” (processo - 431253/2018-8).

À American Geophysical Union, pelo AGU Travel Grant Award, que possibillitou a apresentação dos primeiros resultados desta tese no AGU Fall Meeting 2018 em Washington, D.C.

Aos professores e funcionários do DEES, University of Kentucky, que me auxiliaram nas análises de laboratório, atividades de campo e questões burocráticas, em especial Dr. Ryan Thigpen, Adrianne Gilley, Peter Idstein, Dr. Summer Brown, Dr. Dave Moecher, Dr. Edward W. Woolery e Dr. Kevin M. Yeager.

Às queridas secretárias do PEA Elisabete Custódio da Silva e Jocemara Santos, por sempre me atenderem prontamente, suportarem minha ansiedade e excesso de dúvidas.

Aos bibliotecários Maria Salete Ribelatto Arita e João Fábio Hildebrandt, por sempre tornarem agradável a permanência na Biblioteca Setorial do Nupélia e disponibilização de literatura.

À Universidade Estadual do Paraná, campus Campo Mourão e ao Laboratório de Estudos Paleoambientais da Fecilcam (Lepafe) por toda a estrutura disponibilizada em todas as etapas desta pesquisa.

Ao Grupo de Estudos Multidisciplinares do Ambiente (GEMA) e ao técnico Vanderlei Grze pelo empréstimo de equipamentos para a realização das coletas.

O presente trabalho foi realizado com apoio da Fundação Universidade Federal de Mato Grosso do Sul – UFMS/MEC – Brasil.

À Dra. Heloisa Coe, grande incentivadora das pesquisas com os fitólitos. Sua dedicação, rapidez e eficiência me servem de exemplo a todo momento.

Ao Dr. André Carvalho por todo o auxílio e amizade.

Ao Dr. Cleverson Guizan Silva, pelo empréstimo de equipamentos e ensinamentos no uso do StrataBox.

À Dra. Isabel Leli pela ajuda nos trabalhos de campo e por todo o incentivo.

Ao Prof. Dr. Ulisses Pinheiro por auxiliar no entendimento das esponjas de água doce, na identificação das espécies e por disponibilizar uma vasta bibliografia sobre o tema.

Ao Dr. Edivando Couto, por todo o auxílio, incentivo e inspiração nessa jornada.

À família Lepafe, que esteve presente no convívio diário, em especial Mayara, Fernando, Renan, Eduarda, Thainá, Anne e Katiucia.

Aos alunos do Pioneer Stratigraphy and Paleoenvironments Lab e DEES, em especial Eva Lyon, Bailee Hodelka, Edward Lo, Laura Streib, Hillary Johnson, Cooper Cearley, Autumn Helfrich e Sarah Johnson.

Aos colegas de pós-graduação, que sempre fizeram o caminho ficar mais fácil e alegre.

Aos membros da banca de doutorado Dra. Evanilde Benedito, Dra. Liliana Rodrigues, Dr. Ulisses Pinheiro e Dr. Sidney Kuerten, pela disponibilidade e importantes considerações.

Aos amigos Aline Vieira e Franklin Machado que foram meu suporte emocional em Lexington, sempre trazendo um pouquinho do Brasil para os nossos encontros.

Ao Edward Lo, com quem compartilho as pesquisas, reflexões de vida e as angústias da pós-graduação. Você foi fundamental no incentivo durante as inscrições, auxílios burocráticos e adaptação na cidade de Lexington. Obrigada meu amigo!

Ao Leandro Luz, obrigada por me encorajar, sou grata por sua amizade e por todos os momentos que compartilhamos e todos os lugares que conhecemos juntos, conte sempre comigo.

Ao Renato L. Guerreiro, por todas as discussões, ideias, entusiasmo, parceria e suporte nesses últimos anos. Obrigada por sempre me ajudar, independente do dia e hora.

A Lucia, Juan e família que me acolheram em Washingon D.C., vocês foram incríveis, sou muito feliz em poder compartilhar tantas experiências ao lado de vocês.

À Loyana Docio, pelas discussões de dados, realização de trabalhos campo e principalmente por sempre compartilhar uma boa cerveja.

À Débora Brandt, por me ajudar a manter o equilíbrio emocional, proporcionar a minha reconexão, sua condução e profissionalismo foram essenciais.

À Mayra Stevanato, minha amiga e parceira de pesquisa, entre confissões, desabafos e muitas cervejas discutimos sobre a vida e a ciência. Como é bom contar com você!

À Helivania Sardinha, que por vezes cedeu um colchão para que eu pudesse realizar os créditos, compartilhou almoços e momentos de reflexão.

Aos amigos de década, Willian Schroder, Camila Selzler (que meu deu meu maior presente, o nosso Henrique), João Locastro, Karisa Varella, Luiz Deon, Edward Galina, Josiane Hammes, Ana Carneiro, Nilson Junior, Selmo Junior, Carlos Junior, Priscila Book, Priscila Gregory, Guilherme Salvadori e Karen Silva, que sempre foram meu suporte e a minha válvula de escape para aqueles momentos onde só encontrei paz no aconchego de vocês.

À Andressa Rupulo, nossas conversas e parceria fizeram minha alegria nos últimos anos, obrigada por sempre me apoiar e incentivar.

À minha família, que me forneceu o suporte emocional durante esse processo, pelo constante incentivo e vínculo de amor. Por respeitaram minhas decisões e conviveram com a distância. À minha mãe Oresta Rasbold, por não medir esforços e estar sempre disponível para os abraços e desabafos, sua presença, carinho e compreensão foram fundamentais para manter meu equilíbrio. Ao meu pai Gilberto Rasbold (*in memoriam*), meu maior incentivador, com você apreendi que não existem barreiras para os sonhos e que estudar é o meu bem mais precioso, sei que estaria orgulhoso. Ao meu irmão Jean Rasbold, meu parceiro e amigo, obrigada por sempre me apoiar, me proteger, auxiliar e incentivar.

À todas as pessoas e instituições, que de alguma maneira me auxiliaram e que por falha tenha esquecido de mencionar.

Muito obrigada...

"... Não existe indicação metodológica mais fértil do que fazer os sedimentos de uma bacia sedimentar "contar" a própria história evolutiva do teatro deposicional."

Aziz Ab'saber, 1988

Paleoecologia das lagoas do Pantanal por análises multiproxy

RESUMO

As mudanças climáticas globais resultam em alterações nos padrões de precipitação, que podem ter efeitos dramáticos na ecologia aquática e terrestre. Para criar estratégias de mitigação de impactos é necessário um profundo entendimento dos mecanismos e taxas das mudanças climáticas. Os lagos e as áreas úmidas são considerados sentinelas das mudanças ambientais, porque seus sedimentos e colunas de água servem como registros sensíveis dos processos climáticos, hidrológicos e antropogênicos (induzidos pelo homem) da região. O Pantanal, localizado no alto rio Paraguai, é considerada a maior área úmida do planeta e desempenha inúmeros serviços ecossistêmicos, abriga uma imensa biodiversidade e é fundamental para os ciclos biogeoquímicos globais. As mudanças ambientais ocorridas na borda oeste do Pantanal durante os últimos 19 k anos AP foram interpretadas com base na análise paleolimnológica de testemunhos sedimentares recuperados nas lagoas Negra e Cáceres. Os testemunhos mostram variações na abundância, diversidade e preservação de espículas de esponja, fitólitos e geoquímica dos sedimentos ao longo do tempo. No final do Pleistoceno, as lagoas Negra e Cáceres foram influenciadas fortemente pelo Sistema de Monção Sul-Americano, com atividade fluvial intensa durante um clima mais úmido que o atual. A acumulação de carbono orgânico nas lagoas da planície de inundação do Pantanal variou ao longo do Quaternário Tardio. No Holoceno Médio, entretanto, houve períodos mais secos que o atual, em que essas lagoas foram desconectadas do rio Paraguai. Altos teores de carbono orgânico foram registrados a partir de ~7,3-6 k anos AP. Os registros de $\delta^{13}C_{org}$, $\delta^{15}N_{org}$ e C/N revelaram que a matéria orgânica depositada durante essa fase nas lagoas Gaíva, Castelo, Cáceres e Negra (direcionadas em um transecto Norte-Sul) tem como fonte as macrófitas aquáticas. Sugere-se que o aumento no enterro de carbono ocorreu em um clima mais seco, no qual houve a diminuição da área pelágica dessas lagoas. No entanto, as áreas litorâneas produtivas permaneceram alagadas e sem influência dos pulsos de inundação, as quais foram colonizadas por extensos bancos de macrófitas aquáticas. O clima mais seco prolongado resultou na dessecação e exposição do fundo de alguns dessas lagoas, ocasionando hiatos sedimentares próximo à transição para o Holoceno Tardio. Os dados sugerem que as lagoas da planície de inundação do Pantanal respondem de maneira complexa e, às vezes, indireta às mudanças climáticas. Nesse sentido, a dinâmica do sistema fluvial adjacente deve ser considerada na interpretação dos padrões de paleoidrologia e vegetação. Os resultados deste estudo permitiram novas interpretações sobre os controles hidroclimáticos da ciclagem de carbono lacustre nas zonas úmidas do Pantanal.

Palavras-chave: Holoceno. Áreas úmidas. Carbono orgânico. Espículas de esponja. Fitólitos.

Paleoecology of Pantanal lakes via multiproxy analysis

ABSTRACT

Global climate change influences the precipitation patterns, which can have dramatic effects on aquatic and terrestrial ecology. In order to create mitigation strategies is required a deep understanding of the mechanisms and rates of climate change. Lakes and wetlands are sentinels of environmental changes because their sediments and water columns serve as sensitive records of the climate, hydrology, and anthropogenic (human-induced) processes. The Pantanal, located in the Upper Paraguay River, is considered the largest wetland on Earth, and it performs numerous ecosystem services, has an immense biodiversity and is fundamental to global biogeochemical cycles. The environmental changes that occurred on the western border of the Pantanal during the last 19 cal kyr BP were interpreted based on the paleolimnological analysis of sedimentary cores recovered in the Negra and Cáceres lakes. The cores, show variations in the abundance, diversity, and preservation of sponge spicules, phytoliths, and geochemistry of sediments over time. In the Late Pleistocene, the Lakes Negra and Cáceres were strongly influenced by the South American Monsoon System, with intense fluvial activity during a more humid climate. The accumulation of organic carbon in the Pantanal floodplain lakes varied throughout the Late Quaternary. In the Middle Holocene, however, there were drier periods when these lakes were disconnected from the Paraguay River. High levels of organic carbon have been recorded from ~ 7.3-6 cal kyr BP. The records of $\delta^{13}C_{org}$, $\delta^{15}N_{org}$ and C/N revealed that the organic matter deposited during this phase in the Gaíva, Castelo, Cáceres, and Negra lakes are the source of aquatic macrophytes. It is suggested that the increase in carbon burial in these lakes occurred in a drier climate, in which there was a decrease in the pelagic area. However, the productive coastal areas remained flooded and without the influence of the flood pulses, which were colonized by extensive mats of aquatic macrophytes. The prolonged drier climate resulted in the desiccation and subaerially exposed lake floor, causing sedimentary gaps close to the transition to the Late Holocene. The data suggest that the lakes in the Pantanal floodplain respond in a complex and sometimes indirect way to global climate change. In this sense, the dynamics of the adjacent river system must be considered when interpreting paleohydrology and vegetation patterns. The results of this study allowed new interpretations about the hydroclimatic controls of the lacustrine carbon cycling in the Pantanal wetlands.

***Keywords*:** Holocene. Wetlands. Organic carbon. Sponge spicules. Phytoliths.

Tese elaborada e formatada conforme as normas das publicações científicas: *Palaeogeography Palaeoclimatology Palaeoecology* e *Journal of Paleolimnology*. Disponíveis em: <https://www.journals.elsevier.com/palaeogeography-palaeoclimatology-palaeoecology> and <https://link.springer.com/journal/10933>

SUMÁRIO

1 INTRODUCTION

The Pantanal is considered the largest wetland on the planet, covering approximately 135,000 km² in the interior of the South American continent (POR, 1995). The Pantanal floodplain is composed of complex lentic and lotic systems, including lake systems from different origins, a network of active and inactive river channels, and alluvial fans. The seasonal dynamics of floods shaped heterogeneous landscapes, making the Pantanal one of the primary areas for biodiversity conservation and environmental preservation (JUNK et al., 2006; JUNK et al., 2013). Among its functions, we can mention the importance of ecosystemic and economic services, such as carbon accumulation, a source of livelihood for the Pantanal population and ecotourism (BERGIER et al., 2018).

From a geological point of view, the Pantanal is a tectonically active sedimentary basin, formed as a result of the Andean orogeny during the Tertiary (USSAMI et al., 1999; WARREN et al., 2015). The basin is drained in the North-South direction by the Paraguay River, and it is distributed primarily over Brazilian territory (states of Mato Grosso and Mato Grosso do Sul) with smaller areas in Bolivia and Paraguay (ASSINE, 2015). The Pantanal climate is influenced by the Intertropical Convergence Zone (ITCZ) and the South American Summer Monsoon (SASM) System (ZOU; LAU, 1998; GARREAUD et al., 2009; VUILLE et al., 2012). Annual precipitation ranges from 800 to 1200 mm, with a wet season between October and April, with greater precipitation in December, January and February (ASSINE, 2015). The northern and southern areas of the Pantanal have different flood peaks. In the northern region, flood pulses are synchronized with precipitation. The low gradient of slope and the accumulation of water by the channels, plains, lakes and backwaters mean that the flood pulses of the southern region are delayed or asynchronous, starting after exceeding the storage limits of the northern portion (IVORY et al., 2019).

The flood pulses that seasonally affect the Pantanal Basin by raising river water levels, directly influence the lakes connected to the trunk river and indirectly influence those not connected. The flood pulse helps to homogenize and interconnect the environments that are disconnected during the drought (JUNK et al., 1989). This influence can be through the flooding of the plain, runoff or water table fluctuation, including changes in water balance, sedimentation, and geochemistry of the lake systems (MCGLUE et al., 2015). Seasonal fluctuations in water and sediments in the Pantanal basin are responsible for nutrient cycling and high primary productivity, which support a large, highly complex and diverse food chain (JUNK et al., 2012).

Global climate change can alter patterns of precipitation, hydrology and seasonality by increasing occurrence of extreme summer rains and winter droughts (BERGIER et al., 2018). Wetlands are the first ecosystems affected by climate change, changing hydrological pulses, evapotranspiration patterns, and local patterns of precipitation, temperature and humidity (MITSH et al., 2010). Understanding the environmental behavior of wetlands in the face of global changes is essential to plan and mitigate short and long-term impacts, as well as to outline strategies for regional water security (COLE et al., 2007; SOBEK et al., 2009; MITSCH et al., 2010; BERGIER et al., 2018).

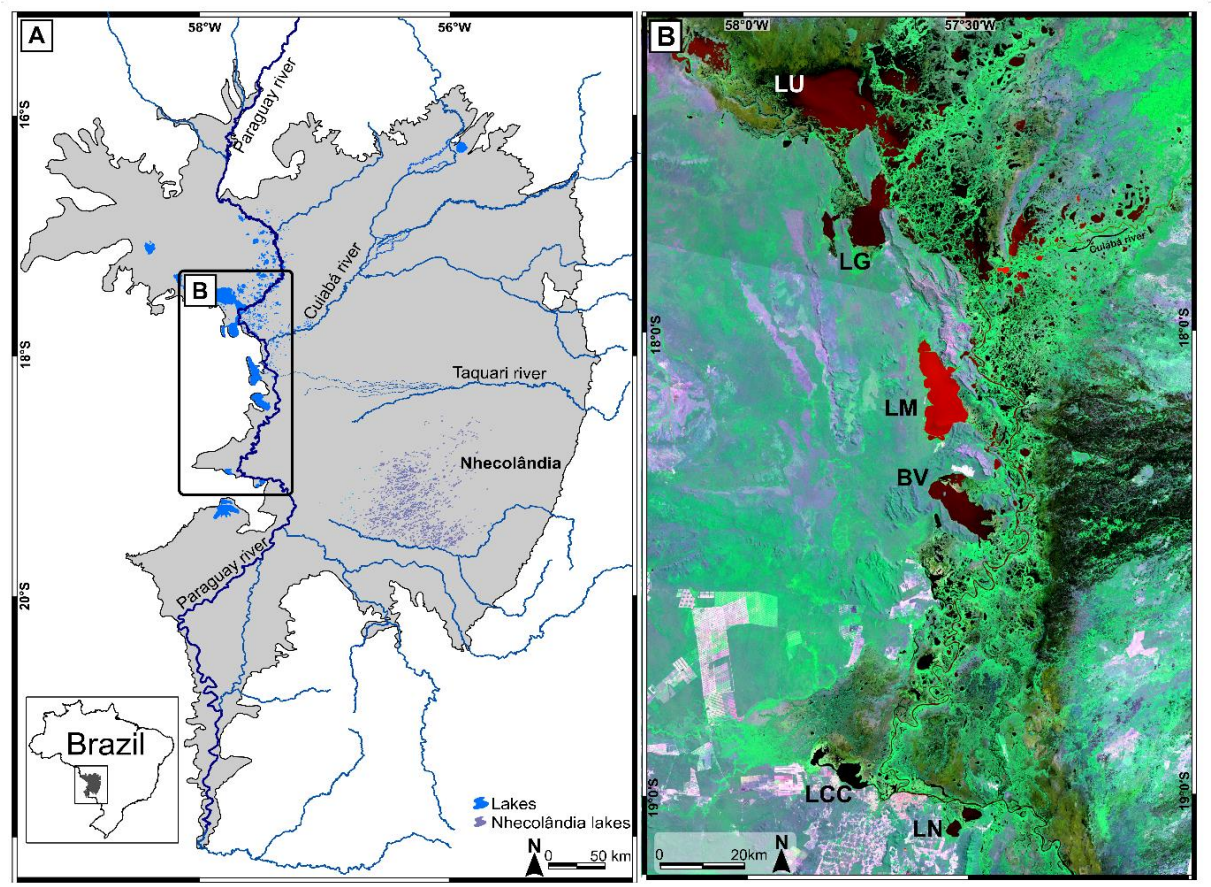

Figure 1. A. Location map of the Pantanal, with emphasis on the floodplain lakes; B. Floodplain lakes connected with the Paraguay River in a North-South transect (~ 200 km). Lake Uberaba (LU), Lake Gaíva (LG), Lake Mandioré (LM), Baía Vermelha (BV), Lake Cáceres (LCC) and Lake Negra (LN). Landsat-8 image, 07/09/2018, OLI-TIRS sensor, orbit/point: 227/072 and 227/073. Landsat-8 courtesy of the U.S. Geological Survey

In order to understand how an ecosystem can respond to climatic variations, one must interpret and document the patterns of change identified in the past thousands of years. In this sense, the sedimentary content of lake depositional systems is essential, as these environments are considered sentinels of climate change. Lacustrine records are less subject to erosion and can preserve important environmental indicators of climatic, hydrological and anthropogenic changes in the region (WILLIAMSON et al., 2009).

Deposition of lake sediments is the result of the dynamics of external inputs, such as sedimentary input, surface and ground water, organic matter and the atmosphere; and internal mechanisms, including primary productivity, chemical processes and decomposition (MULHOLLAND; ELWOOD, 1982). This sedimentary nature allows the preservation of several paleoenvironmental indicators, such as microfossils and, isotopic records. The physical processes, changes in the landscape, and hydroclimatic characteristics be assessed to correlate the chronology, geochemistry and the biological indicators contained in the lake sedimentary record.

Geochronological data and elaboration of high-resolution chronological models are extremely important elements for paleoenvironmental studies since chronology is the most critical problem in establishing the temporal and spatial patterns of climate change (OJALA et al., 2016). Together with the geochronology, the understanding of the nature of the organic material preserved in the sediments provides information regarding the productivity of the algae, aquatic macrophytes, terrestrial plants or transport processes involved. The analysis of total organic carbon (TOC) allows for tracing the paleoproductivity parameters (MEYERS; TERRANES, 2001). However, other analyses are used to identify the origin of organic matter, such as the relationship between the proportion of carbon and nitrogen, called C/N (MEYERS, 2003), which differentiates production via algae or terrestrial plants and the composition of carbon isotopes ($\delta^{13}C$) to distinguish between algae (fresh and marine water), C3 and C4 plants (MEYERS, 1994).

Most of the paleoenvironmental studies of the Late Pleistocene and Holocene use biological indicators through the analysis of fossil assemblages, which mostly comprise organisms that still exist, whose ecological and limnological environments and parameters are well known (COHEN, 2003). The biological indicators composed of silica tend to be more resistant to digenetic and oxidation processes, compared to those of organic origin (e.g. pollen grains, phytoclasts and coal fragments) and can be preserved for thousands of years in the sedimentary record. Among these, the sponge spicules, which comprise the siliceous skeleton

of freshwater sponges, are exceptionally well preserved (VOLKMER-RIBEIRO, 1985). These sessile animals have specific environmental peculiarities for development. The siliceous structure present in the skeletons and the reproductive systems allows for identification at a specific level (VOLKMER-RIBEIRO, 1985). Phytoliths, are structures of silica accumulated by plants, and are also preserved in sediments after the death of plants. Their morphologies are directly related to specific botanical families (PIPERNO, 2006).

The Pantanal has thousands of shallow lakes that can be used as a source of sedimentary records. The Paraguay River is connected with several large floodplain lakes on its right bank, in a North-South transect, including Lake Uberaba, Lake Gaíva, Lake Mandioré, Baía Vermelha, Lake Castelo, Lake Cáceres and Lake Negra (Figure 1). Sedimentary evidence from some of these lakes has been studied in the last two decades to understand the influences of the climate on the dynamics of wetlands. Several biological and geochemical approaches and indicators were used in these analyses, such as sponges spicules (Lake Gaíva - MCGLUE et al., 2012; Lake Negra - BEZERRA et al., 2019), pollen grains (Lake Gaíva - WHITNEY et al., 2011), diatom frustules (Lake Gaíva - METCALFE et al., 2014) and geochemical analyzes (Lake Negra and Lake Castelo - BEZERRA; MOZETO, 2008; Lake Gaíva - MCGLUE et al., 2012; FORNACE et al. , 2016).

Sedimentary records and interpretations of the environmental changes in these lakes have proved to be complex. An isotopic high-resolution oxygen record of speleothems from the Jaraguá cave, Serra do Bodaquena, in the southeast of the Pantanal, indicated that the region had a strong influence from the SASM during the Last Glacial Maximum (~ 27.9- 17.8 k yr BP) and a relatively dry period in the Middle Holocene (NOVELLO et al., 2017). Proxy data from the Late Pleistocene of the caves seem to differ from the pollen and diatoms records of Lake Gaíva (NOVELLO et al., 2017). Therefore, it is necessary to examine the sedimentary records of other floodplain lakes, as well as to perform analyses with multiple indicators that can provide independent and more complete evidence of changes in environmental conditions at the end of the Pleistocene and Holocene for the Pantanal.

The scope of this dissertation includes the study of high temporal resolution of sedimentary cores recovered from lakes Negra and Cáceres. The first article was published in the journal Palaeogeography, Palaeoclimatology, Palaeoecology (RASBOLD et al., 2019) and concerning a paleoecological and sedimentological analysis of a sedimentary core recovered from Lake Negra, using phytoliths, sponge spicules, organic carbon, and geochronology by 14C. The results were compared with the records of other lake systems and regional

paleoclimatic data, providing more information on the dynamics of the Pantanal floodplain in the last 19 k cal yr BP.

The addition of new paleoenvironmental data from sediments recovered from lakes Gaíva and Castelo to those from Lake Negra and Lake Cáceres (RASBOLD et al., 2019) enabled the identification of a period of the high deposition rate of organic carbon and siliceous microfossils accumulation rate in large lakes on the western edge of the Pantanal around 7.3-6 k cal yr BP. This period is characterized by the dominance of drier phases in the Pantanal during the Holocene (GUERREIRO et al. 2017; MCGLUE et al 2017; NOVELLO et al., 2017; NOVELLO et al., 2019). Discussions about which mechanisms had the greatest influence on the high deposition of organic carbon in dry periods guided the second article of the dissertation, submitted to the Journal of Paleolimnology. The hypothesis defended is that this deposition is related to the expansion of the marginal wetland of these lakes and the decrease of the pelagic area, similar to what currently occurs. In drier periods, the lakes lose their connection with the Paraguay River, causing an increase in the proportion of the shallower areas and allowing the colonization of aquatic macrophytes. From these conclusions it was possible to make a paleoenvironmental analysis of the main lakes on the western margin of the Pantanal during the Middle Holocene, correlating it to the regional paleoclimatic context, and seeking to understand the interactions between climate, vegetation and hydrology and their influence on paleoproduction in humid areas.

REFERENCES

AB'SABER, A. N. O Pantanal Mato-Grossense e a teoria dos refúgios. **Revista Brasileira de Geografia**. v. 50, n. 2, p. 9–57, 1988.

ASSINE, M. L. Brazilian Pantanal: A Large Pristine Tropical Wetland. In: Vieira, B. C. et al. (Eds.), **Landscapes and Landforms of Brazil, World Geomorphological Landscapes**, 2015. pp. 135-146. https://doi.org/10.1007/978-94-017-8023-0_12.

BERGIER, I.; ASSINE, M. L.; MCGLUE, M. M.; ALHO, C. J. R.; SILVA, A.; GUERREIRO, R. L.; CARVALHO, J. C. Amazon rainforest modulation of water security in the Pantanal wetland. **Science Total Environmental**. v. 619-620, 2018. pp.1116–1125. https://doi.org/10.1016/j.scitotenv.2017.11.163.

BEZERRA, M. A. O.; MOZETO, A. A. Deposição de carbono orgânico na planície de inundação do Rio Paraguai durante o Holoceno médio. **Oecologia Brasiliensis,** v. 12, n. 1, 2008. pp. 155–171.

BEZERRA, M. A. O.; MOZETO, A. A.; OLIVEIRA, P. E.; VOLKMER-RIBEIRO, C.; RODRIGUES, V. V.; ARAVENA, R. Late Pleistocene/Holocene environmental history of

the Southern Brazilian Pantanal wetlands. **Oecologia Australis**, v. 23, n. 4, 2019. pp. 712-729. https://doi.org/ 10.4257/oeco.2019.2304.02.

COHEN, A.S. **Paleolimnology**: The History and Evolution of Lake Systems. Oxford University Press, Oxford, 2003, 528p.

COLE, J. J.; PRAIRIE, Y. T.; CARACO, N. F.; MCDOWELL, W. H.; TRANVIK, L. J.; STRIEGL, R. G.; DUARTE, C. M.; KORTELAINEN, P.; DOWNING, J. A.; MIDDELBURG, J. J.; MELACK, J. Plumbing the Global Carbon Cycle: Integrating Inland Waters into the Terrestrial Carbon Budget. **Ecosystems**, v. 10, 2007. pp. 171-184. https://doi.org/10.1007/s10021-006-9013-8.

FORNACE, K. L.; WHITNEY, B. S.; GALY, V.; HUGHEN, K. A.; MAYLE, F. E. Late Quaternary environmental change in the interior South American tropics: new insight from leaf wax stable isotopes. **Earth Planet. Sci. Lett**. v. 438, 2016. pp. 75–85. https://doi.org/10.1016/j.epsl.2016.01.007.

GARREAUD, R. D.; VUILLE, M.; COMPAGNUCCI, R.; MARENGO, J. Present-day South American climate. **Palaeogeogr. Palaeoclimatol. Palaeoecol**. v. 281, 2009. pp. 180–195. https://doi.org/10.1016/j.palaeo.2007.10.032.

GUERREIRO, R. L.; MCGLUE, M. M.; STONE, J. R.; BERGIER, I.; PAROLIN, M.; SILVA C., SILANE A. F.; WARREN, L. V.; ASSINE, M. L. Paleoecology explains Holocene chemical changes in lakes of the Nhecolândia (Pantanal-Brazil). **Hydrobiologia** v.1, 2017. pp. 1-19. https://doi.org/10.1007/s10750-017-3429-3

IVORY, S.; MCGLUE, M. M.; SPERA, S.; SILVA, A.; BERGIER, I. Vegetation, rainfall, and pulsing hydrology in the Pantanal, the world's largest tropical wetland. **Environ. Res. Lett**. v. 14, 2019. pp. 124017. https://doi.org/10.1088/1748-9326/ab4ffe.

JUNK, W.J., BAYLEY, P.B., SPARKS, R.E. The flood pulse concept in river-floodplain systems. **Canadian Special Publications for Fisheries and Aquatic Sciences**, v. 106, 1989. pp.110-127.

JUNK, W. J.; BROWN, M.; CAMPBELL, I. C.; FINLAYSON, M.; GOPAL, B.; RAMBERG, L.; WARNER, B.G. The comparative biodiversity of seven globally important wetlands: a synthesis. **Aquat. Sci**. v. 68, 2006. pp. 400–414. https://doi.org/10.1007/s00027-006-0856-z.

JUNK, W. J.; PIEDADE, M. T. F.; SCHÖNGART, J.; WITTMANN, F. A classification of major natural habitats of Amazonian whitewater river floodplains (várzeas). **Wetlands Ecology and Management**, v. 20, 2012. pp. 461–475.

JUNK, W. J.; AN, S.; FINLAYSON, C. M.; GOPAL, B.; KVĚ, M.; STEPHEN, A.; MITSCH, W. J.; ROBARTS, R. D. Current state of knowledge regarding the world-s wetlands and their future under global climate change: a synthesis. **Aquat. Sci**. v. 75, 2013. pp. 151–167. https://doi.org/10.1007/s00027-012-0278-z.

MCGLUE, M. M.; SILVA, A.; ZANI, H.; CORRADINI, F. A.; PAROLIN, M.; ABEL, E. J.; COHEN, A. S.; ASSINE, M. L.; ELLIS, G. S.; TREES, M. A.; KUERTEN, S.; GRADELLA, F. S.; RASBOLD, G. G. Lacustrine records of Holocene flood pulse dynamics in the Upper

Paraguay River watershed (Pantanal wetlands, Brazil). **Quat. Res.** v.78, 2012. pp. 285–294. https://doi.org/10.1016/j.yqres.2012.05.015.

MCGLUE, M. M.; SILVA, A.; ASSINE, M. L.; STEVAUX, J. C.; PUPIM, F. N. Paleolimnology in the Pantanal: using lake sediments to track quaternary environmental change in the world's largest tropical wetland. In: Bergier, I., Assine, M.L. (Eds.), **Dynamics of the Pantanal Wetland in South America**. The Handbook of Environmental Chemistry 37. Springer, Cham, pp. 51–81. 2015. https://doi.org/10.1007/698_2015_350.

MCGLUE, M. M.; GUERREIRO, R. L.; BERGIER, I.; SILVA, A.; PUPIM, F. N.; OBERC, V.; ASSINE, M. L. Holocene stratigraphic evolution of saline lakes in Nhecolândia, southern Pantanal wetlands (Brazil). **Quaternary Research** v. 1, 2017. p. 1-19. https://doi.org/10.1017/qua.2017.57

METCALFE, S. E.; WHITNEY, B. S.; FITZPATRICK, K. A.; MAYLE, F. E.; LOADER, N. J.; STREET-PERROTT, F. A.; MANN, D. G. 2014. Hydrology and climatology at Laguna La Gaiba, lowland Bolivia: complex responses to climatic forcings over the last 25 000 years. **J. Quat. Sci**. v. 29, n. 3, 2015. pp. 289–300. https://doi.org/10.1002/jqs.2702.

MEYERS, P.A.; TERANES, J.L. Sediment organic matter. In: Last, W.M.; Smol, J.P. (Eds.), **Tracking Environmental Changes Using Lake Sediments**, v.2: Physical and Chemical Techniques. Kluwer, Dordrecht, pp. 239–269, 2001.

MEYERS, P.A. Preservation of source identification of sedimentary organic matter during and after deposition. **Chemical Geology**, v. 144, n. 3-4, 1994. pp.289–302, https://doi.org/10.1016/0009-2541(94)90059-0

MEYERS, P.A. Applications of organic geochemistry to paleolimnological reconstructions: a summary of examples from the Laurentian Great Lakes. **Organic Geochemistry**, v. 34, 2003. pp. 261–289, https://doi.org/10.1016/S0146-6380(02)00168-7

MITSCH, W. J.; NAHLIK, A.; WOLSKI, P.; BERNAL, B.; ZHANG, L.; RAMBERG, L. Tropical wetlands: seasonal hydrologic pulsing, carbon sequestration, and methane emissions. **Wetlands Ecology and Management**, v. 18, n. 5, 2010. pp. 573-586, https://doi-org.ez79.periodicos.capes.gov.br/10.1007/s11273-009-9164-4

MULHOLLAND, P. J.; ELWOOD, J. W. The role of lake and reservoir sediments as sinks in the perturbed global carbon cycle. **Tellus** v. 34, 1982 pp. 490-499. https://doi.org/10.3402/tellusa.v34i5.10834

NOVELLO, V. F.; CRUZ, F. W.; VUILLE, M.; STRÍKIS, N. M.; EDWARDS, R. L.; CHENG, H.; EMERICK, S.; SAITO DE PAULA, M.; LI, X.; BARRETO, E. S.; KARMANN, I.; SANTOS, R.V. A highresolution history of the South American Monsoon from Last Glacial Maximum to the Holocene. **Sci. Rep.**, v. 7, 2017. pp. 44267. https://doi.org/10.1038/srep44267.

NOVELLO, V. F.; CRUZ, F. W.; MCGLUE, M. M.; WONG, C. I.; WARD, B. M.; VUILLE, M.; SANTOS, R. A.; JAQUETO, P.; PESSENDA, L. C.; ATORRE, T.; RIBEIRO, L. M. Vegetation and environmental changes in tropical South America from the last glacial to the

Holocene documented by multiple cave sediment proxies. **Earth and Planetary Science Letters**, v. 524, 2019. pp. 115717.

OJALA, A. E. K.; ARPPE, L.; LUOTO, T. O.; WACKER, L.; KURKU, E.; ZAJĄCZKOWSKI, M.; PAWŁOWSKA, J.; DAMRAT, M.; OKSMAN, M. Sedimentary environment, lithostratigraphy and dating of sediment sequences from Arctic lakes Revvatnet and Svartvatnet in Hornsund, valbard. **Polish Polar Research**, v. 37, n. 1, 2016. pp. 23-48, https://doi.org/10.1515/popore−2016−0005

PIPERNO, D. R. **Phytoliths**: A Comprehensive Guide for Archaeologists and Paleoecologists. AltaMira Press, Oxford 238 p. 2006.

POR, F. D. **The Pantanal of Mato Grosso (Brazil)**: World's Largest Wetlands. Kluwer Academic, Dordrecht. 125 p. 1995. https://doi.org/10.1007/978-94-011-0031-1.

RASBOLD, G. G.; MCGLUE, M.M.; STEVAUX, J. C.; PAROLIN, M.; SILVA, A.; BERGIER, I. Sponge spicule and phytolith evidence for Late Quaternary environmental changes in the tropical Pantanal wetlands of western Brazil. **Palaeogeogr Palaeoclimatol Palaeoecol**, v. 518, 2019. pp. 119-133. https://doi.org/10.1016/j.palaeo.2019.01.015

SOBEK, S.; SCHERBER, C.; STEFFAN-DEWENTER, I.; TSCHARNTKE, T. Sapling herbivory, invertebrate herbivores and predators across a natural tree diversity gradient in Germany's largest connected deciduous forest. **Oecologia**, v. 160, 2009. pp. 279-288. https://doi.org/10.1007/s00442-009-1304-2.

USSAMI, N.; SHIRAIWA, S.; DOMINGUEZ, J. M. L. Basement reactivation in a sub-Andean foreland flexural bulge: the Pantanal wetland, SW Brazil. **Tectonics**, v. 18, n. 1, 1999. pp. 25-39. https://doi.org/10.1029/1998TC900004.

VOLKMER-RIBEIRO, C. **Esponjas de Água doce**. Manuais Técnicos para a Preparação de Coleções Zoológicas, v. 3, pp. 1–6, 1985.

VUILLE, M.; BURNS, J. S.; TAYLOR, B. L.; CRUZ, F. W.; BIRD, B. W.; ABBOTT, M. B.; KANNER, L. C.; CHENG, H.; NOVELLO, V. F. A review of the South American monsoon history as recorded in stable isotopic proxies over the past two millennia. **Clim. Past**, v. 8, 2012. pp. 1309–1321. https://doi.org/10.5194/cpd-8-637-2012.

WARREN LV, Q. F.; SIMÕES, M. G.; FREITAS, B. T.; ASSINE, M. L.; RICCOMINI, C. Underneath the Pantanal Wetland: A Deep- Time History of Gondwana Assembly, Climate Change, and the Dawn of Metazoan Life. In: Bergier I, Assine M (eds) **Dynamics of the Pantanal Wetland in South America**, pp. 1-21, 2015. The Handbook of Environmental Chemistry, vol 37. Springer, Cham, https://doi.org/ 10.1007/698_2014_326.

WHITNEY, B. S.; MAYLE, F. E.; PUNYASENA, S.W.; FITZPATRICK, K. A.; BURN, M. J.; GUILLEN, R.; CHAVEZ, E.; MANN, D.; PENNINGTON, R.T.; METCALFE, S. E. A 45 kyr palaeoclimate record from the lowland interior of tropical South America. **Palaeogeogr. Palaeoclimatol. Palaeoecol**. v. 307, n. 1–4, 2011. pp. 177–192. https://doi.org/10.1016/j.palaeo.2011.05.012.

WILLIAMSON, C. E.; SAROS, J. E.; VINCENT, W. F.; SMOL, J. P. Lakes and reservoirs as sentinels, integrators, and regulators of climate change. Limnology and **Oceanography**, v. 54, 2009. 2273-2282. https://doi.org/10.4319/lo.2009.54.6_part_2.2273.

ZHOU, J.; LAU, K. M. Does a monsoon climate exist over South America? **J. Clim.** v. 11, 1998. pp. 1020–1040. https://doi.org/10.1175/1520-0442(1998)011<1020:DAMCEO>2.0.CO;2.

2 SPONGE SPICULE AND PHYTOLITH EVIDENCE FOR LATE QUATERNARY ENVIRONMENTAL CHANGES IN THE TROPICAL PANTANAL WETLANDS OF WESTERN BRAZIL

ABSTRACT

The environmental history of the central Pantanal wetlands of western Brazil is inferred for the last 19 kyrs based on a multi-indicator paleolimnological analysis of a sediment core from Lake Negra. The core, dated by ^{14}C and OSL, shows variations in the abundance, diversity, and preservation of sponge spicules and phytoliths through time, consistent with changing aquatic environments. In the late Pleistocene, Lake Negra was influenced by a strong monsoon and fluvial depositional processes, whereas in the Holocene, there was a drier interval where the lake was more isolated on the floodplain. Hiatuses in the stratigraphy resulted from both wet and dry conditions, through fluvial channel scour or subaerial exposure of the lake floor, respectively. Data suggest that floodplain lakes in the Pantanal wetlands and similar riverine wetlands respond in a complex and, at times, indirect manner to climate change, and the dynamics of the adjacent fluvial system must be accounted for when interpreting paleohydrology and vegetation patterns.

Keywords: Biological indicators; Lake sediments; Lake Negra; Paleolimnology; Wetlands.

2.1 Introduction

Tropical wetlands are important to global biogeochemical cycling and patterns of biodiversity (Junk, 2002), but the response of many of these aquatic ecosystems to future environmental changes is still uncertain (e.g., Bridgham et al., 2013). A number of modeling studies have concluded that higher concentrations of atmospheric carbon dioxide (CO_2) could impart dramatic changes to tropical wetlands in the future, including an increase in the flux of methane (CH_4) to the atmosphere (Gedney et al., 2004; Shindell et al., 2008; Melton et al., 2013). Other studies note the key role that tropical wetlands may play in the future for carbon sequestration, which could counterbalance any net radiative forcing from CH_4 emissions (Mitsch et al., 2013).

Melton et al. (2013) suggest that CH_4 flux from tropical wetlands due to increasing heterogeneity in the water cycle is less clear, which underscores the need for new paleohydrological research to expand our understanding of wetland function under different scenarios of water availability. At the regional scale, wetlands provide ecosystem services that are economically valuable, including opportunities for ranching, fishing, agriculture, and tourism (Bergier et al., 2018). Large riverine wetlands at low latitudes in the Americas (e.g., the Everglades, Llanos, and Pantanal), have received some attention for the threats posed to them by changes in precipitation, temperature, sea level, wildfire, agriculture, and urbanization (Foti et al., 2013; Junk et al., 2013). Due to their seasonal or "pulsing" hydrology, these wetlands are believed by Mitsch et al. (2010) to be particularly sensitive to changes in climate.

One way to add to our understanding of the response of tropical wetlands to environmental variability is through an examination of late Quaternary strata, which holds the promise of recording sedimentological and ecological changes. Yet tropical wetlands with pulsing hydrology pose unique challenges for the development of continuous stratal records, particularly from floodplain lakes. For example, the Pantanal of central South America, a lowland savanna floodplain type wetland, is strongly impacted by the annual flooding of the Paraguay River. The arrival of the Paraguay River flood pulse varies spatially and temporally within the Pantanal (Assine et al., 2015a). For many floodplain lakes directly connected to the Paraguay River, rising stage elevation can influence lake level and therefore influence facies development (McGlue et al., 2011). The discharge, slope, sediment load, and channel morphology of the Paraguay River therefore also play roles in governing sedimentary processes for floodplain lakes, and these characteristics can be altered by processes other than climate, including landform evolution, fault movements, earthquakes, subsidence, and vegetation dynamics (Assine and Soares, 2004; Zani et al., 2012; McGlue et al., 2015; Assumpção et al., 2016; Dias et al., 2016). Nonetheless, pursuit of additional knowledge on how transitions in tropical climate have influenced the Pantanal since the Last Glacial Maximum remains an important task, since this information provides insight that can be used by water managers to inform policy, aid sustainable development, and build conservation plans. At present, only historical datasets are available for these tasks in the Pantanal (Bergier et al., 2018), but these data do not encompass the full range of environmental perturbations likely to affect the wetlands in the Anthropocene.

The large floodplain lakes on the western margin of the Paraguay River are among the best studied limnogeological systems in the Pantanal (Bezerra and Mozeto, 2008; McGlue et al., 2015). Today, these lakes are hydrologically open on a seasonal basis, but the strength of the outflow to the Paraguay River varies. Sedimentary records of environmental change from these lakes have proven complex, especially at Lake Gaíva (Mato Grosso do Sul state). For example, Whitney et al. (2011) and Metcalfe et al. (2014) analyzed pollen and diatom assemblages from Lake Gaíva, and they found evidence for a relatively cool and dry environment from ~45.0 to 19.5 kyr BP. Those authors suggested that Pantanal remained dry until ~12.8–12.2 kyr BP, at which time the lake level rose, connecting Lake Gaíva to the Paraguay River. A later study using biomarkers made by Fornace et al. (2016) largely supported the results and interpretations of these earlier studies, indicating abundant C_4 vegetation (grasses) and C_3 herbs on the landscape from ~41 to 20 kyr BP, with a peak in drought tolerant vegetation inferred from carbon isotopes at the Last Glacial Maximum (LGM). McGlue et al. (2012) documented the presence of mid-late Holocene unconformities in Lakes Gaíva and Mandioré, which were attributed to drought-induced lake level low stands. Neither Whitney et al. (2011) nor Metcalfe et al. (2014) found evidence for drought in the mid-late Holocene.

Adding to the complexity of Pantanal's environmental history, a paleo-precipitation proxy record was produced from the Serra do Bodaquena (Mato Grosso do Sul) in southeastern Pantanal. A high resolution oxygen isotope record from Jaraguá cave speleothems indicated that the region experienced a strong monsoon during the LGM (~27.9–17.8 ka) and a relatively dry early-mid Holocene (Novello et al., 2017). The cave proxy data for the late Pleistocene appear to conflict with the pollen and diatom records from Lake Gaíva, but support the presence and severity of dry conditions at the transition into the late Holocene. Novello et al. (2017) suggested that changes in vegetation may have been decoupled from precipitation patterns of the last glacial maximum. It is also plausible that the complex depositional setting along the margin of the Paraguay River may decouple prevailing environmental conditions from the information recorded in lake sediments. It is therefore valuable to examine floodplain lake records other than those from Lake Gaíva, which could provide independent evidence of changing environmental conditions in the late Pleistocene and Holocene. The purpose of this study is a paleoecological and sedimentological analysis

of a sediment core collected from Lake Negra (LN), which is a large floodplain lake connected to the Paraguay River (Fig. 1A), situated about 150 km south of Lake Gaíva (Fig. 1A) and ~200 km northwest of the Jaraguá cave (Fig. 1A). Lake Negra's hydrological balance is controlled by the arrival of the Paraguay River flood pulse in the late austral summer and fall. We used siliceous microfossils and carbon content from a well-dated lake sediment core from LN to document environmental changes since ~19 ka. The results add to a growing spatial network of Quaternary lake sediments datasets for Pantanal and help illustrate how hydroclimatic signals are recorded in floodplain lakes.

2.2 Geological setting

The Pantanal is a tectonically active sedimentary basin that most likely formed due to the Andean orogeny in the Tertiary (Ussami et al., 1999; Assine et al., 2015a). The Pantanal is a lake-rich lowland basin situated at ~16–21°S latitude and ~55–58.5°W longitude (Cohen et al., 2015). Drained north to south by the Paraguay River (PR), the Pantanal is considered one of the largest natural wetlands in the world; it extends over ~150,000 km^2 covering areas of western Brazil in Mato Grosso and Mato Grosso do Sul states, and small areas of eastern Bolivia and Paraguay (Por, 1995; Assine et al., 2015a). The geology surrounding the study site is comprised of Quaternary sediments, such as the Xaraiés and Pantanal Formations that make up alluvial terraces and colluvial deposits (Brasil Ministério de Minas e Energia, 1982; Lacerda Filho et al., 2006). The lowland landscape is intermittently fringed by hills that consist of ancient meta-sedimentary rocks, such as the Morraria do Urucum, Tromba dos Macacos, Jacadigo, Santa Cruz, São Domingos, Grande, and Rabichão, which belong to the Urucum and Santa Cruz Formations of the Neoproterozoic Jacadigo Group. Localized outcrops of Bocaina and Tamengo Formation (Neoproterozoic Corumbá Group) limestones are also present (Brasil Ministério de Minas e Energia, 1982; Lacerda Filho et al., 2006).

The climate of the Pantanal is influenced by the Intertropical Convergence Zone (ITCZ) and by the South American Summer Monsoon (SASM) (Zhou and Lau, 1998; Garreaud et al., 2009; Vuille et al., 2012). A prominent wet season occurs from October to April. In general, high precipitation occurs in the months of December, January and February in the northern and central portion of the Pantanal (McGlue et al., 2011). Vegetation in the Pantanal is a mosaic of different types (Brasil Ministério de

Minas e Energia, 1982). Seasonal flooding patterns, local topography, and soils are the main controls on the distribution of plant life, which Pott and da Silva (2015) described as "self-organized chaos". Terrestrial plants in the Pantanal include deciduous seasonal forests, semi-deciduous seasonal forests, and cerrado (savanna). Both lotic and lentic aquatic vegetation types are present, and zonation is dependent on water depth; plants may be floating, partially submerged, or rooted (Pott and da Silva, 2015).

Ab'Saber (1988) classified the lakes of the Pantanal into four distinct types, taking into account formation processes, shape, depth, and residence time. These lake types are: (i) oxbow lakes, (ii) small circular lakes (ovate ponds, especially those formed on the Taquari River megafan, (iii) karst lakes, and (iv) large floodplain lakes. Floodplain lakes are typically shallow and can be maintained on the landscape for hundreds to thousands of years, through a combination of surface water inflows, groundwater infiltration, and direct precipitation (Hutchinson, 1957; Cohen, 2003). The largest lakes in the Pantanal are on the floodplain of the Paraguay River and are located on the western border of the basin, including Lakes Gaíva, Mandioré, Baía Vermelha, Cáceres, Castelo, Negra and Uberaba (McGlue et al., 2011).

Lake Negra has an area of ~10.8 km^2 with an irregular shape. The lake has a maximum long axis length of ~4.1 km and a maximum width of ~3.5 km (Bezerra and Mozeto, 2008). The bathymetry of LN is relatively simple, with gradually increasing water depths towards the basin center that reach ~2.6m when the Paraguay River is flooded. The southeastern border of LN is at the base of Ladário Mountain (maximum elevation is ~150m above sea level); the higher elevations are colonized by seasonal forest with abundant Bromeliaceae and Cactaceae. The water inputs to LN include direct precipitation on the lake surface, local river channels (e.g., the Banda Alta Stream that drains the Urucum Massif), and inflow from Paraguay River floods during the wet season. Along the northwestern margin of LN, a natural tie channel formerly connected the lake to the Paraguay mainstem, but a road built across that channel in 1974 separated the lake from the river (Fig. 1B). Today, that abandoned channel exists on the floodplain as a periodically inundated swamp. Following the construction of the road, a Paraguay River flood formed a new permanent lake (Lagoa do Arroz) to the northeast of LN (Bezerra, 1998).

The modern limnogeology of LN provides important context for understanding its sedimentary archives. Today, LN has a pH of 6.5–7, high alkalinity (853.7–1281.5

mg $CaCO_3$/L), low electrical conductivity (32.2–130.6 µS/cm) and turbidity values that range from ~30 to 197 NTU, with maximum values typically encountered on the southwestern lake margin. Modern sediments accumulating on the LN floor consist of clays and silts; a small delta that deposits sand and gravel forms on the southern shoreline, where the Alta Banda Stream enters the lake (Fig. 1).

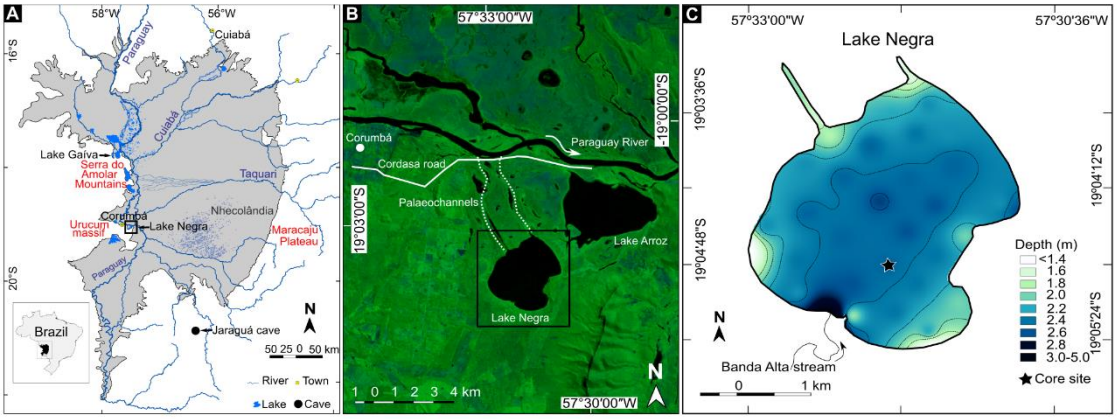

Fig. 1. Study area location maps. (A) Pantanal Basin (gray) in western tropical Brazil. (B) Satellite image showing Lake Negra on the right side of the Paraguay River, near the city of Corumbá. Landsat 8 image, 2017/04, OLI-TIRS, orbit/point: 227/073. (C) Bathymetry of Lake Negra. The star indicates the location of the core site.

2.3 Material and methods

Bezerra (1998) retrieved two sediment cores from adjacent boreholes in LN in 1995 via vibro-coring (LN95/L1 and LN95/L2) (Fig. 1C). Details about core LN95/L1, including its age-depth model, appear in Bezerra and Mozeto (2008). Core LN95/L2 was kept in cool, dry storage prior to opening in 2016. The core was opened in a dark room at the Federal University of Mato Grosso do Sul, Pantanal Campus, in order to facilitate the collection of sand samples for OSL dating. Core LN95/L2 was photographed and described following the methods outlined in Schnurrenberger et al. (2003). Discrete sediment sub-samples were collected every 3 cm (n=87) along the length of the core, in order to analyze sponge spicules and plant phytoliths, as well as for total carbon.

The stratigraphy of LN95/L2 is virtually identical to the LN95/L1 core, allowing the correlation of strata and ^{14}C dates reported on by Bezerra (1998) and Bezerra and Mozeto (2008) (Table 1, Fig. 2). Two prominent sand beds were sampled

for OSL dating. The OSL dating followed the SAR protocol (Wallinga et al., 2000) at Dating, Trade, and Provision of Services Ltd., São Paulo (Table 2). The SAR protocol obtains a mean age derived from samples with a minimum of five aliquots. The samples were subjected to chemical treatment with H_2O_2, HF, and HCl to isolate quartz. Following chemical pre-treatment, the samples were dried and passed through 100–60 mesh (0.149–0.25 mm) Tyler sieves. For the two dated horizons in LN95/L2, 15 aliquots were measured from each horizon, though only one aliquot (~7 mg) was used for the determination of paleodose (P). Values of equivalent dose, tests forrecycling and tests for recovery of each aliquot were obtained, from which the annual dose rate (μGy/yr), paleodose average (Gy) and average age (years) were derived (Table 2).

All radiocarbon dates in Bezerra (1998) and Bezerra and Mozeto (2008) (Table 1), as well as new OSL dates, were input into BACON for R in order to generate an age-depth model (Blaauw and Christen, 2011) (Fig. 3). The radiocarbon dates were calibrated using the SHCal13 curve (Hogg et al., 2013), and the post-bomb date at 1 cm was calibrated using the SH3 post-bomb calibration curve (Hogg et al., 2013; Hua et al., 2013). The visual stratigraphy of the LN95/L2 suggested the presence of three hiatuses, at ~60, 180, and 240 cm below the lake floor; these were input into the BACON model with an estimated length of ~1000 yr. The accumulation rate mean was set at 50 years/cm and an alternative depth was set at 272 cm, the base of the core.

Table 1. Radiocarbon dates used in the age-depth model for LN95/L2 (Lake Negra). [a]Liquid scintillation counting. [b]Accelerator mass spectrometry; Material: Total organic carbon (TOC). See text for details.

Depth (cm)	Lab code	$\delta^{13}C$ (‰)	Age (^{14}C yr BP)	Error	Median calibrated age (cal yr BP)	2-σ range (cal yr BP)	Material
21-30	WAT-4036[a]	-26.3	1,060	90	1,030	860 – 1,220	TOC
60-70	WAT-2967 [a]	-19.3	5,190	90	3,950	4,170 – 3,750	TOC
101-110	WAT-4037 [a]	-25.0	7,480	160	6,300	6,600 – 6,000	TOC
125-135	WAT-2975 [a]	-23.4	8,770	120	7,820	8,030 – 7,580	TOC
181-191	WAT-2976 [a]	-23.4	10,200	190	9,850	10,480 – 9,280	TOC
243-254	TO-6178 [b]	-22.9	14,870	160	16,100	16,480 – 15,690	TOC

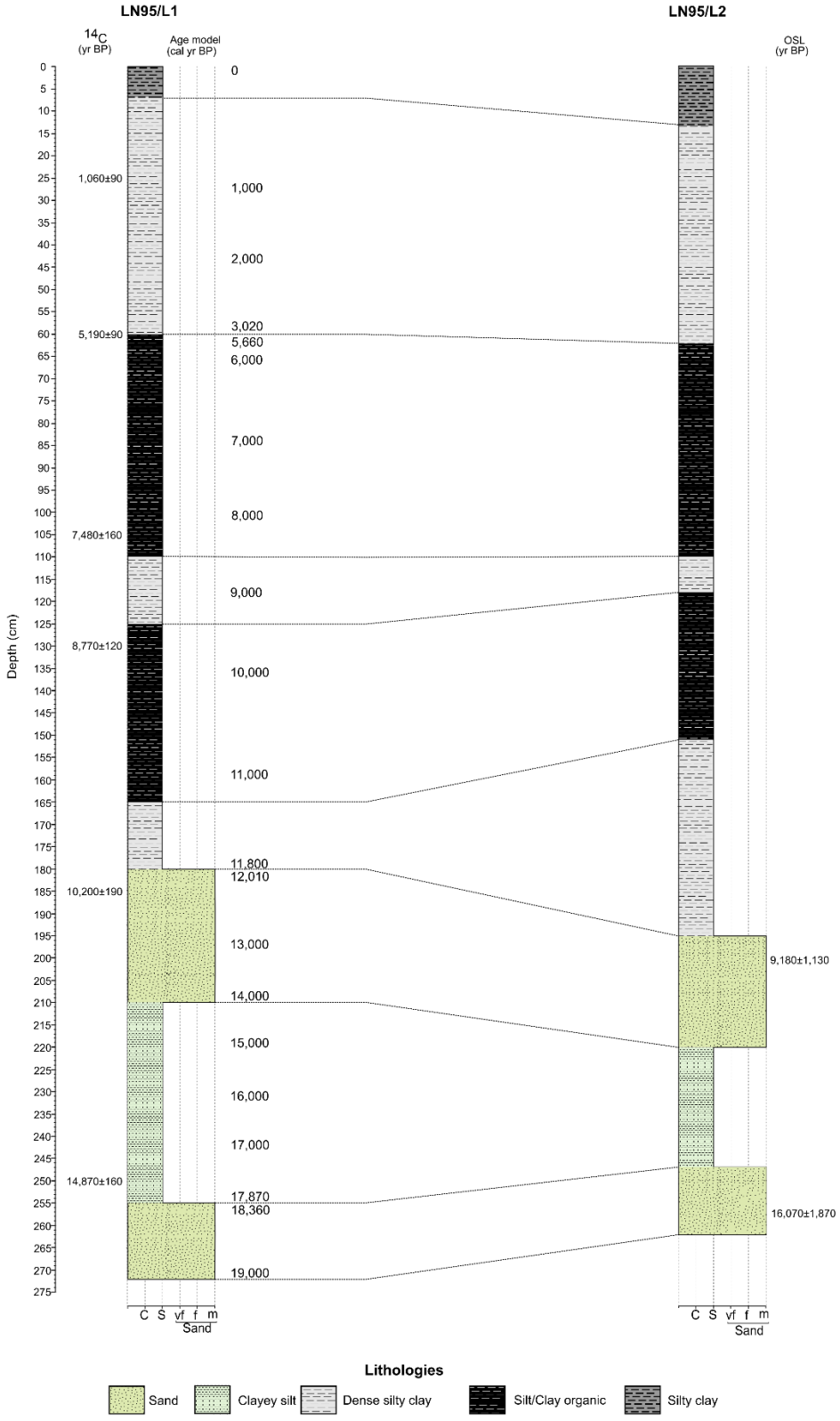

Fig. 2. Correlated beds between cores LN95/L1 (Bezerra and Mozetto, 2008) and LN95/L2 (this study). Radiocarbon dates from LN95/L1 were placed at equivalent depths in LN95/L2, and two additional OSL/SAR dates were added to improve the age-depth model (see text for details). C, clay. S, silt. Vf, very fine sand. F, fine sand. M, medium sand.

Table 2. Equivalent doses, dose rates and OSL/SAR ages for the studied samples from LN95/L2 obtained from Lake Negra.

ID	Depth (cm)	Th (ppm)	U (ppm)	K (%)	Water content (%)	Annual Dose rate (µGy/yr)	Aliquots	P (Gy)	OSL age (yr)
4897	180-188	5,471± 299	1,570± 137	1,351± 272	1.8	2,230± 225	15	20.5	9,180± 1,130
4907	250-262	6321± 311	1,969± 143	1,248± 239	4.2	2,260± 195	15	36.5	16,070± 1,870

Sponge spicules and phytoliths were extracted at the Paleoenvironmental Studies Laboratory (Lepafe), following a modified protocol of Volkmer-Ribeiro (1985). In brief, the procedure called for the following: (i) each sample was oven dried, crushed, and ~1 g of sediment was packed into a clean test tube, (ii) ~5 ml of HNO_3 was added to each test tube, (iii) the sediment samples plus acid were heated to a boil and allowed to react overnight, (iv) the samples were washed with distilled water until a neutral pH was achieved, (v) ~50 µl of acidified sample was dripped onto a cleaned microscope slide and dried on a hot plate, and (vi) Entellan® resin and a coverslip were used to fix the sample.

Sponge spicules and plant phytoliths were counted and identified on three randomly selected transects on each slide, and three slides were prepared for each sample. Thus, nine transects per sample were assessed for the sponge spicule analysis, and an average of 315 spicules were counted per sample. Taxonomic identification was performed through systematic observations of the slides and distinguishing among the different sponge skeletal elements (megascleres, gemmuloscleres, and microscleres). Identification of different species followed the sponge identification key of the Class Demospongiae Sollas, 1885, Order Spongillida Manconi and Pronzato, 2002 - proposed by Morrow and Cárdenas (2015). Sponge abundances were classified using the following observation system: 1–3 observations (very rare), 4–6 observations (rare), 7–10 observations (common), and>11 observations (abundant). Where sponge assemblages were characteristic of typical aquatic environments, we classified those intervals as spongiofacies, as defined by Parolin et al. (2008). The sponge spicules were recorded in two ways. Images of sponge spicules (gemmuloscleres and microscleres) were obtained with a scanning electron microscope (FEI, model Quanta 250) at the Laboratory of Biomass Conversion, Embrapa Pantanal, Corumbá, Brazil and photomicrographs of the other biological indicators were collected using an optical

microscope (×640 magnification). For internal consistency, a single analyst (GGR) completed the sponge spicule analysis. Morphological identification and quantification of plant phytoliths followed the International Code for Phytolith Nomenclature 1.0 (Madella et al., 2005). Spicule assemblages and phytoliths were statistically sorted into zones using a stratigraphically constrained cluster analysis in CONISS® in the Tilia® program (Grimm, 1987).

An additional split of each sediment sample was freeze-dried, ground, and analyzed for weight percent total organic carbon (TOC), which provides an indicator of processes responsible for organic enrichment of the lake sediments, including biological productivity, preservation, and dilution. Total carbon (TC) content was determined on a LECO SC-144DR device and total inorganic carbon (TIC) on a UIC™ carbonate coulometer at the Kentucky Geological Survey. The precision of the TIC analysis was±0.2%, whereas the precision for TC was better than 1.0%. The TOC was computed as the mass difference between LECO-derived TC and coulometry derived TIC values.

2.4 Results and interpretations

Analysis of megascleres, gemmuloscleres, and microscleres revealed seven different freshwater sponge species of the family Spongillidae Gray, 1867 (Fig. 4): *Corvoheteromeyenia heterosclera* (Ezcurra de Drago, 1974) (Fig. 5 A–D), *Corvospongilla seckti* Bonetto & Ezcurra de Drago, 1966, *Dosilia pydanieli* Volkmer-Ribeiro, 1992, *Heteromeyenia barlettai* Pinheiro, Calheira & Hajdu, 2015 (Fig. 5E), *Tubella variabilis* Bonetto & Ezcurra de Drago, 1973 (Fig. 5F), *Tubella paulula* (Bowerbank, 1863) (Fig. 5G), and *Radiospongilla amazonensis* Volkmer & Maciel, 1983 (Fig. 5H). For the phytoliths, several botanical families were evident (Figs. 4, 5) including abundant Poaceae (bilobate, cross, saddle, and rondel short cells and cuneiform and parallepipedal bulliforms) and lesser abundances of dicotyledons (globular granulate and psilate), Bromeliaceae (globular echinate), and Areaceae (globular echinate). The assemblages of sponge spicules and phytoliths were used to define six units within the core using cluster analysis (labeled I-VI, from oldest to youngest, respectively).

2.4.1 Stratigraphy and geochronology

Core LN95/L2 chiefly consists of dark, massively bedded muds and green-grey sands (Figs. 2 and 4). Most of the bedding contacts in the core are gradational, however sharp and distinct contacts separate units I and II, III and IVa, and V and VI. Mud-over-sand transitions mark the Unit I-II and III-IVa contacts, which we interpret as evidence for fluvial scour in an environment marked by strong riverine baseflow and flooding. In contrast, the contact separating units V and VI is marked by the presence of a thin, light brown-red silty clay layer containing sand sized iron oxide nodules overlying much darker, lower density muds. We attribute this sedimentology, and the associated abrupt transition in the biological indicators, to reflect subaerial exposure of the LN floor, most likely due to late Holocene drought. We used this information to condition the BACON age-depth model by placing hiatuses at these contacts. Six ^{14}C dates and two OSL dates were used to generate an age depth model for LN95/L2 in BACON (Fig. 3). The model produced by BACON generates a good fit for all of the dated horizons, with three multi-centennial gaps where section is missing (Hiatus I=~18,360–17,870 cal yr BP, Hiatus II=~12,010–11,800 cal yr BP, and Hiatus III=~5660–3020 cal yr BP).

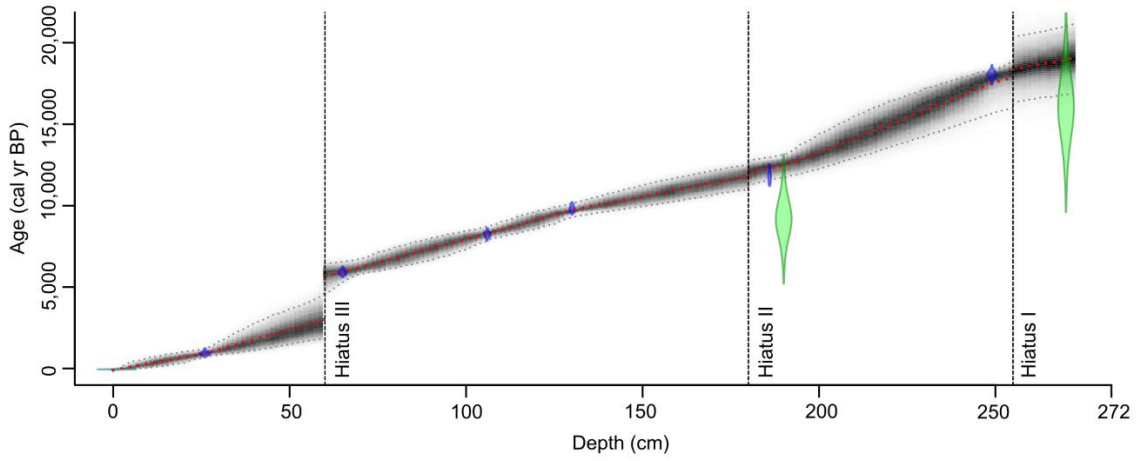

Fig. 3. BACON-derived age model for LN95/L2 from Lake Negra. Hiatus I is dated 18,360–17,870 cal yr BP, Hiatus II is dated 12,010–11,800 cal yr BP, and Hiatus III is dated 5660–3020 cal yr BP. Blue markers denote ^{14}C dates horizons, green markers are OSL ages. (For interpretation of the references to color in this figure legend, the reader is referred to the web version of this article.)

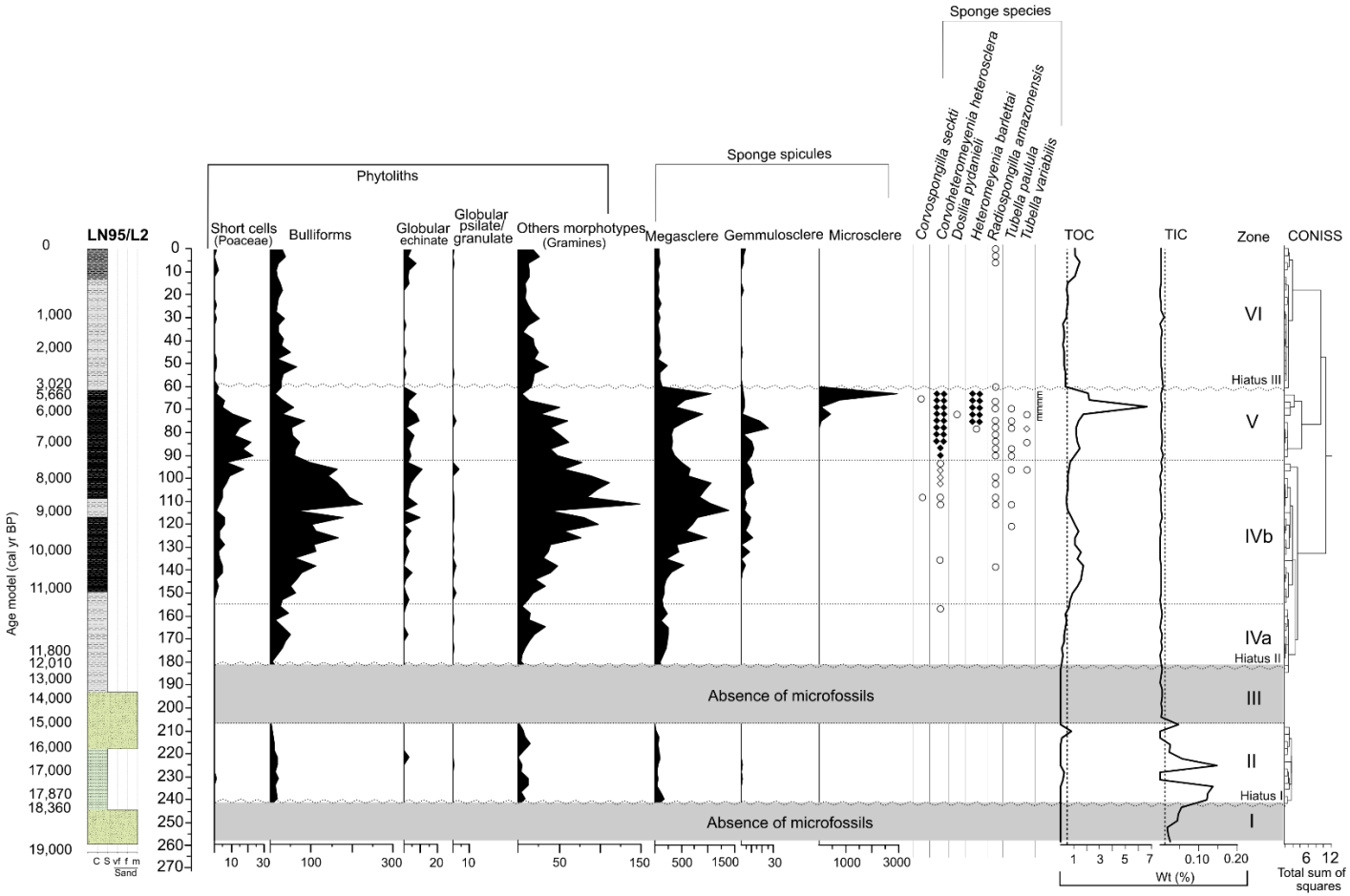

Fig. 4. Phytoliths, sponge spicules, total organic carbon (TOC), total inorganic carbon (TIC), and paleoenvironmental zones for the core LN95/L2 using a stratigraphically constrained cluster analysis in CONISS. Vertical dashed line indicates mean TOC and TIC values for the core. Sponge species: very rare occurrence (white circles), rare occurrence (white lozenges), common occurrence (black lozenges), abundant occurrence (two black lozenges), Sponge-rich facies (E).

Fig. 5. Scanning electron micrographs of freshwater sponge spicules (A–L) and phytoliths (M–S) from late Quaternary sediments of Lake Negra. (A) Pseudobirotule microsclere with pseudobirotules of long hooks. (B) Pseudobirotule microsclere with pseudobirotules of short hooks. (C–D) Acanthoxea microscleres. (E) Acanthoxea microsclere. (F) Gemmulosclere birotule of *Tubella variabilis*. (G) Gemmulosclere birotule of *Tubella paulula*. (H) Gemmulosclere spiny strongyles of *Radiospongilla amazonensis*. (I). Gemmulosclere birotule with a long spiny shaft. (J–L) Gemmuloscleres birotules with a long spiny shaft of *Heteromeyenia barlettai*. (M) Bilobate. (N) Saddle. (O) Rondel. (P) Elongate psilate. (Q) Elongate echinate. (R) Parallepipedal bulliform. (S) Cuneiform bulliform. All scale bars=10 μm.

2.4.2 Unit I (19,000–18,360 cal yr BP)

Unit I (260–240 cm below lake floor [cmblf]) consists of massive green muddy sands that lack obvious sedimentary structures or macrofossils. Phytoliths and sponge spicules are absent in this unit (Fig. 4). The TOC concentrations were uniformly below the detection limit, whereas concentrations of TIC were very low (0.02–0.06 wt.%). We interpret Unit I to indicate a fluvial-lacustrine paleoenvironment (Fig. 4). Sand encountered in the core suggests that considerable Paraguay River flooding was occurring at this time, and it is plausible that a secondary channel of the Paraguay mainstem was positioned adjacent to the coring site. The absence of biological indicators may be due to the strength of the riverine flow and abrasion of fossils by suspended silts or bedload sands.

2.4.3 Unit II (17,870–15,000 cal yr BP)

Overlying a hiatus at the top of Unit I, Unit II (240–205 cmblf) consists of massively bedded fine grained sandy mud. The base of Unit II is green and it transitions into a mottled green color near the upper contact. Phytoliths and sponge spicules are present but in low total concentrations (< 50 phytoliths and<250 spicules). The phytolith morphologies present are dominated by bulliform cuneiform, parallepipedal, and elongate psilate (Figs. 4, 5). The sponge spicules in Unit II are dominantly megascleres with varying degrees of taphonomic overprint, ranging from mostly intact fossils to extensively damaged fragments. No morphologies were present that allowed species identification. Unit II TOC concentrations range up to ~1.0 wt.%, whereas TIC reaches the maximum encountered in the core, with values up to ~0.16 wt.% (Fig. 4).

We interpret Unit II to reflect deposition in a floodplain paleoenvironment characterized by ephemeral wetlands that received occasional riverine inputs (Figs. 4, 6). The sponge spicules may have been fragmented during transport through grain impacts, or following deposition due to bioturbation, as mottling suggests a fluctuating redox front. Carbonate precipitation in this environment suggests that evaporation of standing water was a common process, potentially resulting from long dry seasons. Bulliform phytolith morphologies that were deposited in this unit are consistent with water stress in floodplain grasses (Parry and Smithson, 1958; Sangster and Parry, 1969; Bremond et al., 2005).

2.4.4 Unit III (15,000–12,010 cal yr BP)

Unit III (205–180 cmblf) comprised mottled sandy mud that grades into green medium sand. The sands in Unit III are fine grained and lack sedimentary structures. Siliceous microfossils are absent from Unit III, and TOC and TIC concentrations are minimal (Fig. 4).

We interpret Unit III as an interval when LN was strongly influenced by pulses of seasonal flooding from the Paraguay River that reached the core site by a secondary channel associated with the Paraguay, similar to Unit I (Figs. 4, 6).

2.4.5 Unit IVa (11,800–11,000 cal yr BP)

Unit IVa (180–155 cmblf) overlies hiatus II and consists of medium green sands that transition upward into gray sandy muds. Concentrations of both TOC and TIC are very low throughout Unit IVa. Sponge gemmuloscleres and microscleres are absent, and the total presence of megascleres is limited (< 250 spicules). These megascleres are characterized by heavy taphonomic damage; spicule fragmentation was moderate-to-high in ~75% of the microfossils examined. The concentration of phytoliths is low (< 70 fossils). The predominant phytolith morphologies are robust, such as bulliform parallepipedal, cuneiform, and elongate psilate. Bulliform morphologies (parallepipedal and cuneiform) are indicators of water stress in plants, especially grasses that can tolerate long dry seasons and high evapotranspiration (Parry and Smithson, 1958; Sangster and Parry, 1969; Bremond et al., 2005).

The biological indicators and damage patterns to spicules suggest the periodic influence of Paraguay River floods on the depositional environment. The high ratio of fragmented to whole megascleres suggests occasional floodplain inundation with variable persistence of ponded water (Kuerten et al., 2013). The phytolith assemblage of Unit IVa is interpreted to reflect the presence of herbaceous vegetation and soils with relatively low moisture in the LN watershed during deposition.

2.4.6 Unit IVb – 155–90 cm (11,000–8000 cal yr BP)

Unit IVb (155–90 cmblf) consists of dark gray silty clays and light gray clays with charcoal. In this unit, TOC concentrations rise to ~ 2.0 wt.%, whereas TIC remains very low. Unit IVb is marked by a large increase in the diversity and abundance of sponge megascleres (> 1000 total spicules). Sponge spicules from *C. heterosclera*, *R. amazonensis*, *T. paulula*, *T.*

variabilis, and *C. seckti* are present in rare to very rare abundances. The concentration of phytoliths reaches a peak of ~380 fossils per sample in this unit. Globular morphologies such as globular echinate (Bromeliaceae - Piperno, 1985, 2006; Bremond et al., 2005 and Arecaceae - Piperno, 2006; Runge, 1999; Mercader et al., 2009), globular granulate and psilate (woody dicotyledons), bilobate (C_4 mesophytic grasses), rondel (C_3 grasses), and saddle (C_4 xerophytic grasses) were present (Bremond et al., 2005) (Fig. 5).

The vegetation succession around LN based on the phytolith record suggests that an environmental change took place between Unit IVa and IVb. Bulliform phytolith morphologies in Unit IVa suggest a relatively dry paleoenvironment that, when coupled with the sedimentological characteristics, are best interpreted as an ephemerally inundated floodplain associated with a secondary channel of the Paraguay River. By contrast, in Unit IVb, the phytoliths suggest the presence of a diverse mixture of vegetation, including both C_3 and C_4 plants. Moreover, the sedimentology of Unit IVb is most consistent with a shallow lacustrine paleoenviroment with relative water column stability that allowed delicate lentic sponge spicules to be preserved. Carbon coulometry data show that this paleo-lake accumulated organic matter, suggesting environmental conditions favorable for aquatic primary production and preservation and lower potential for dilution, even in light of slightly higher sedimentation rates.

2.4.7 Unit V (8000–5660 cal yr BP)

Unit V (90–60 cmblf) consists of interbedded light gray sandy clay and dark gray clay. Unit V is distinguished by high concentrations of TOC (up to ~7.0 wt.%) and an upward increase in phytoliths, sponge megascleres, and gemmuloscleres. Preservation of sponge spicules is excellent in Unit V, in evidence by abundant whole microscleres of *C. heterosclera*, and *H. barlettai*. Spicules of *T. paulula*, *T. variabilis*, *R. amazonensis*, *D. pydanieli*, and *C. seckti* were also present, in rare to very rare abundances. Unit V is interpreted as a spongiofacies from 6500 to 5700 cal yr BP due to the abundance of spicules. For the phytoliths, we observed a reduction in the robust bulliform and elongate psilate morphologies and an increase in the concentration of bilobate morphological characteristics of the subfamily Panicoideae (Poaceae), indicating wetter conditions either across the region, or an increase in soil moisture around LN (Coe et al., 2014).

We interpret Unit V to reflect a perennial lacustrine paleoenvironment with relatively constant water levels based on the abundance of *C. heterosclera* and *H. barlettai*, the near pristine state of spicule preservation, and high concentrations of sedimentary organic carbon, which suggests elevated primary productivity and preservation (Figs. 4, 5). *C. heterosclera* has been characterized as an indicator species of shallow lakes among dunes in tropical Brazil (Volkmer-Ribeiro and Machado, 2007). However, there are records of this species for several habitat types, including ephemeral freshwater ponds in the Nhecolândia lake district of the Pantanal (Guerreiro et al., 2018). *C. heterosclera* is the most widely distributed freshwater sponge species in the Brazilian state of Pernambuco, and it has been found in aquatic environments affected by pollution (Nicacio and Pinheiro, 2015). Calheira and Pinheiro (2016) consider it an endemic from Neotropical Region species that can resist adverse conditions. A spongiofacies of *Metania spinata* Carter, 1881, *T. variabilis*, *R. amazonensis* and *Heterorotula fistula* Volkmer & Motta, 1995 was reported as characteristic of an isolated lentic environments on the Nabileque megafan ~3900 yr BP (Kuerten et al., 2013). *H. barlettai* was abundant and consistently encountered in the upper sediments of Unit V. Little data exists on natural ecological preferences and distribution of this species, but aquarium specimens in São Paulo (Pinheiro et al., 2015) suggest that it can thrive in lentic environments, adhering to leaves, roots of aquatic plants, and tree trunks. We interpret the presence of this species to reflect a seasonal influence of riverine floodwaters entering LN.

2.4.8 Unit VI (3020 cal yr BP to the present)

Unit VI (60–0 cmblf) consists of massive gray-green clay overlying a prominent layer of reddish-brown silty clay that defines the unconformable Unit V-Unit VI contact. Towards the top of the unit, Unit VI muds become dark brown, and TOC concentrations rise to a maximum of ~2.0 wt.% from ~1000 cal yr BP to the present. The abundance of microfossils abruptly decreases in Unit VI (< 100 phytoliths,< 200 megascleres,<4 gemmuloscleres, and 1 microsclere). For the sponges, *R. amazonensis* was identified at the top of the unit (Fig. 4). The predominant phytoliths are the robust bulliform cuneiform, parallepipedal, and elongate psilate morphologies. After ~1000 cal yr BP, globular echinate phytoliths (Bromeliaceae - Piperno, 1985, 2006; Bremond et al., 2005 and Arecaceae - Piperno, 2006; Runge, 1999; Mercader et al., 2009) are encountered in the core sediments. These phytoliths correspond to the vegetation growing in the area surrounding the lake today.

For example, bromeliads are dominant in the Ladário Mountain on the western boundary of the lake, and specimens of *Copernica alba* (Carandá-Arecaceae) are a major component of the flora to the northwest and southwest of LN.

Unit VI reflects the transition from a period of very dry conditions that produced Hiatus III into a wetter paleoenvironment. The biological indicators and core sedimentology are most consistent with a small, shallow permanent lake environment, mostly similar to modern LN, at the coring site by ~1000 yr BP.

2.5 Discussion

The Pantanal region is still difficult to access and sample, and as a result, relatively few studies have appeared that contain paleoenvironmental information for the Pleistocene-Holocene transition (McGlue et al., 2015). Lake records that cover the Last Glacial Maximum and deglacial are rare, and those that do exist provide different information on the environmental conditions. For example, palynological data from Lake Gaíva suggests drier and cooler conditions than present from 42.0 to 19.5 kyr BP (Whitney et al., 2011). Similarly, diatom paleoecology suggests that from 24.5 to 13.1 kyr BP, Lake Gaíva was very shallow (Metcalfe et al., 2014). Metcalfe et al. (2014) also indicate rapid hydroclimate changes from ~12.2 to 11.8 kyr BP, with strong flooding alternating with brief dry periods. By contrast, lithofacies and sponge spicules from the Nhecolândia region of the Pantanal show that extant saline lake environments were likely occupied by rivers in the latest Pleistocene, suggesting the potential for strong baseflow in an area that today experiences only ephemeral river flow (Guerreiro et al., 2018). Thus, new data from LN hold the potential for helping to clarify environmental conditions in the wetlands during the late glacial and deglacial period. In general, our data suggest that fluvial dynamics are important controls on floodplain depositional environments and local vegetation patterns (Fig. 7). Precipitation in the catchment is the primary regulator of river flooding, which responds to the intensity, duration, and recurrence time of the South America summer monsoon (Stevaux and Latrubesse, 2017). Because floodplain lakes share hydrological and morphological connections to rivers that vary, the sedimentary records of these basins must be interpreted through the filter of fluvial history.

Our study used new geochronology, core sedimentology, phytoliths and sponge spicules in order to improve paleoenvironmental interpretations for LN over the last 19,000 yr (Fig. 7). In Brazil, studies that use phytoliths as indicators of paleoenvironments have been

restricted to coastal environments, peatlands, or soils from only a few states, including Rio de Janeiro (Coe et al., 2013; Coe et al., 2014), Espírito Santo (Lorente et al., 2015), São Paulo (Calegari et al., 2015), Paraná (Rasbold et al., 2016; Parolin et al., 2017; Monteiro et al., 2015), and Minas Gerais (Augustin et al., 2014; Coe et al., 2015; Barros et al., 2016).

Thus, our study is the first to apply phytolith analysis to fluvial lacustrine sediments from the Pantanal. Additional geochronological information revealed the presence of three hiatuses in the LN sedimentary sequence. Late Pleistocene hiatuses are interpreted to be the result of erosion from fluvial scour that removed section; these are consistent with wet climatic conditions and riverine processes affecting the core site inferred by Bezerra and Mozeto (2008). The late Holocene hiatus was non-depositional and most likely driven by subaerial exposure of LN during a prolonged interval of drought, which has been observed in other paleoenvironmental archives from central Pantanal (McGlue et al., 2012).

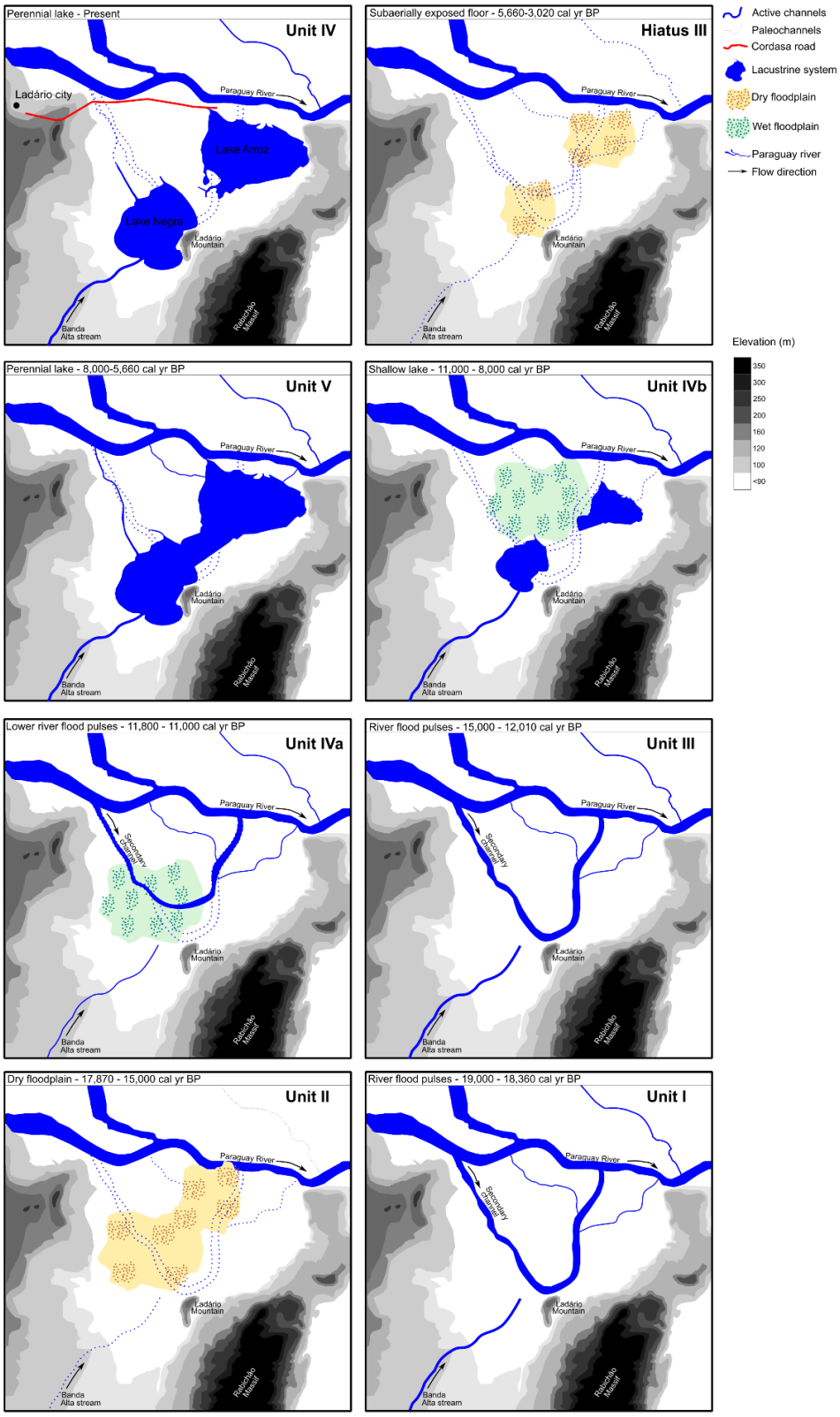

Fig. 6. Paleogeographic sketch maps relating the evolution of Lake Negra based on paleolimnological analysis of core LN95/L2. (A) Modern day. (B) 5660–3020 cal yr BP. (C) 8000–5660 cal yr BP. (D) 11,000–8000 cal yr BP. (E) 11,800–11,000 cal yr BP. (F) 15,000–12,010 cal yr BP. (G) 17,870–15,000 cal yr BP. (H) 19,000–18,360 cal yr BP.

2.5.1 Pleistocene late glacial and deglacial

The presence of massive sand and an absence of siliceous microfossils reveal that, unlike the modern LN condition, the environment was strongly influenced by fluvial channel sedimentary processes during two intervals of the late Pleistocene: ~19,000–18,360 and ~15,000–12,010 cal yr BP (e.g., Units I and III). The geochemical data presented in Bezerra and Mozeto (2008) for LN suggest that prior to ~11,000 cal yr BP, there were two peaks of deposition under the strong influence of the Paraguay River, separated by an intervening phase with only minor fluvial influence when fine grained, organic rich sediments were deposited. These interpretations are supported by our microfossil data and age model refinements for Units I, II and III. We interpret that wet climatic conditions during Units I and III allowed riverine flooding and potentially avulsions to influence the LN floodplain. Some of the best late Pleistocene paleo-precipitation data available for the Pantanal comes from Jaraguá cave speleothem $\delta^{18}O$, which provide a proxy for monsoon strength (Novello, 2016; Novello et al., 2017). These datasets confirm that the monsoon was strong during the last glacial period (~27.9–17.8 kyr BP), Heinrich Stadial 1 (~17.7–14.8 kyr BP), and the Younger Dryas (12.9–11.6 kyr BP). By contrast, the cave carbonate records indicate a relatively dry Bølling-Allerød period (~14.7–12.9 kyr BP). Deposition of river-derived sand at the LN coring site began during wet phases in the Pantanal, when the SASM was strong. We interpret that floods from the Paraguay River trunk channel itself, or from an associated secondary channel, helped to deliver sand to the core site on the LN floodplain.

Anabranching channels are common for the Paraguay River in the Pantanal basin. Secondary channels that bifurcate from and rejoin the Paraguay River vary in morphology, size, permanence, and many of them are active only during floods. LN is located in the Paraguay-Corumbá geomorphic compartment of the Pantanal, which is a ~27 km wide heterogenous floodplain with both active and ancient channels (Assine et al., 2015b). We interpret that a secondary channel connected to the Paraguay River that formed in the late Pleistocene was responsible for depositing Unit I and III sands. Anastomosing river channels are often narrow and complex, bifurcating numerous times around relatively stable vegetated islands. Makaske (2001) noted that avulsions are key for anastomosing rivers to evolve, and avulsion frequency can be driven by depositional rates and channel discharge, or changes in base level and regional gradient. High depositional rates and the formation of alluvial ridges and levees can spur avulsions, which allows for the development of multiple active channel belts. Secondary channel development and the deposition of muddy sands are consistent with

the period of intense monsoon rainfall in the late deglacial recorded at Jaraguá cave (Novello et al., 2017). The Pantanal basin's geomorphology is amenable to the development of anastomosing river channels due to low gradient valleys and flood-prone discharge, as well as cohesive bank sediments and abundant organic debris in certain locales.

Separating the two fluvio-lacustrine phases there was a shallow wetland phase from ~17,880 to 15,000 cal yr BP, which we interpret to have resulted from drier conditions and evaporation of ponded water on the floodplain. The presence of carbonate at the core site, as well as bulliform-type phytoliths and fragmented sponge megascleres, are consistent with a seasonally dry climate and a floodplain lake that experienced evaporative conditions and a fluctuating shallow water column. The nearly exclusive deposition of fragmented megascleres indicates an unstable aquatic environment, with possible reworking by occasional floods (Kuerten et al., 2013). A perennial lake is much less likely than an ephemeral lake from ~17,800 to 15,000 cal yr BP, because perennial lakes in the Pantanal typically contain sponge fossils with preserved gemmuloscleres and microscleres that are highly dissimilar to the fossil record of Unit II. Yet this time interval overlaps with Heinrich Stadial 1 (HS1), when the Pantanal was hydroclimatically complex. According to Novello et al. (2017), HS1 was marked by a wet early phase (~17.7–16.8 kyr BP), a relatively dry intermediate phase (~16.5–16.0 kyr BP), and a wet conclusion (~16.0–14.8 kyr BP). Unit II deposits suggest that the LN site responded to the dry middle phase of HS1, and that depositional patterns were influenced by a decline in precipitation. Bezerra and Mozeto (2008) suggested that late Pleistocene intervals characterized by lacustrine sedimentation may have occurred during relatively dry intervals, when baseflow within the adjacent rivers was low. This interpretation is consistent with evidence from our record, though we suggest that residence time was too short for a true lacustrine environment to develop. Mottled muds in Unit II are more consistent with a fluctuating floodplain wetland that received rare floods from the adjacent river system, which was mostly confined to its channel.

2.5.2 Early Holocene

Several lines of evidence suggest that the transition into the early Holocene was marked by a change in environmental conditions at LN. Beginning with Unit IVb, the abundance and diversity of sponge microfossils increase markedly, and phytoliths morphotypes from C_3 and C_4 grasses as well as globular morphologies increase. Furthermore,

the organic carbon content of core sediments increases in Unit IVb and reaches a maximum in Unit V (Fig. 4). We interpret that by ~8000 cal yr BP, a perennial lake had formed at the LN core site (Fig. 6). Our data suggest that very limited riverine flooding occurred during the deposition of Units IVb and V. Oxygen isotope data from Jaraguá cave show that the last ~11,000 yrs were drier compared to the LGM and deglacial, with very short intervals of high rainfall occurring occasionally (Novello et al., 2017). Although precipitation overall was lower in the Holocene relative to the Pleistocene, seasonal rainfall was apparently sufficient to maintain a perennial lake system while keeping the Paraguay River mostly confined within its channel, as evidence for flooding is minimal.

Sponges respond to local environmental conditions, and they are particularly sensitive to changes associated with flowing versus stagnant waters and transport distance. For example, sponge assemblages marked by robust structures (e.g., megascleres) and a high degree of fragmentation are most consistent with long distance fluvial transport, whereas a biodiverse assemblage of delicate spicules suggests a local lacustrine population under stable conditions (Wilding and Drees, 1968; Sifeddine et al., 2001; Santos et al., 2016). The development of a spongiofacies in Unit V indicates that the environmental conditions at LN were a shallow lake with abundant macrophytes on its margins. Excellent preservation of *C. heterosclera* and *H. barlettai* spicules between~8000 and 5700 cal yr BP is a lodestar of this stable lacustrine Environment. Microcleres and gemmuloscleres are the smallest siliceous structures of the freshwater sponge skeleton. The elongate and spined microscleres in Unit V do not exceed ~100 μm long, and their unique and pristine preservation state suggests that remobilization was uncommon (Fig. 5). Besides the taphonomic condition of the spicules, the ecological characteristics of the species are valuable for characterizing the paleoenvironment. *Heteromeyenia barlettai* are characteristic of lentic environments, and they are frequently found attached to roots of aquatic plants (Pinheiro et al., 2015). *C. heterosclera* prefers to settle on floating macrophyte roots in highly vegetated ponds (Ezcurra de Drago, 1974). The spicules of *C. heterosclera* in the sediments of the LN were well preserved, in evidence from the positive identification of three types of microscleres that are characteristic of this species: (i) Pseudobirotule microsclere with pseudobirotules of long hooks, (ii) Pseudobirotule microsclere with pseudobirotules of short hooks, and iii) Acanthoxea microscleres (Fig. 7). Although *C. heterosclera* and *H. barlettai* are dominant in Unit V, the presence of *T. paulula*, *T. variabilis*, *R. amazonensis* are further evidence of a lentic ecosystem, as these species are known from modern environments to prefer lakes with abundant submerged vegetation

(Volkmer-Ribeiro et al., 1975; Volkmer-Ribeiro and De Rosa-Barbosa, 1985; Tavares et al., 2003). The less common spicules like *D. pydanieli* and *C. seckti* are known to attach submerged roots, stems of aquatic plants or on rocky substrates that experience period inflows (Volkmer-Ribeiro and Parolin, 2010).

Bezerra and Mozeto (2008) indicate that around 11,000 yr BP, a set of levees may have developed that isolated LN from the Paraguay River; they pointed towards elevated organic carbon in the early Holocene as key evidence for this geomorphological change. Those authors argued that regional evidence for fluvial transport of bedload sediment in the late Pleistocene under conditions of high rainfall may have built floodplain landforms that allowed lake development to occur in isolation from large rivers. If accurate, the development of positive relief constructional landforms in the area of LN may have helped the lake expand during a time of relatively low precipitation. Cohen et al. (2015) note that in the foreland settings, the development of topographic closure and lakes occurs under conditions where sediment infill from large rivers is modulated, by a dry climate or geomorphic processes that isolate the available accommodation for water and sediment.

The transition between units V and VI is unconformable, and we interpret that regional drought was responsible for setting in motion processes that removed section at the mid-to-late Holocene transition. The stratal contact in LN95/2 is marked by a sharp boundary with strong evidence for oxidation of a formerly subaqueous depositional environment, including sand and gravel-sized iron oxide grains overlying dark muds. Our BACON age model suggests that this event took place at the transition to the late Holocene. The existence of severe mid-Holocene drought in the Pantanal has been debated. McGlue et al. (2012) reported the existence of a hiatus that removed section from 5300 to 2600 cal yr BP in lakes Gaíva and Mandiore, which were attributed to the exposure of the lake's floor due to a drought-induced regression accompanying a low, channel confined Paraguay River. However, Metcalfe et al. (2014), also studying Lake Gaiva, found no evidence for a prolonged drought. Rather, those authors suggested a deep and stable lake based on diatom assemblages from 5000 to 2100 cal yr BP. Similarly, a Pediastrum (green siliceous algae) paleoecological record described in Whitney and Mayle (2012) from Lake Gaiva indicates relatively low water levels in the early Holocene, followed by progressively wetter conditions after ~4400 cal yr BP. Yet a paucity of growth bands in stalagmites from Mato Grosso do Sul suggested limited water availability between 3800 and 2500 yr BP (Bertaux et al., 2002). Most recently, stalagmites from Jaraguá cave provides compelling evidence for dry conditions ~3670–2170 yr BP, when

stalagmite growth halted entirely (Novello, 2016). Given the robust dating associated with the Jaraguá cave record, we suggest that a prolonged drought at the transition to the late Holocene was most likely, and that this event desiccated LN.

2.5.3 Late Holocene

The quantity of biological indicators abruptly decreases at the transition into Unit VI (< 100 phytoliths, <200 megascleres,<4 gemmuloscleres, and 1 microsclere) and remains low throughout the unit. R. amazonensis sponge spicules were found in the top of the unit (Fig. 4). This is a lentic sponge that tends to occupy shallow lakes with abundant vegetation (Volkmer-Ribeiro and Parolin, 2010). The predominant phytoliths in Unit VI are the robust cuneiform, parallepipedal, and elongate psilate morphologies. After ~1000 yr BP, globular echinate phytoliths are present, (Bromeliaceae - Piperno, 1985, 2006; Bremond et al., 2005 and Arecaceae - Piperno, 2006; Runge, 1999; Mercader et al., 2009) and this type corresponds to vegetation surrounding the lake today, such as bromeliads are dominant in the Ladário Mountain and specimens of *C. alba* (Carandá-Arecaceae) dominate the landscape along the northwest and southwestern shores of LN. Together, the biological indicators and sedimentology of Unit VI suggest a reorganization of the depositional environment following late Holocene drought that produced a shallow, fluctuating floodplain lake that accumulates little organic carbon, most likely due to conditions that do not favor preservation. We interpreted that LN achieved a near modern morphology and bathymetry ~1000 cal yr BP, as the sponge fauna and vegetation assemblies become similar to the present at that time. This interpretation is consistent with regional paleoclimate archives that suggest wetter conditions in the latest Holocene, including a stalagmite from João Arruda cave (Bonito, MS), which showed approximately constant growth since ~2500 yr BP (Bertaux et al., 2002). Oxygen isotopes from the Pau d'Alho cave (northern border of Pantanal) indicate that the Little Ice Age was wet, and that a persistent rainfall cycle has occurred over the past ~1500 yr BP in the area (Novello et al., 2016). Lakes from elsewhere in the Pantanal, including the Nhecolândia region, recorded shifting depositional conditions after ~3200 cal yr BP, with marked change in salinity and alkalinity in the last millennium (Guerreiro et al., 2018; McGlue et al., 2017).

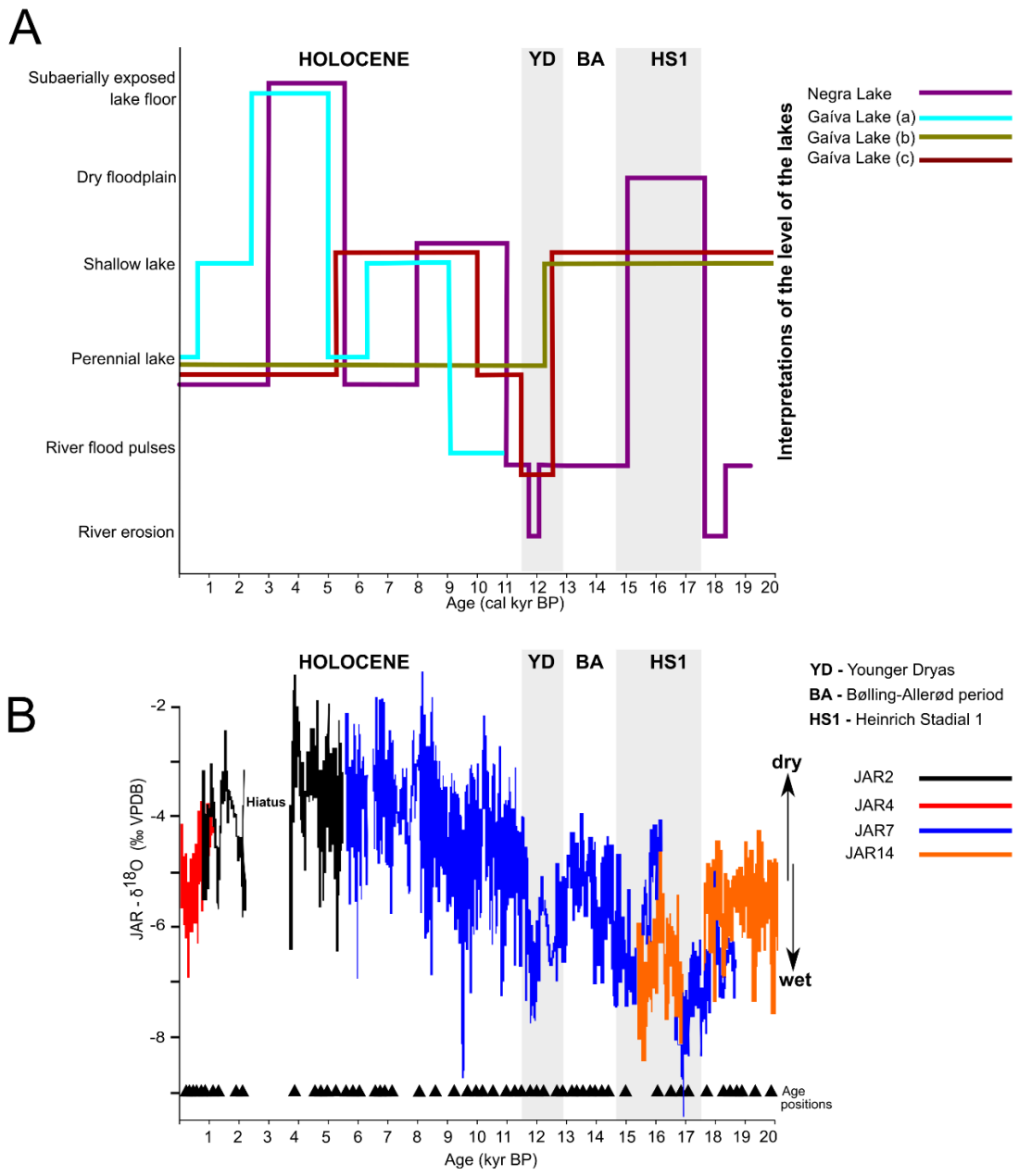

Fig. 7. Regional comparison of our data with paleo-records from elsewhere in the Pantanal wetlands of Brazil. (A) Data from floodplain lakes in central Pantanal (Lakes Negra and Gaíva; Whitney et al., 2011; McGlue et al., 2012; Metcalfe et al., 2014) plotted against (B) $\delta^{18}O$ records from caves (Novello et al., 2017; Novello, 2016).

2.6 Conclusions

1. A sediment core from Lake Negra, a shallow floodplain lake in central Pantanal, tropical western Brazil, provides new paleoenvironmental information for a region that remains difficult to access. Late Quaternary responses of tropical wetlands to climate are important for understanding the sensitivity of these aquatic ecosystems to alterations in the water cycle. The chronology of the core was established using ^{14}C dating and OSL. The

sedimentary record extends to ~19,000 cal yr BP and it is punctuated by three short hiatuses. The study is the first of its kind to integrate core sedimentology with phytolith and sponge spicule analysis for the purpose of reconstructing environmental history in the Pantanal. Proportional changes in the abundance of sponges and phytoliths show considerable sensitivity to hydroclimatic and changes in depositional environment.

2. The accumulation of muddy sands in the late Pleistocene is consistent with deposition influenced by fluvial processes under a strong monsoon. A secondary anabranching channel associated with the Paraguay River system may have occupied the area of the present- day LN during the deglacial when the climate was wet. A brief dry episode during the complex Heinrich Stadial 1 appears to have resulted in an ephemeral wetland at the LN site.

3. In spite of a decline in monsoon rainfall in the early-middle Holocene in Pantanal, a stable lacustrine environment expanded at Lake Negra beginning ~11,000 yr BP, which may be explained by isolation of the floodplain from the Paraguay River system, either from channel confinement (low baseflow) or from the construction of levees. The immaculate preservation of phytoliths and delicate sponge spicules (microscleres) indicate that this lacustrine environment, though shallow, was stable between ~8000 and ~5660 cal yr BP.

4. Missing section from ~5660 to 3020 cal yr BP suggests that a late Holocene drought dessicated LN at the transition into the late Holocene; this evidence is consistent with oxygen isotopes and growth rings in speleothems from elsewhere in the Pantanal. LN appears to have established near-modern characteristics around 1000 cal yr BP.

5. Data from LN suggest that floodplain lakes in the Pantanal respond in a complex and at times indirect manner to climate change, and the dynamics of the adjacent fluvial system must be accounted for when interpreting paleohydrology and vegetation patterns.

REFERENCES

Ab'Saber, A.N., 1988. O Pantanal Mato-Grossense e a teoria dos refúgios. Rev. Bras. Geogr. 50 (2), 9–57.

Assine, M.L., Soares, P.C., 2004. Quaternary of the Pantanal, west-central Brazil. Quat. Int. 114, 23–34. https://doi.org/10.1016/S1040-6182(03)00039-9.

Assine, M.L., Merino, E.R., Pupim, F.N., Macedo, H.A., Santos, M.G.M., 2015a. The Quaternary alluvial systems tract of the Pantanal Basin, Brazil. Brazilian Journal of Geology 45 (3), 475–489. https://doi.org/10.1590/2317-4889201520150014.

Assine, M.L., Merino, E.R., Pupim, F.N., Warren, L.V., Guerreiro, R.L., McGlue, M., 2015b. Geology and geomorphology of the Pantanal Basin. In: Bergier, I., Assine, M.L. (Eds.), Dynamics of the Pantanal Wetland in South America. The Handbook of Environmental Chemistry 37. Springer, Cham, pp. 23–50. https://doi.org/10.1007/698_2015_349.

Assumpção, M., Dias, F.L., Zevallos, I., Naliboff, J.B., 2016. Intraplate stress field in South America from earthquake focal mechanisms. J. S. Am. Earth Sci. 71, 278–295. https://doi.org/10.1016/j.jsames.2016.07.005.

Augustin, C.H.R.R., Coe, H.H.G., Chueng, K.F., 2014. Analysis of geomorphic dynamics in ancient quartzite landscape using phytolith and carbon isotopes, Espinhaço Mountain Range, Minas Gerais, Brazil. Geomorphologie 4, 355–376.

Barros, L.F.P., Coe, H.H.G., Seixas, A.P., Magalhães, A.P., Macario, K.C.D., 2016. Paleobiogeoclimatic scenarios of the Late Quaternary inferred from fluvial deposits of the Quadrilátero Ferrífero (Southeastern Brazil). J. S. Am. Earth Sci. 67, 71–88. https://doi.org/10.1016/j.jsames.2016.02.004.

Bergier, I., Assine, M.L., McGlue, M.M., Alho, C.J.R., Silva, A., Guerreiro, R.L., Carvalho, J.C., 2018. Amazon rainforest modulation of water security in the Pantanal wetland. Sci. Total Environ. 619-620, 1116–1125. https://doi.org/10.1016/j.scitotenv.2017.11.163.

Bertaux, J., Sondag, F., Santos, R., Soubies, F., Casse, C., Plagnes, V., Le Cornec, F., Seidel, F., 2002. Palaeoclimatic record of speleothems in a tropical region: study of laminated sequences from a Holocene stalagmite in central-west Brazil. Quat. Int. 89, 3–16. https://doi.org/10.1016/S1040-6182(01)00077-5.

Bezerra, M.A.O., 1998. Uso de multi-traçadores na reconstrução de Holoceno no Pantanal Mato-grossense, Corumbá, MS. Ph.D. Thesis In: Ecologia e Recursos Naturais. Universidade de São Carlos, São Carlos, SP 254 p.

Bezerra, M.A.O., Mozeto, A.A., 2008. Deposição de carbono orgânico na planície de inundação do Rio Paraguai durante o Holoceno médio. Oecologia Brasiliensis 12 (1), 155–171.

Blaauw, M., Christen, J.A., 2011. Flexible paleoclimate age-depth models using an autoregressive gamma process. Bayesian Anal. 6 (3), 457–474.

Brasil Ministério de Minas e Energia. Secretaria-Geral. Projeto RADAMBRASIL. Folha SE. 21 Corumbá e parte da Folha SE.20; geologia, geomorfologia, pedologia, vegetação e uso potencial da terra. Rio de Janeiro, 1982. 452 p.

Bremond, L., Alexandre, A., Peyron, O., Guiot, J., 2005. Grass water stress estimated from phytoliths in West Africa. J. Biogeogr. 32, 311–327. ttps://doi.org/10.1111/j.1365-2699.2004.01162.x.

Bridgham, S.D., Cadillo-Quiroz, H., Keller, J.K., Zhuang, Q., 2013. Methane emissions from wetlands: biogeochemical, microbial, and modeling perspectives from local to global scales. Glob. Chang. Biol. 19 (5), 1325–1346. https://doi.org/10.1111/gcb.12131.

Calegari, M.R., Madella, M., Buso Jr., A.A., Osterrieth, M., Lorente, F.L., Pessenda, L.C.R., 2015. Holocene vegetation and climate inferences from phytoliths and pollen from Lagoa do Macuco, North Coast of Espírito Santo State (Brazil). Quaternary and Environmental Geosciences 6, 41–50. https://doi.org/10.5380/abequa.v6i1.36426.

Calheira, L., Pinheiro, U., 2016. Corvoheteromeyenia Ezcurra de Drago, 1979 (Spongillidae, Porifera): genus review with proposal of neotype of Corvoheteromeyenia heterosclera (Ezcurra de Drago, 1974). Zootaxa 4126 (3), 351–374. https://doi.org/10.11646/zootaxa.4126.3.3.

Coe, H.H.G., Alexandre, A., Carvalho, C.N., Santos, G.M., Da Silva, A.S., Sousa, L.O.F., Lepsch, I.F., 2013. Changes in Holocene tree cover density in Cabo Frio (Rio de Janeiro, Brazil): evidence from soil phytolith assemblages. Quat. Int. 287, 63–72. https://doi.org/10.1016/j.quaint.2012.02.044.

Coe, H.H.G., Kita, M., Gomes, J.G., Chueng, K.F., Oliveira, F., Gomes, P.R.S., Carvalho, C., Linares, R., Alves, E., Santos, G.M., 2014. Understanding Holocene variations in the vegetation of Sao Joao River basin, southeastern coast of Brazil, using phytolith and carbon isotopic analyses. Palaeogeogr. Palaeoclimatol. Palaeoecol. 415, 59–68. https://doi.org/10.1016/j.palaeo.2014.01.009.

Coe, H.H.G., Seixas, A.P., Gomes, J.G., Barros, L.F.P., 2015. Reconstituição Paleobiogeoclimática através de Fitólitos e Isótopos de Carbono no Quadrilátero Ferrífero, MG. Revista Equador 4, 1439–1447.

Cohen, A.S., 2003. Paleolimnology: The History and Evolution of Lake Systems. Oxford University Press, Oxford 528p.

Cohen, A.S., McGlue, M.M., Ellis, G.S., Zani, H., Swarzenski, P.W., Assine, M.L., Silva, A., 2015. Lake formation, characteristics, and evolution in retroarc deposystems: a synthesis of the modern Andean orogen and its associated basins. In: DeCelles, P.G., Ducea, M.N., Carrapa, B., Kapp, P.A. (Eds.), Geodynamics of a Cordilleran Orogenic System: The Central Andes of Argentina and Northern Chile. Geological Society of America Memoir 212. https://doi.org/10.1130/2015.1212(16).

Dias, F.L., Assumpcão, M., Facincani, E.M., Franca, G.S., Assine, M.L., Paranhos Filho, A.C., Gamarra, R.M., 2016. The 2009 earthquake, magnitude mb 4.8, in the Pantanal Wetlands, west-central Brazil. An. Acad. Bras. Cienc. 88 (3), 1253–1264.

Ezcurra de Drago, I., 1974. Las especies sudamericanas de Corvomeyenia Weltner (Porifera, Spongillidae). Physis 33 (87), 233–240.

Fornace, K.L., Whitney, B.S., Galy, V., Hughen, K.A., Mayle, F.E., 2016. Late Quaternary environmental change in the interior South American tropics: new insight from leaf wax stable isotopes. Earth Planet. Sci. Lett. 438, 75–85. https://doi.org/10.1016/j.epsl.2016.01.007.

Foti, R., del Jesus, M., Rinaldo, A., Rodriguez-Iturbe, I., 2013. Signs of critical transition in the Everglades wetlands in response to climate and anthropogenic changes. Proc. Natl. Acad. Sci. 110 (16), 6296–6300. https://doi.org/10.1073/pnas.1302558110.

Garreaud, R.D., Vuille, M., Compagnucci, R., Marengo, J., 2009. Present-day South American climate. Palaeogeogr. Palaeoclimatol. Palaeoecol. 281, 180–195. https://doi.org/10.1016/j.palaeo.2007.10.032.

Gedney, N., Cox, P.M., Huntingford, C., 2004. Climate feedback from methane emissions. Geophysical Research Letters 31, L20503. https://doi.org/10.1029/22004GL020919.

Grimm, E.C., 1987. CONISS: a Fortran 77 program for stratigraphically constrained cluster analysis by the method of incremental sum of squares. Comput. Geosci. 13 (1),13–35. https://doi.org/10.1016/0098-3004(87)90022-7.

Guerreiro, R.L., McGlue, M.M., Stone, J.R., Bergier, I., Parolin, M., Caminha, S.A.F.S., Warren, L., Assine, M., 2018. Paleoecology explains Holocene chemical changes in lakes of the Nhecolândia (Pantanal-Brazil). Hydrobiologia 815 (1), 1–19. https://doi.org/10.1007/s10750-017-3429-3.

Hogg, A.G., Hua, Q., Blackwell, P.G., Niu, M., Buck, C.E., Guilderson, T.P., Heaton, T.J., Palmer, J.G., Reimer, P.J., Reimer, R.W., Turney, C.S.M., Zimmerman, S.R.H., 2013.

SHCal13 Southern Hemisphere calibration, 0–50,000 years cal BP. Radiocarbon 55 (4), 1889–1903. https://doi.org/10.2458/azu_js_rc.55.16783.

Hua, Q., Barbetti, M., Rakowski, A.Z., 2013. Atmospheric radiocarbon for the period 1950–2010. Radiocarbon 55 (4), 2059–2072. https://doi.org/10.2458/azu_js_rc.v55i2.16177.

Hutchinson, G.E., 1957. A Treatise on Limnology, v. 1. Geography, Physics and Chemistry J. Wiley and Sons, New York 1015 p.

Junk, W.J., 2002. Long-term environmental trends and the future of tropical wetlands.Environ. Conserv. 29 (4), 414–435. https://doi.org/10.1017/S0376892902000310.

Junk, W.J., An, S., Finlayson, C.M., Gopal, B., Kvě, M., Stephen, A., Mitsch, W.J., Robarts, R.D., 2013. Current state of knowledge regarding the world-s wetlands and their future under global climate change: a synthesis. Aquat. Sci. 75, 151–167. https://doi.org/10.1007/s00027-012-0278-z.

Kuerten, S., Parolin, M., Assine, M., McGlue, M.M., 2013. Sponge spicules indicate

Holocene environmental changes on the Nabileque River floodplain, southern Pantanal, Brazil. J. Paleolimnol. 49 (2), 171–183. https://doi.org/10.1007/s10933- 012-9652-z.

Lacerda Filho, J.V., Silva, M.G., Hardy, J., 2006. Geologia e recursos minerais do Estado de Mato Grosso do Sul: texto explicativo dos mapas geológico e de recursos minerais do Estado de Mato Grosso do Sul: escala 1:1.000.000. CPRM-Serviço Geológico do Brasil, Campo Grande 121 p.

Lorente, F.L., Pessenda, L.C.R., Calegari, M.R., Cohen, M.C.L., Rossetti, D.F., Giannini, P.C.F., Buso Junior, A.A., Castro, D.F., Franca, M.C., Bendassolli, J.A., Macario, K., 2015. Fitólitos como indicadores de mudanças ambientais durante o Holoceno na costa norte do estado do Espírito Santo (Brasil). Quaternary and Environmental Geosciences 6, 26–40. https://doi.org/10.5380/abequa.v6i1.36239.

Madella, M., Alexandre, A., Ball, T., 2005. International code for phytolith nomenclature 1.0. Ann. Bot. 96 (2), 253–260. https://doi.org/10.1093/aob/mci172.

Makaske, B., 2001. Anastomosing rivers: a review of their classification, origin and sedimentary products. Earth-Sci. Rev. 53, 149–196. https://doi.org/10.1016/S0012-8252(00)00038-6.

Manconi, R., Pronzato, R., 2002. Sub-order Spongillina subord. nov.: freshwater sponges. In: Hooper, J.N.A., Van Soestr, W.M. (Eds.), Systema Porifera: A Guide to the Classification of Sponges. Kluwer Academic/Plenum Publ, New York, pp. 921–1019. https://doi.org/10.1007/978-1-4615-0747-5_97.

McGlue, M.M., Silva, A., Corradini, F.A., Zani, H., Trees, M.A., Ellis, G.E., Parolin, M., Swarzenski, P.W., Cohen, A.S., Assine, M.L., 2011. Limnogeology in Brazil's “forgotten wilderness”: a synthesis from the large floodplain lakes of the Pantanal. J. Paleolimnol. 46, 273–289. https://doi.org/10.1007/s10933-011-9538-5.

McGlue, M.M., Silva, A., Zani, H., Corradini, F.A., Parolin, M., Abel, E.J., Cohen, A.S., Assine, M.L., Ellis, G.S., Trees, M.A., Kuerten, S., Gradella, F.S., Rasbold, G.G., 2012. Lacustrine records of Holocene flood pulse dynamics in the Upper Paraguay River watershed (Pantanal wetlands, Brazil). Quat. Res. 78, 285–294. https://doi.org/10.1016/j.yqres.2012.05.015.

McGlue, M.M., Silva, A., Assine, M.L., Stevaux, J.C., Pupim, F.N., 2015. Paleolimnology in the Pantanal: using lake sediments to track quaternary environmental change in the world's largest tropical wetland. In: Bergier, I., Assine, M.L. (Eds.), Dynamics of the Pantanal Wetland in South America. The Handbook of Environmental Chemistry 37. Springer, Cham, pp. 51–81. https://doi.org/10.1007/698_2015_350.

McGlue, M.M., Guerreiro, R.L., Bergier, I., Silva, A., Pupim, F., Oberc, V., Assine, M., 2017. Holocene stratigraphic evolution of saline lakes in Nhecolândia, Southern Pantanal wetlands (Brazil). Quat. Res. 88 (3), 472–490. https://doi.org/10.1017/qua.2017.57.

Melton, J.R., Wania, R., Hodson, E.L., Poulter, B., Ringeval, B., Spahni, R., Bohn, T., Avis, C.A., Beerling, D.J., Chen, G., Eliseev, A.V., Denisov, S.N., Hopcroft, P.O., Lettenmaier, D.P., Riley, W.J., Singarayer, J.S., Subin, Z.M., Tian, H., Zürcher, S., Brovkin, V., Bodegom, Van, Kleinen, T., Yu, Z.C., Kaplan, J.O., 2013. Present state of global wetland extent and wetland methane modelling: conclusions from a model intercomparison project (WETCHIMP). Biogeosciences 10, 753–788. https://doi.org/10.5194/bg-10-753-2013.

Mercader, J., Bennett, T., Esselmont, C., Simpson, S., Walde, D., 2009. Phytoliths in woody plants from the Miombo woodlands of Mozambique. Ann. Bot. 104, 91–113. https://doi.org/10.1093/aob/mcp097.

Metcalfe, S.E., Whitney, B.S., Fitzpatrick, K.A., Mayle, F.E., Loader, N.J., Street-Perrott, F.A., Mann, D.G., 2014. Hydrology and climatology at Laguna La Gaiba, lowland Bolivia: complex responses to climatic forcings over the last 25 000 years. J. Quat. Sci. 29 (3), 289–300. https://doi.org/10.1002/jqs.2702.

Mitsch, W.J., Nahlik, A., Wolski, P., Bernal, B., Zhang, L., Ramberg, L., 2010. Tropical wetlands: seasonal hydrologic pulsing, carbon sequestration, and methane emissions. Wetl. Ecol. Manag. 18 (5), 573–586. https://doi.org/10.1007/s11273-009-9164-4.

Mitsch, W.J., Bernal, B., Nahlik, A.M., Mander, Ü., Zhang, L., Anderson, C.J., Jørgensen, S.E., Brix, H., 2013. Wetlands, carbon, and climate change. Landsc. Ecol. 28 (4), 583–597. https://doi.org/10.1007/s10980-012-9758-8.

Monteiro, M.R., Parolin, M., Caxambu, M.G., 2015. Análise da assembléia fitolítica em solo superficial e serrapilheira em dois fragmentos de cerrado em área urbana de Campo Mourão-Paraná. Revista Brasileira de Geografia Física 8 (4), 1256–1272.

Morrow, C., Cárdenas, P., 2015. Proposal for a revised classification of the Demospongiae (Porifera). Front. Zool. 12, 7. https://doi.org/10.1186/s12983-015-0099-8.

Nicacio, G., Pinheiro, U., 2015. Biodiversity of freshwater sponges (Porifera: Spongillina) from northeast Brazil: new species and notes on systematics. Zootaxa 3981 (2), 220–240. https://doi.org/10.11646/zootaxa.3981.2.4.

Novello, V.F., 2016. Paleoclima do Centro-Oeste do Brasil desde o último período glacial com base em registros isotópicos de espeleotemas. Ph.D. Thesis In: Geoquímica e Geotectônica. Universidade de São Paulo, São Paulo, SP, Brazil 145 p.

Novello, V.F., Vuille, M., Cruz, F.W., Stríkis, N.M., Paula, M.S., Edwards, R.L., Cheng, H., Karmann, I., Jaqueto, P.F., Trindade, R.I.F., Hartmann, G.A., Moquet, J.S., 2016. Centennial-scale solar forcing of the South American Monsoon System recorded in stalagmites. Sci. Rep. 6, 24762. https://doi.org/10.1038/srep24762.

Novello, V.F., Cruz, F.W., Vuille, M., Stríkis, N.M., Edwards, R.L., Cheng, H., Emerick, S., Saito de Paula, M., Li, X., Barreto, E.S., Karmann, I., Santos, R.V., 2017. A highresolution history of the South American Monsoon from Last Glacial Maximum to the Holocene. Sci. Rep. 7, 44267. https://doi.org/10.1038/srep44267.

Parolin, M., Volkmer-Ribeiro, C., Stevaux, J.C., 2008. Use of Spongofacies as a proxy for river-lake paleohydrology in Quaternary deposits of central-western Brazil. Revista Brasileira de Paleontologia 11 (3), 187–198. https://doi.org/10.4072/rbp.2008.3.05.

Parolin, M., Monteiro, M.R., Coe, H.H.G., Colavite, A.P., 2017. Considerações Paleoambientais do Holoceno Médio por Meio de Fitólitos na Serra do Cadeado, Paraná. Revista do Departamento de Geografia USP 5, 96–103. https://doi.org/10.11606/rdg.v0ispe.132609.

Parry, W.D., Smithson, F., 1958. Silicification of bulliform cells in grasses. Nature 181, 1549–1550. https://doi.org/10.1038/1811549b0.

Pinheiro, U., Calheira, L., Hajdu, E., 2015. A new species of freshwater sponge, Heteromeyenia barlettai sp. nov. from an aquarium in São Paulo, Brazil (Spongillida: Spongillidae). Zootaxa 4034 (2), 351–363. https://doi.org/10.11646/zootaxa.4034. 2.7.

Piperno, P., 1985. Phytolith analysis and tropical paleo-ecology: production and taxonomic signifcance of siliceous forms in new world plant domesticates and wild species. Rev. Palaeobot. Palynol. 45, 185–228. https://doi.org/10.1016/0034-6667(85)90002-8.

Piperno, D.R., 2006. Phytoliths: A Comprehensive Guide for Archaeologists and Paleoecologists. AltaMira Press, Oxford 238 p.

Por, F.D., 1995. The Pantanal of Mato Grosso (Brazil): World's Largest Wetlands. Kluwer Academic, Dordrecht. https://doi.org/10.1007/978-94-011-0031-1. 125 p.

Pott, A., da Silva, J.S.V., 2015. Terrestrial and aquatic vegetation diversity of the Pantanal Wetland. In: Bergier, I., Assine, M. (Eds.), Dynamics of the Pantanal Wetland in South America. The Handbook of Environmental Chemistry 37. Springer, Cham, pp. 111–131. https://doi.org/10.1007/698_2015_352.

Rasbold, G.G., Parolin, M., Caxambu, M.G., 2016. Reconstrução Paleoambiental de um depósito sedimentary por análises multiproxy, Turvo, estado do Paraná, Brasil. Revista Brasileira de Paleontologia 19 (2), 315–324. https://doi.org/10.4072/rbp.2016.2.13.

Runge, F., 1999. The opal phytolith inventory of soils in central Africa-quantities, shapes, classifcation, and spectra. Rev. Palaeobot. Palynol. 107, 23–53. https://doi.org/10.1016/S0034-6667(99)00018-4.

Sangster, G., Parry, W.D., 1969. Some factors in relation to bulliform cell silicifcation in the grass leaf. Ann. Bot. 33, 315–323. https://doi.org/10.1093/oxfordjournals.aob.

a084285.

Santos, G.B., Castro, P.T.A., Parolin, M., Doio, L., Costa, D.H., 2016. Análise de espículas de esponjas como indicadores paleoambientais em sedimentos lacustres no oeste da Bahia. Revista Brasileira de Paleontologia 19 (3), 439–448. https://doi.org/10.4072/rbp.2016.3.09.

Schnurrenberger, D., Russell, J.M., Kelts, K., 2003. Classification of lacustrine sediments based on sedimentary components. J. Paleolimnol. 29 (2), 141–154. https://doi.org/10.1023/A:1023270324800.

Shindell, D.T., Chin, M., Dentener, F., Doherty, R.M., Faluvegi, G., Fiore, A.M., Hess, P., Koch, D.M., MacKenzie, I.A., Sanderson, M.G., Schultz, M.G., Schulz, M., Stevenson, D.S., Teich, H., Textor, C., Wild, O., Bergmann, D.J., Bey, I., Bian, H., Cuvelier, C., Duncan, B.N., Folberth, G., Horowitz, L.W., Jonson, J., Kaminski, J.W., Marmer, E., Park, R., Pringle, K.J., Schroeder, S., Szopa, S., Takemura, T., Zeng, G., Keating, T.J., Zuber, A., 2008. A multi-model assessment of pollution transport to the Arctic. Atmos. Chem. Phys. 8, 5353–5372. https://doi.org/10.5194/acp-8-5353-2008.

Sifeddine, A., Martin, L., Turcq, B., Volkmer-Ribeiro, C., Soubiès, F., Cordeiro, R.C., Suguio, K., 2001. Variations of the Amazonian rainforest environment a sedimentological record covering 30,000 years. Palaeogeogr. Palaeoclimatol. Palaeoecol. 168, 221–235. https://doi.org/10.1016/S0031-0182(00)00256-X.

Stevaux, J.C., Latrubesse, E.M., 2017. Geomorfologia Fluvial. Oficina de Textos, São Paulo 336 p.

Tavares, M.C.M., Volkmer-Ribeiro, C., De Rosa-Barbosa, R., 2003. Primeiro registro de Corvoheteromeyenia australis (Bonetto & Ezcurra de Drago) para o Brasil com chave taxonômica para os poríferos do Parque Estadual Delta do Jacuí, Rio Grande do Sul, Brasil. Revista Brasileira de Zoologia 20 (2), 169–182. https://doi.org/10.1590/S0101-81752003000200001.

Ussami, N., Shiraiwa, S., Dominguez, J.M.L., 1999. Basement reactivation in a sub-Andean foreland flexural bulge: the Pantanal wetland, SW Brazil. Tectonics 18 (1),25–39. https://doi.org/10.1029/1998TC900004.

Volkmer-Ribeiro, C., 1985. Esponjas de Água doce. Manuais Técnicos para a Preparação de Coleções Zoológicas 3, 1–6.

Volkmer-Ribeiro, C., De Rosa-Barbosa, R., 1985. Redescription of the freshwater sponges Trochospongilla repens (Hinde, 1888) and Trochospongilla amazonica (Weltner, 1895) with an account of the South American species of Trochospongilla (Porifera, Spongillidae). Iheringia, Série Zoologia 65, 77–93.

Volkmer-Ribeiro, C., Machado, V.S., 2007. Freshwater sponges (Porifera, Demospongiae) indicators of some coastal habitats in South America: redescriptions and key to identification. Iheringia, Série Zoologia 97 (2), 157–167. https://doi.org/10.1590/S0073-47212007000200005.

Volkmer-Ribeiro C, Parolin M. 2010. As Esponjas. In: Parolin M, Volkmer-Ribeiro C, Leandrini JA (orgs.) Abordagem ambiental interdisciplinar em bacias hidrográficas no Estado do Paraná. Editora da Fecilcam, Campo Mourão, pp 105-130.

Volkmer-Ribeiro, C., Grosser, K.M., De Rosa-Barbosa, R., Pauls, S.M., 1975. Primeiro relato da ocorrência de Espongílideos (Porifera) na Bacia do Guaíba, Estado do Rio Grande do Sul. Iheringia, Série Zoologia 46, 33–49.

Vuille, M., Burns, J.S., Taylor, B.L., Cruz, F.W., Bird, B.W., Abbott, M.B., Kanner, L.C., Cheng, H., Novello, V.F., 2012. A review of the South American monsoon history as recorded in stable isotopic proxies over the past two millennia. Clim. Past 8, 1309–1321. https://doi.org/10.5194/cpd-8-637-2012.

Wallinga, J., Murray, A., Wintle, A., 2000. The single-aliquot regenerative-dose (SAR) protocol applied to coarse-grain feldspar. Radiat. Meas. 32 (5–6), 529–533. https://doi.org/10.1016/S1350-4487(00)00091-3.

Whitney, B.S., Mayle, F.E., 2012. Pediastrum species as potential indicators of lake-level change in tropical South America. J. Paleolimnol. 47, 601–615. https://doi.org/10.1007/s10933-012-9583-8.

Whitney, B.S., Mayle, F.E., Punyasena, S.W., Fitzpatrick, K.A., Burn, M.J., Guillen, R., Chavez, E., Mann, D., Pennington, R.T., Metcalfe, S.E., 2011. A 45 kyr palaeoclimate record from the lowland interior of tropical South America. Palaeogeogr. Palaeoclimatol. Palaeoecol. 307 (1–4), 177–192. https://doi.org/10.1016/j.palaeo.2011.05.012.

Wilding, L.P., Drees, L.R., 1968. Distribution and implications of sponge spicules insurficial deposits in Ohio. The Ohio Journal of Science 68 (2), 92–99.

Zani, H., Assine, M.L., McGlue, M.M., 2012. Remote sensing analysis of depositional landforms in alluvial settings: method development and application to the Taquari megafan, Pantanal (Brazil). Geomorphology 161-162, 82–92. https://doi.org/10.
1016/j.geomorph.2012.04.003.

Zhou, J., Lau, K.M., 1998. Does a monsoon climate exist over South America? J. Clim. 11, 1020–1040. https://doi.org/10.1175/1520-0442(1998)011<1020:DAMCEO>2.0. CO;2.

APPENDIX A - Quantification of phytoliths, sponge spicules, total organic carbon (TOC), and total inorganic carbon (TIC), in the core LN95/L2 from Lake Negra

			Phytoliths														Sponge spicules						Sponge species					
Depht (cm)	Total Organic Carbon (wt %)	Total Inorganic Carbon (wt %)	Bilobate	Cross	Sadlle	Rondel	Cuneiform	Paralelepipedl	Cylindrical traceid	Elongate echinate	Elongate psilate	Trapeziform polylobate	Globular echinate	Globular granulate	Globular psilate	Phytoliths concentration	Megasclere concentration	Gemmulosclere concentration	Microsclere concentration	Sponge spicules concentration	*Corvospongilla seckti*	*Corvoheteromeyenia heterosclera*	*Dosilia pydanieli*	*Heteromeyenia barlettai*	*Radiospongilla amazonensis*	*Tubella paulula*	*Tubella variabilis*
0	1.07	0.0031	1	0	0	0	7	23	0	0	18	1	4	0	1	55	77	4	0	162	0	0	0	0	1	0	0
3	1.16	0.0034	0	0	0	0	3	33	0	2	22	0	2	0	0	64	91	2	0	186	0	0	0	0	2	0	0
6	1.47	0.0021	1	0	0	0	9	11	1	1	6	0	7	0	1	41	110	2	0	224	0	0	0	0	1	0	0
9	1.32	0.0022	1	0	0	1	3	11	0	2	11	0	3	0	0	33	72	0	0	144	0	0	0	0	0	0	0
12	1.12	0.0035	0	0	0	0	7	10	1	0	10	0	2	0	0	33	74	0	0	148	0	0	0	0	0	0	0
15	0.59	0.0017	0	0	0	0	9	15	0	0	6	0	3	0	0	36	72	0	0	144	0	0	0	0	0	0	0
18	0.44	0.0008	0	0	0	0	11	19	0	0	9	0	0	0	0	40	82	2	0	168	0	0	0	0	0	0	0
21	0.58	0.0000	0	0	0	0	3	17	0	0	8	0	0	0	0	28	57	0	0	114	0	0	0	0	0	0	0
24	0.54	0.0032	1	0	0	0	9	9	0	1	8	0	0	0	0	31	113	0	0	226	0	0	0	0	0	0	0
27	0.50	0.0018	0	0	0	0	4	12	0	0	14	0	0	0	0	33	58	0	0	116	0	0	0	0	0	0	0
30	0.49	0.0105	1	0	0	0	6	28	0	0	21	0	0	0	0	61	92	0	0	184	0	0	0	0	0	0	0
33	0.23	0.0008	0	0	0	0	3	16	0	0	9	0	1	0	0	32	59	0	0	118	0	0	0	0	0	0	0
36	0.27	0.0043	0	0	0	0	5	16	0	0	5	0	0	0	0	27	84	0	0	168	0	0	0	0	0	0	0
39	0.32	0.0040	0	0	0	0	7	26	0	0	16	0	0	0	0	51	103	0	0	206	0	0	0	0	0	0	0
42	0.25	0.0028	0	0	0	0	8	18	0	0	17	0	0	0	0	46	86	0	0	172	0	0	0	0	0	0	0
45	0.28	0.0041	0	0	0	0	13	37	0	1	21	0	1	0	0	76	126	1	0	254	0	0	0	0	0	0	0

48	0.31	0.0024	1	0	0	0	3	14	0	1	18	0	0	0	0	38	62	0	0	124	0	0	0	0	0	0	0
51	0.27	0.0024	0	0	0	1	15	49	1	1	26	0	0	0	0	102	233	0	0	466	0	0	0	0	0	0	0
54	0.40	0.0057	0	0	0	0	9	22	1	0	18	0	1	0	1	53	96	0	0	192	0	0	0	0	0	0	0
57	0.41	0.0056	0	0	0	0	2	25	0	0	14	0	0	0	0	45	110	0	0	220	0	0	0	0	0	0	0
60	0.40	0.0079	2	0	0	0	4	24	0	0	10	0	0	0	0	46	136	1	1	275	0	0	0	0	1	0	0
63	2.13	0.0021	1	0	0	0	2	11	0	0	4	1	7	0	0	26	1045	2	2913	5007	0	0	0	>100	0	0	0
66	2.18	0.0018	6	0	0	0	4	27	1	0	10	0	3	0	0	54	570	3	784	1930	1	0	0	>100	2	0	0
69	6.65	0.0061	4	0	1	0	9	48	0	4	35	0	2	0	0	115	399	3	83	887	0	>11	0	>11	2	1	0
72	1.81	0.0025	11	0	0	0	6	24	1	5	20	0	7	0	0	75	897	1	450	2246	0	>11	1	>11	0	0	1
75	1.44	0.0032	14	0	5	3	11	72	1	10	41	4	9	0	2	176	593	18	97	1319	0	>11	0	0	1	1	0
78	1.21	0.0039	12	0	2	1	9	43	0	1	34	2	1	0	0	107	350	25	24	774	0	>11	0	1	3	1	4
81	1.19	0.0055	9	0	2	1	7	47	2	5	40	1	6	0	0	124	323	2	24	674	0	>11	0	0	1	0	0
84	1.29	0.0054	16	0	4	2	14	57	1	4	43	2	4	0	0	159	333	10	24	710	0	>11	0	0	3	0	1
87	1.45	0.0024	13	0	2	2	18	43	1	9	24	1	3	0	0	120	317	12	11	669	0	8	0	0	2	1	0
90	1.12	0.0088	18	0	4	1	9	51	2	2	31	7	4	0	0	135	371	10	12	774	0	8	0	0	1	1	0
93	0.79	0.0019	5	0	1	1	13	83	2	8	60	2	2	0	0	183	509	5	2	1030	0	2	0	0	0	0	0
96	0.68	0.0045	13	0	3	2	35	128	0	2	50	4	11	3	1	252	667	9	5	1357	0	6	0	0	0	1	1
99	0.59	0.0013	5	0	3	1	28	113	0	6	68	1	7	0	0	246	621	10	6	1268	0	5	0	0	3	0	0
102	0.59	0.0017	3	1	1	2	24	139	1	7	81	2	4	0	0	285	1048	12	0	2120	0	5	0	0	2	0	0
105	0.59	0.0002	3	0	1	1	35	143	1	6	67	1	3	0	0	282	944	4	0	1896	0	0	0	0	0	0	0
108	0.48	0.0031	3	0	2	0	46	147	1	6	54	1	2	0	1	285	839	3	2	1686	1	1	0	0	1	0	0
111	0.50	0.0031	2	0	1	0	52	173	1	7	124	1	8	1	0	386	1030	5	0	2070	0	2	0	0	2	1	0
114	0.61	0.0040	1	0	0	0	20	45	0	0	25	0	0	1	0	105	1380	3	0	2766	0	0	0	0	0	0	0
117	0.85	0.0047	2	0	1	3	34	144	0	3	66	1	10	0	1	275	800	9	1	1619	0	0	0	0	0	0	0
120	1.12	0.0015	3	0	2	1	19	83	0	0	74	2	0	0	0	206	712	7	0	1438	0	0	0	0	0	1	0
123	1.37	0.0021	1	0	2	0	28	83	1	2	49	1	4	0	0	173	590	4	0	1188	0	0	0	0	0	0	0
126	1.08	0.0002	0	0	1	2	25	140	1	1	72	2	1	1	0	246	984	11	1	1991	0	0	0	0	0	0	0

129	1.17	0.0002	2	0	3	1	11	95	0	1	34	0	1	0	0	153	404	0	0	808	0	0	0	0	0	0	0
132	1.54	0.0002	0	0	0	2	16	96	0	2	34	1	3	0	1	155	456	8	0	928	0	0	0	0	0	0	0
135	1.27	0.0013	2	0	0	1	14	46	0	0	30	0	1	0	0	95	227	0	1	455	0	1	0	0	0	0	0
138	1.78	0.0032	3	0	0	2	23	88	0	0	47	1	0	2	0	166	544	4	0	1096	0	0	0	0	1	0	0
141	1.67	0.0023	4	0	0	1	12	64	0	1	33	1	5	1	0	127	312	1	2	628	0	0	0	0	0	0	0
144	1.59	0.0026	1	0	0	0	11	54	0	0	21	0	1	0	0	88	217	0	0	434	0	0	0	0	0	0	0
147	1.31	0.0017	0	0	2	0	7	42	0	1	28	1	0	0	0	84	186	0	0	372	0	0	0	0	0	0	0
150	0.93	0.0029	1	0	0	0	10	52	0	1	16	1	1	0	2	84	183	0	0	366	0	0	0	0	0	0	0
153	0.72	0.0013	0	0	0	0	9	21	0	0	9	0	3	0	0	45	141	0	0	282	0	0	0	0	0	0	0
156	0.69	0.0032	0	0	0	0	2	23	0	0	5	0	1	0	0	31	165	0	3	333	0	2	0	0	0	0	0
159	0.39	0.0045	0	0	0	0	15	30	0	0	12	0	0	0	0	60	231	0	0	462	0	0	0	0	0	0	0
162	0.49	0.0041	0	0	0	0	0	12	0	0	14	0	0	0	1	27	123	0	0	246	0	0	0	0	0	0	0
165	0.38	0.0004	0	0	0	0	3	27	0	0	30	0	0	0	0	63	252	0	0	504	0	0	0	0	0	0	0
168	0.31	0.0051	0	0	0	0	5	45	0	0	20	0	2	0	0	72	264	0	0	528	0	0	0	0	0	0	0
171	0.30	0.0016	0	0	0	0	2	35	0	0	14	0	0	0	0	51	239	0	0	478	0	0	0	0	0	0	0
174	0.16	0.0043	0	0	0	0	0	30	0	0	8	0	0	0	1	39	211	0	0	422	0	0	0	0	0	0	0
177	0.21	0.0012	0	0	0	0	0	18	0	0	4	0	0	0	0	23	156	0	0	312	0	0	0	0	0	0	0
180	0.14	0.0038	0	0	0	0	0	6	0	0	0	0	0	0	0	9	96	0	0	192	0	0	0	0	0	0	0
183	0.04	0.0052	0	0	0	0	0	17	0	0	10	0	1	0	0	29	137	0	0	274	0	0	0	0	0	0	0
186	0.00	0.0030	0	0	0	0	0	6	0	0	0	0	0	0	0	6	15	0	0	30	0	0	0	0	0	0	0
189	0.00	0.0003	0	0	0	0	0	0	0	0	0	0	0	0	0	0	0	0	0	0	0	0	0	0	0	0	0
192	0.00	0.0044	0	0	0	0	0	0	0	0	0	0	0	0	0	0	0	0	0	0	0	0	0	0	0	0	0
195	0.00	0.0059	0	0	0	0	0	0	0	0	0	0	0	0	0	0	0	0	0	0	0	0	0	0	0	0	0
198	0.00	0.0018	0	0	0	0	0	0	0	0	0	0	0	0	0	0	0	0	0	0	0	0	0	0	0	0	0
201	0.00	0.0065	0	0	0	0	0	0	0	0	0	0	0	0	0	0	0	0	0	0	0	0	0	0	0	0	0
204	0.01	0.0034	0	0	0	0	0	0	0	0	0	0	0	0	0	0	0	0	0	0	0	0	0	0	0	0	0
207	0.03	0.0463	0	0	0	0	1	2	0	0	1	0	0	0	0	4	13	0	0	26	0	0	0	0	0	0	0

210	0.82	0.0001	0	0	0	0	0	6	0	0	6	0	0	0	0	12	21	0	0	42	0	0	0	0	0	0	0
213	0.16	0.0000	0	0	0	0	1	6	0	0	8	0	0	0	0	15	75	0	0	150	0	0	0	0	0	0	0
216	0.00	0.0253	0	0	0	0	3	6	0	0	12	0	0	0	0	24	57	0	0	114	0	0	0	0	0	0	0
219	0.01	0.0241	0	0	0	0	3	8	0	0	7	0	0	0	0	18	87	0	0	174	0	0	0	0	0	0	0
222	0.01	0.0589	0	0	0	0	6	12	0	0	0	0	3	0	0	21	108	0	0	216	0	0	0	0	0	0	0
225	0.02	0.1473	0	0	0	0	1	16	0	0	4	0	0	0	1	23	54	1	0	110	0	0	0	0	0	0	0
228	0.26	0.0000	0	0	0	0	0	12	0	0	3	0	0	0	0	15	48	0	0	96	0	0	0	0	0	0	0
231	0.21	0.0000	1	0	0	0	3	17	0	0	12	0	0	0	0	33	55	1	0	112	0	0	0	0	0	0	0
234	0.03	0.1357	0	0	0	0	6	6	0	0	6	0	0	0	0	24	48	0	0	96	0	0	0	0	0	0	0
237	0.00	0.1225	0	0	0	0	0	15	0	0	4	0	0	0	0	19	124	0	0	248	0	0	0	0	0	0	0
240	0.01	0.1206	0	0	0	0	12	6	0	0	9	0	0	0	0	27	177	0	0	354	0	0	0	0	0	0	0
243	0.00	0.0565	0	0	0	0	0	0	0	0	0	0	0	0	0	0	0	0	0	0	0	0	0	0	0	0	0
246	0.01	0.0467	0	0	0	0	0	0	0	0	0	0	0	0	0	0	0	0	0	0	0	0	0	0	0	0	0
249	0.00	0.0449	0	0	0	0	0	0	0	0	0	0	0	0	0	0	0	0	0	0	0	0	0	0	0	0	0
252	0.00	0.0187	0	0	0	0	0	0	0	0	0	0	0	0	0	0	0	0	0	0	0	0	0	0	0	0	0
255	0.00	0.0201	0	0	0	0	0	0	0	0	0	0	0	0	0	0	0	0	0	0	0	0	0	0	0	0	0
258	0.00	0.0252	0	0	0	0	0	0	0	0	0	0	0	0	0	0	0	0	0	0	0	0	0	0	0	0	0

APPENDIX B - Age model of the L95/L2 core from Lake Negra

Depth (cm)	Age min	Age max	Age median	Agen mean	Depth (cm)	Age min	Age max	Age median	Agen mean
0	-170.5	-35.5	-82.5	-87.3	137	9555.2	10529.5	10011.5	10033.3
1	-76.3	-15	-45.4	-44.9	138	9584.5	10584	10052.8	10073.4
2	-56.2	78.4	-8.1	-2.1	139	9615	10654.1	10092	10113.7
3	-49.4	194.6	26.3	39.8	140	9639.5	10732.1	10129.5	10153.4
4	-45.8	312.3	60.5	81.6	141	9680.6	10767.1	10172.2	10194.3
5	-41.7	431.9	95.7	123.6	142	9711.8	10814.2	10214.5	10235.8
6	-12	458.8	138.6	163.3	143	9745.7	10863.4	10255.9	10276.9
7	4.9	498.1	182.7	202.9	144	9771	10927.7	10297.4	10318.8
8	17.9	546.8	222.8	241.5	145	9791.1	11007.6	10334.9	10359.5
9	27.4	608.7	259	279.2	146	9835.5	11046.1	10376.6	10401.8
10	35	683.4	294.6	316.9	147	9869.7	11091.6	10421.4	10443.8
11	75.8	709.1	336.4	354.7	148	9898.1	11142.1	10464.7	10485.3
12	103.7	736.2	378.6	392.8	149	9927.9	11196.4	10506	10527.3
13	124.5	769.3	421.2	431.1	150	9949.9	11268.3	10546.4	10569.3
14	144.1	816.6	461.9	469.1	151	9996.5	11304.6	10588.7	10612.3
15	161.8	878.9	499.7	507.2	152	10032.2	11351.5	10633.4	10655.1
16	216.9	901.4	538.3	545.6	153	10064	11403.3	10677	10697.8
17	256.9	926.9	577.3	583.9	154	10087.3	11456.7	10717.3	10738.6
18	290.6	957.8	616.6	622.2	155	10110.9	11518.5	10757.1	10779
19	317.1	993.9	657.5	660.7	156	10156	11553.5	10799.7	10821.2
20	339.8	1042.9	696.6	699	157	10194.1	11596.1	10845.7	10863.5
21	419.7	1061.3	731.1	737.5	158	10225.6	11632.2	10889.2	10906
22	492.9	1083	766.1	775.8	159	10256.5	11676.8	10933.5	10947.8
23	555.1	1105.8	805.3	814.9	160	10285.7	11731.4	10976	10989.8
24	601.3	1141.4	845	854.3	161	10327.9	11769	11018.7	11031.5
25	638.2	1190.6	884.4	893.7	162	10373.5	11805.7	11061.8	11073.3
26	720	1236	936	950.1	163	10410.2	11849.2	11105.5	11114.9
27	763.4	1301.5	991.8	1006.4	164	10439.4	11897.7	11145.5	11156.4
28	793.4	1398.2	1044.4	1062.8	165	10462.9	11950.8	11185.7	11195.9
29	814.1	1533.8	1094.1	1119	166	10505.4	11986.8	11226.6	11237.7
30	831.3	1675.4	1140.2	1174.3	167	10544.7	12023.3	11269.8	11279.8
31	873.2	1744.9	1202.8	1235	168	10589.4	12063.5	11313.8	11321.7
32	900.2	1847.6	1263	1295.4	169	10621.7	12112.3	11355.6	11363.7
33	917.8	1980.5	1319.1	1356.5	170	10652.3	12166.8	11396.8	11405.8
34	937.8	2121.5	1370.5	1417.4	171	10703.3	12194	11438.7	11448.1
35	950.8	2261.6	1421.4	1477.9	172	10744.5	12225.7	11481.8	11490.8
36	997.3	2335.7	1487.4	1541	173	10781.4	12266.8	11526.9	11533.7
37	1036.7	2431.5	1552	1604.4	174	10811.3	12309.4	11571.3	11576.3
38	1067.9	2548.5	1615.9	1667.7	175	10843	12363.8	11614.9	11619.2
39	1090.5	2661.3	1674	1730.1	176	10889.4	12376.9	11651.5	11656.2
40	1108.5	2791.3	1726.4	1791.7	177	10917.9	12413.6	11689.5	11691.8
41	1155	2869.1	1786.7	1854	178	10943.2	12453.6	11726	11727.9
42	1198	2951.8	1849.8	1916.1	179	10969.6	12489.2	11762.7	11763.3
43	1234.1	3038.1	1911.7	1978.2	179.99	10987.6	12533.9	11798.2	11799.1
44	1256.8	3150.9	1967.8	2037.5	180	11210.3	12784.9	12006.7	12011.3

45	1275	3281.9	2019.7	2097.6	181	11303	12810.5	12053.7	12059.9
46	1336.3	3332.7	2085	2160	182	11372.9	12837.8	12103	12108.3
47	1384.1	3395.9	2150.5	2222.9	183	11428	12867.7	12155.2	12155.9
48	1418.7	3472.1	2212.9	2285.7	184	11477.1	12897.3	12208	12204.6
49	1455.7	3562.4	2275.3	2349	185	11513.4	12941.5	12259.5	12252.2
50	1483.1	3680.5	2333.9	2411.1	186	11572.8	12969.7	12305.4	12294.1
51	1536.6	3731.1	2393.4	2470.2	187	11617.6	13009.3	12346.7	12336
52	1583.4	3797	2456.9	2530.5	188	11659.6	13046.5	12391.1	12377.9
53	1619.9	3866.4	2516.4	2590.7	189	11698.9	13086.5	12435.7	12420.1
54	1656.1	3956.3	2575.4	2650.6	190	11707.6	13135.4	12461.4	12445.7
55	1687.7	4045.6	2631	2710.5	191	11776.3	13206.5	12535.3	12522.9
56	1741.7	4129.4	2705.3	2783.8	192	11830.5	13311.4	12605.1	12599
57	1770	4239.5	2759	2844	193	11883.7	13461.7	12674.5	12675.8
58	1795	4357.1	2813.1	2902.9	194	11923.5	13632.7	12740.7	12753.5
59	1818.4	4489.5	2869.2	2962.2	195	11962	13804.1	12807	12830.4
59.99	1835.3	4634.8	2921.7	3021.7	196	12040	13881.8	12893.3	12915.1
60	4537	6450	5718.6	5662.7	197	12099	13973.6	12976.7	13000.3
61	4694.1	6464.8	5763.3	5718.8	198	12149.4	14101.1	13061.6	13085.7
62	4841.2	6484.9	5807.4	5774.6	199	12196.1	14239.2	13137.8	13170.3
63	4994.2	6504.5	5849.5	5830.7	200	12243.3	14406.2	13210.6	13255.5
64	5146.4	6526.7	5894.6	5886.4	201	12326.1	14480.6	13301.8	13343.2
65	5290.2	6555.7	5941	5942.7	202	12401.5	14565.4	13391.7	13431.2
66	5421.8	6583.6	5987.2	5997.2	203	12464.5	14674.6	13480.6	13518.8
67	5545.4	6614.1	6033.8	6052.1	204	12526.2	14802.7	13567.5	13606.6
68	5652.3	6650.7	6083.4	6107	205	12569	14966.4	13650.1	13694.3
69	5744.2	6681.9	6134.3	6161.9	206	12666.6	15038.4	13743.1	13782.5
70	5803.9	6736.6	6186.9	6215.4	207	12735.5	15122.9	13838.7	13871.2
71	5852.8	6790.2	6245.2	6271.7	208	12802.9	15226.7	13928.9	13959.4
72	5890.1	6858.3	6304.9	6327.6	209	12853	15351.4	14015.5	14045.8
73	5921.4	6939.6	6363	6383.8	210	12900.8	15495.1	14096.1	14131.3
74	5945.8	7034.7	6415.9	6439.5	211	12986.7	15572.5	14182.6	14216.2
75	5967.3	7141.5	6465.3	6493.4	212	13054.8	15651.8	14269	14301.4
76	6030.8	7180.9	6527.2	6550.3	213	13115.2	15738.9	14356.3	14386.6
77	6076.3	7237.3	6587.9	6607	214	13167.1	15848.4	14442.3	14471.5
78	6113.3	7297.5	6645.4	6663.2	215	13208.5	15976	14528.7	14555.3
79	6143.3	7376.2	6701.6	6719.7	216	13294.5	16042.7	14619	14642.7
80	6171	7467.8	6756.3	6776.9	217	13386.7	16112.3	14707.9	14730.1
81	6241.5	7506.7	6818.6	6835.9	218	13454.3	16196.2	14803	14817.6
82	6297.5	7552.8	6882.5	6894.4	219	13518	16293	14893.1	14904.1
83	6341	7607.8	6945.5	6953.2	220	13573.7	16411.1	14979.8	14991.4
84	6374.4	7670.3	7004.8	7011.7	221	13656.6	16464.4	15069	15077.9
85	6402.6	7763.4	7064.4	7070.3	222	13726.8	16517.6	15156.9	15163.5
86	6474.8	7791.5	7123.6	7128.5	223	13797.2	16588.3	15249	15251.1
87	6528.6	7829.7	7181	7186.1	224	13850.7	16674.9	15338.1	15336.3
88	6573.5	7876.2	7242.6	7244	225	13901.8	16793.5	15426.5	15421.2
89	6611.1	7934.6	7300.8	7300.9	226	14000	16844.5	15514.8	15508.7
90	6644.2	8006.7	7356.8	7356.9	227	14078.5	16908	15603.4	15596.7
91	6724	8043.2	7413.6	7416	228	14142.1	16978.3	15694.6	15685.5

92	6796.2	8079.1	7477.2	7475.3	229	14197.2	17073.9	15786.5	15773.3
93	6852.7	8127.2	7539.7	7534.1	230	14253	17179	15874.6	15860.5
94	6896.7	8186.4	7602.2	7593.4	231	14350.6	17232.3	15969.8	15947
95	6937.6	8259.4	7661.8	7651.9	232	14425.2	17292.1	16063	16031.2
96	7036.3	8286.6	7715	7707.7	233	14489.7	17357.3	16159.5	16116.9
97	7128.6	8314.2	7772.7	7764.4	234	14542.4	17436.4	16251.9	16202.4
98	7198.7	8352.7	7831.6	7821.1	235	14596.3	17521.6	16339.7	16286.7
99	7253.9	8402.6	7890.8	7878.1	236	14693.5	17572.3	16433.3	16373.4
100	7296.4	8463.2	7947.8	7934.1	237	14773.5	17620.3	16529.2	16460.1
101	7421.1	8487.2	7995.2	7989.6	238	14842.8	17687.2	16622.2	16546.9
102	7522.2	8517.5	8046.9	8046.9	239	14912.6	17758.6	16717	16633.6
103	7609.6	8562.7	8103.2	8104.7	240	14969.3	17855.7	16806.1	16719.2
104	7682.8	8615.4	8160.7	8162.3	241	15069	17901	16899.1	16807.3
105	7741.8	8679.1	8218.9	8219.9	242	15143	17942.6	16996.1	16894.1
106	7855.3	8727.4	8276.4	8281.2	243	15212.6	17999.9	17093.9	16982.2
107	7941.4	8782.1	8336.5	8343.2	244	15275.3	18076.3	17191.3	17070.4
108	8002.7	8834.9	8399.6	8404.7	245	15336	18169.4	17284.6	17158.3
109	8045.6	8906.9	8456.2	8464.6	246	15426.5	18201.1	17380.7	17246.4
110	8081.9	9014.5	8508.9	8523.5	247	15501.4	18233.7	17480.3	17333.6
111	8147	9058.6	8569.8	8582.7	248	15574.6	18283	17583.2	17421.6
112	8201.3	9118.7	8632.1	8643.5	249	15654.1	18334.9	17682.9	17509.3
113	8245.9	9191.5	8692.6	8704.6	250	15717.2	18416.7	17781.9	17597.6
114	8278.2	9275.7	8751	8764.9	251	15799	18446.3	17811.4	17632
115	8306.6	9389.2	8808.7	8825.7	252	15837.5	18529.1	17868.1	17690.8
116	8389.6	9421.4	8869.5	8884.5	253	15895.9	18631.6	17919.7	17749.9
117	8446.7	9464.5	8934.4	8944.3	254	15926	18755.7	17969.5	17807.5
118	8490.5	9518	8998	9003.9	254.99	15967	18886.4	18016.5	17866.4
119	8532.2	9586.2	9060.4	9064.2	255	16312.6	20371.3	18290.8	18356.4
120	8566.1	9668.8	9118.6	9124.5	256	16362.2	20394.6	18339.2	18401.6
121	8654.1	9698.5	9179	9183	257	16405.1	20433.1	18395.1	18447
122	8730.6	9734.8	9241.4	9242.7	258	16445.6	20471.2	18443.9	18492.3
123	8783.5	9781.3	9306.1	9302.9	259	16489.2	20502.9	18497.6	18538.3
124	8826.9	9837.6	9371.3	9363.3	260	16523.2	20552.6	18542.7	18583.2
125	8862.3	9914.2	9433.7	9423.3	261	16556.9	20592	18578.8	18619
126	8981.9	9940.8	9484.8	9482	262	16594.9	20619.7	18619.5	18657.7
127	9083.8	9978.3	9537.6	9542.2	263	16642.2	20673.3	18654.7	18693.7
128	9166	10026.4	9591.5	9602	264	16667.7	20701.2	18690.3	18729.2
129	9224.8	10084.2	9646.6	9661.8	265	16623.1	20778.2	18698	18738.7
130	9274.6	10154.2	9706	9722.6	266	16679.4	20823.6	18744.4	18784.6
131	9335.9	10193.6	9750.4	9768.9	267	16719.4	20863.6	18790.1	18831
132	9379.8	10237.2	9796.5	9815.3	268	16763	20907.9	18837.6	18877.1
133	9415	10287.4	9843.1	9862	269	16799.5	20966.6	18882.4	18922.9
134	9442.3	10356	9887.1	9908.9	270	16809.7	21018	18925.4	18968.1
135	9470.5	10448.1	9926.8	9953.8	271	16883.3	21068.6	18975.3	19016.7
136	9515.9	10484.4	9968	9993.1	272	16934.9	21136.7	19022	19065.2

3 CONTROLS ON ENHANCED MID HOLOCENE ORGANIC CARBON BURIAL IN FLOODPLAIN LAKES OF THE PANTANAL

ABSTRACT

An important yet environmentally sensitive ecosystem service of wetlands and their shallow lakes is carbon storage. Carbon burial in the floodplain lakes of the Pantanal (tropical South America) appears to have varied during the late Quaternary, but several paleolimnological studies have recorded unusually high sedimentary organic carbon content from ~7.3-6.0 cal kyr BP in lakes connected to the Upper Paraguay River. In this study, we present results of a new multi-indicator (phytoliths, sponge spicules, and geochemistry) sediment core analysis from Lake Cáceres (Bolivia), which replicates the signal of enhanced organic carbon burial in the middle Holocene and provides additional insight on the flooding history of the Upper Paraguay River. $\delta^{13}C_{org}$, $\delta^{15}N_{org}$, and C/N data reveal that organic matter deposited in this early Holocene phase of enhanced carbon burial in Lake Cáceres is from a macrophyte source, and allied data from three other lakes are consistent with this finding. We suggest that enhanced carbon burial occurs when the lakes shoal in a drying climate, which increases the area of productive littoral wetland at the expense of open water and captures floating macrophyte islands. The results of this study shed new light on the hydroclimatic controls on lacustrine carbon cycling in the Pantanal wetlands, and improves on interpretations of bulk organic matter geochemical data in floodpain lake cores.

***Keywords*:** biological indicators; lake sediments; organic carbon; paleolimnology; wetlands.

3.1 Introduction

Tropical wetlands are diverse landscapes of considerable ecological importance, and may include swamps, marshes, bogs, fens, floodplains, and shallow lakes (Neue et al. 1997; Einsele et al. 2001; Junk et al. 2013). Tropical wetlands perform many ecosystem services harbor exceptional biodiversity, and are critical for regional primary productivity and nutrient cycling, particularly in environments influenced by seasonal hydrology (Junk et al. 2013; Mitsch et al. 2013). Wetland biogeochemical processes and vegetation also produce various greenhouse gases, including CH_4 and N_2O (Mitsch and Gosselink, 2015). Wetlands are also important to carbon cycling, in part because of their capacity to generate and bury organic matter (OM) (Tockner et al. 1999; Mitsch et al. 2013). However, not all wetlands, even if

waterlogged, accumulate vast stores of carbon. Indeed, wetlands under the influence of changing hydrology and climate may vary between carbon source and sink, as the process which control the balance between OM inputs and outputs change (Neue et al. 1997). Climate changes that favor consecutive years of drought threaten wetland hydrology and may make them vulnerable to methane emission and oxidation of carbon stores from wildfires or microbial activity as soils desiccate under subaerial conditions (Cole et al. 2007; Sobek et al. 2009; Mitsch et al. 2010). Changes to carbon storage may have feedbacks on the global climate system, as well as hold potential for regional losses in biodiversity (Shindell et al. 2004; Carey et al. 2018).

The Pantanal is the world's largest tropical wetland (Por 1995; Warren et al. 2015), and it is located in the Upper Paraguay River watershed (Assine et al. 2015). The Paraguay River is a trunk river system on the Pantanal's western margin, and seasonal flooding holds great importance to the vegetation and ecology of the wetlands (Ivory et al. 2019). The seasonal fluctuation of flood waters and riverine sediment produces a nutrient recycling effect that supports primary productivity and a complex and diverse food web (Junk et al. 2013). Carbon cycling in the Pantanal is still understudied, but the available data indicates that the flooding cycle of the Paraguay River is important to OM transformations and emissions of CO_2 and CH_4 (Bergier et al 2015; Dalmagro et al. 2018).

The concentration of sedimentary organic carbon (measured as total organic carbon; hereafter TOC) is a commonly employed indicator of paleoproduction in South American lakes (Cohen et al. 2015). Organic matter in lake sediments have two primary sources: an autochthonous origin, derived from algae and aquatic plants, or an allochthonous origin, resulting from the transport of terrestrial plant debris, pollen, biochar, and soils (Talbot 1990; Meyers 1994; Meyers 2003). Waterlogged lentic depositional environments often causes incomplete anaerobic decomposition, leading to a delay in decomposition and an accumulation of carbon rich sediments and nutrients (Neue et al. 1997; Sawakuchi et al. 2015). Differing concentrations of TOC in floodplain lake sediments from the Pantanal has provided evidence of climate dynamics, riverine flooding, and paleoproduction (McGlue et al., 2015).

Paleolimnological studies of large floodplain lakes in the Pantanal demonstrate that the middle Holocene (~7.5-5.0 kyr) was an interval of enhanced sedimentary carbon accumulation, and this ~2.5 kyr interval is unique within the latest Pleistocene and Holocene. High TOC has been measured in middle Holocene sediments in a north-south transect along

the western margin of the Pantanal in lakes Castelo (Bezerra and Mozeto 2008; Bezerra et al. 2019), Gaíva (McGlue et al. 2012; Metcalfe et al. 2014), and Negra (Bezerra and Mozeto 2008; Bezerra et al. 2019; Rasbold et al. 2019). These lakes are located adjacent to the Paraguay River, and their water levels are sensitive to the seasonal flood pulse (McGlue et al. 2011). Enhanced carbon burial in the middle Holocene is somewhat counterintuitive, considering that paleo-precipitation proxies from a high-resolution oxygen isotope dataset indicate that the early-mid Holocene (11.0-5.5 kyr) was a relatively dry period in the Pantanal (Novello et al. 2017). Yet soil formation and vegetation may have been influenced by the drier climate and this could have altered carbon dynamics (Novello et al. 2019).

What hydroclimatic conditions influenced organic carbon burial in the Pantanal's floodplain lakes during the middle Holocene? Given the importance of the seasonal water cycle in the Pantanal to primary productivity in the wetlands, it is important to understand how aquatic ecosystems responded to environmental changes at this time. Modern limnogeological sampling has revealed that some of Pantanal's floodplain lakes show a gradient in sedimentary TOC that increases with water depth and distance to the shoreline (McGlue et al. 2011). These data might suggest that deeper lake phases, and hence a wetter climate, favor higher sedimentary TOC. New paleo-precipitation proxy data suggest this interpretation warrants further examination (Novello et al. 2017). We hypothesize that floodplain lake depressions retain enough water during dry periods to allow aquatic plants to flourish, thus allowing OM generation and burial to continue as the climate system changes. To test this hypothesis, we studied carbon burial during the mid-Holocene in Lake Cáceres (LCC), a large floodplain lake connected to the Paraguay River in the Bolivian Pantanal. We conducted a paleoecological and sedimentological analysis of a recently collected sediment core, and compared the results with previously published paleolimnological data from lakes Gaíva, Castelo, and Negra. Together, we used these data to assess the interactions among climate, vegetation, and hydrology and their influence on paleoproduction in wetlands. The results have implications for improving paleolimnological interpretations of TOC data from tropical floodplain lakes, and for understanding the role of tropical wetlands as atmospheric carbon sinks.

3.2 Geological setting

The Paraguay River is connected to several large floodplain lakes on its western margin (Fig. 1), which from north to south are: Lake Uberaba (LU), Lake Gaíva (LG), Lake

Mandioré (LM), Baía Vermelha (BV), Lake Castelo (LC), Lake Cáceres (LCC), and Lake Negra (LN) (McGlue et al. 2015). The climate in the Pantanal Basin is influenced by the migration of the Intertropical Convergence Zone (ITCZ) and the South American summer monsoon (SASM) (Garreaud et al. 2009; Vuille et al. 2012; Ivory et al. 2019). The precipitation ranges between 800 and 1300 mm annually, and a distinct wet season occurs from October to April. The mean annual temperature is ~25° C (Por 1995). In the north, the response of the floods is synchronous with the rains. Floods to the south, however, are delayed for months, as storage occurs first by the channels and lakes, only after exceeding the limits does the pulse start south (Ivory et al. 2019).

The geology surrounding Lake Cáceres consists of Quaternary sediments such as the Xaraiés and Pantanal Formations, which make up alluvial terraces and colluvial deposits (Brasil 1982; Lacerda Filho et al. 2006). The lowland landscape is intermittently fringed by hills that consist of ancient meta-sedimentary rocks that belong to the Urucum and Santa Cruz Formations of the Neoproterozoic Jacadigo Group. Localized outcrops of Bocaina and Tamengo Formation (Neoproterozoic Corumbá Group) limestones are also present (Brasil 1982; Lacerda Filho et al. 2006).

The Pantanal's vegetation consists of periodically flooded savannas, with plants and animals adapted to the seasonal flood pulse (Junk et al. 2014). The terrestrial vegetation is composed of seasonal deciduous forest, seasonal semi-deciduous forest, pioneer woodlands, savannah (*cerrado*), steppic savanna (*chaco*), and refugia savanna vegetation (grasslands and *cerrado* woodland) (Pott and da Silva 2015). The aquatic vegetation is comprised of emergent, submerged, and floating plants. Submerged and floating plants occur mostly in ponds, oxbow lakes, and streams (Pott and da Silva 2015; Lo et al. 2017). The emergent plants (e.g., smartweeds) develop along river courses, growing as rooted floating mats or in shallow channel margins. However, some plants are found in flooding-prone grasslands and savannas, and can grow either with or without standing water and saturated soils (Pott and da Silva 2015).

Lake Cáceres was connected with the Paraguay River via the Tuiuiú paleochannel (Fig. 2B). Currently, the lake has two primary inflows: (a) the direct connection to the Paraguay River through the Tamengo channel (Fig. 2B) and, (b) groundwater seepage. The Tamengo channel is important to Bolivia, as it connects the landlocked nation's eastern frontier to the Atlantic Ocean via the Paraguay-Paraná waterway. Lake Cáceres has two outflows at the Pimiento and Sicuri rivers (Fig. 2B). The predominant vegetation on the

southern border of Lake Cáceres consists of extensive herbaceous swamp communities that develop very thick (~ 50-80 cm) mats. These mats grow in shallow water < 50 cm deep (Frey 1995). In slightly deeper water (> 1 m), the mats are replaced by a dense cover of free-floating *Ipomoea carnea* ssp. *fistulosa* (Frey 1995). Towards the ca. 30 m high plateau south of the lake, weedy vegetation is found growing on dry soils. Frey (1995) recorded that the norther border of Lake Cáceres contained dense floating mats of Poaceae (e.g., *Hymenachne amplexicaulis*, *Leersia hexandra*, *Oryza rufipogon*), and isolated populations of the giant lily pads, *Victoria amazonica*.

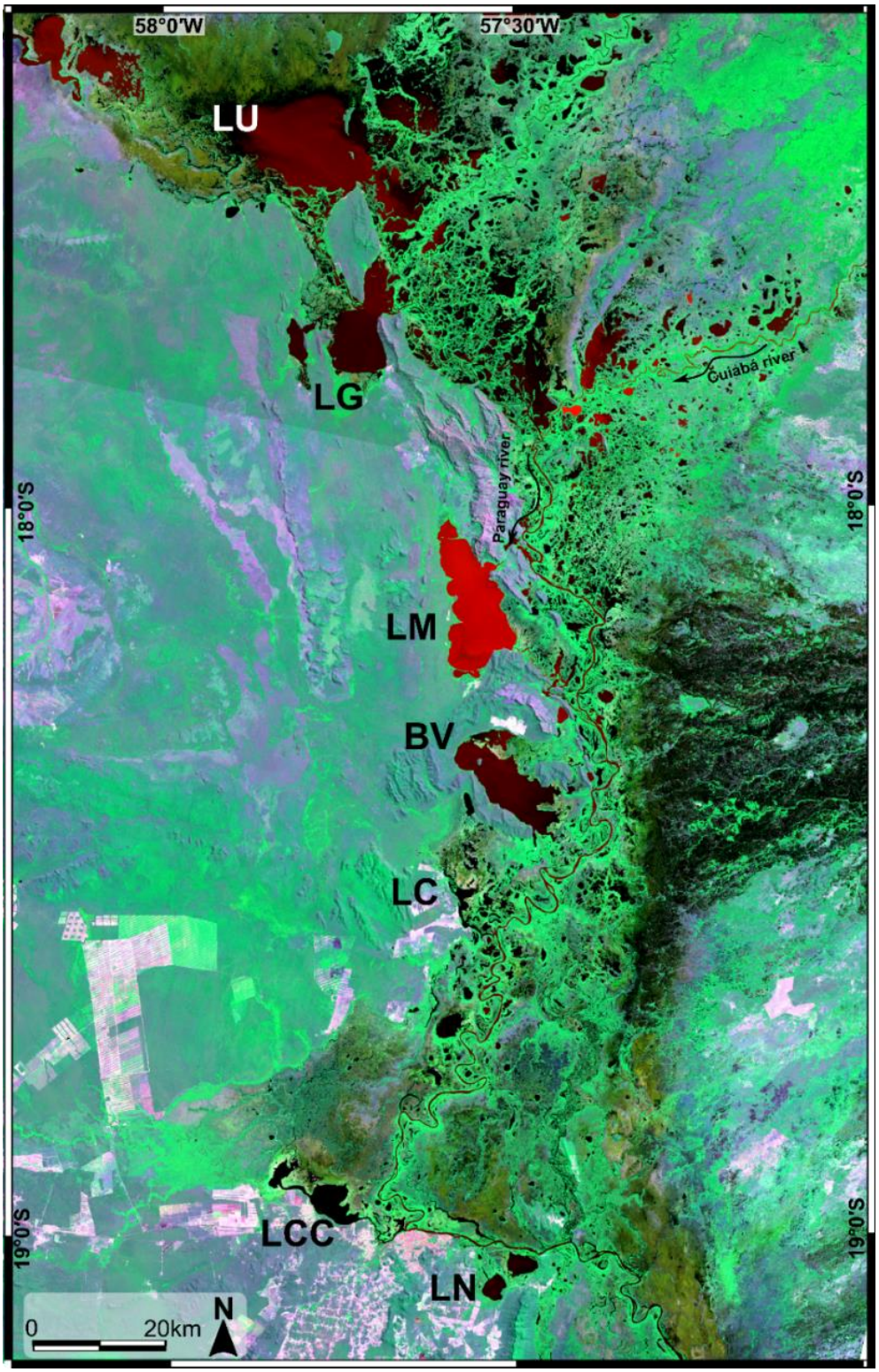

Figure 1. Floodplain lakes connected to the Paraguay River in an N-S transect (~ 200 km). Lake Uberaba (LU), Lake Gaíva (LG), Lake Mandioré (LM), Baía Vermelha (BV), Lake Castelo (LC), Lake Cáceres (LCC), and Lake Negra (LN). Landsat image, 2018/09/07, OLI-TIRS, orbit/point: 227/072 and 227/073. Landsat-8 image courtesy of the U.S. Geological Survey.

3.3 Material and methods

Bathymetric soundings (*n = 61*) were manually collected in June 2016 with a handheld depth finder; the survey was a mesh covering the entire open water area (Fig. 2). The data were analyzed in QGIS 2.18.21 software using an inverse distance weighting interpolation for contouring. Lake morphometrics were assessed using remote sensing data products from the USGS database (earthexplorer.usgs.gov). Lake morphology was determined from a 30 m resolution Landsat-5 image (1984/09/09, TM, orbit/point: 227/073 and 2002/03/01, TM, orbit/point: 227/073). Image enhancement and morphometrics calculations were made in QGIS 2.18.21 (Fig. 2).

Modern sediment samples and a sediment core were collected from Lake Cáceres using standard techniques (Fig. 2). The upper 2–3 cm of modern lake floor sediments (*n = 61*) were collected using a Van Veen sampler, in order to assess the concentrations of total organic carbon (TOC), sponge spicules and phytolith assemblages. The surface sediment sampling mesh was constructed to provide maximum coverage of the different environments encountered in the field.

A sediment core was recovered at 18º57'40.16"S latitude and 57º46'14.59"W longitude, in water ~ 3.2 m deep (Fig. 2). To collect the core, an aluminum barrel was hammered into the lake floor, which met refusal after 102 cm. The top of the core (8-0 cmblf) consist of massive green very fine clay with iron oxide staining. Checking the sedimentary characteristics, absence of dating in this range and possible long hiatus, we assume this interval is modern and we prefer to exclude it from the analysis. The core was sealed in the field and transported to the Federal University of Mato Grosso do Sul, Pantanal Campus in Corumbá Brazil. This core, named LCC/16, was photographed and described following the methods outlined in Schnurrenberger et al. (2003). Six sediment subsamples from the core were sieved to separate <63 μm organic matter for radiocarbon (^{14}C) dating (Table 1). The acid-insoluble fraction was analyzed by accelerator mass spectrometry at Beta Analytical Inc. All radiocarbon dates were input into Bacon for R in order to generate an age-depth model (Blaauw and Christen 2011) (Fig. 3). The radiocarbon dates were calibrated using the SHCal13 curve (Hogg et al. 2013). The accumulation rate mean was set at 50 years/cm and an alternative maximum depth was set at 102 cm.

Discrete sediment sub-samples were collected every 2 cm (*n* = 47) along the length of the core in order to analyze TOC, sponge spicules, plant phytolith content. Each sediment sample was freeze-dried, ground, and analyzed for weight percent total carbon on a LECO

SC-144DR at the Kentucky Geological Survey. The LECO device determines total carbon content by combustion at 1350º C; each sample (~0.15-0.2 g) was mixed in a 1:1 ratio with the combustion catalyst standard (Com-Cat 502-321) and run for 60-70 s. Two synthetic carbon standards and a carbonaceous shale (SARM-41) were used to track analytical performance, and the precision was better than 1.0 %. Sample splits were also analyzed for total inorganic carbon (wt.% TIC) on a UIC CM5130 carbonate coulometer, and the precision for the analysis was ±0.2 %. The wt. % TOC value was calculated by subtracting TIC from total carbon.

Sedimentary TN, $\delta^{15}N_{org}$, and $\delta^{13}C_{org}$ was measured at the University of Kentucky using a Costech ECS 4010 interfaced with a ConFlo IV and Thermo Finnigan DELTAplus XP isotope ratio mass spectrometer. The precision of the %N, $\delta^{15}N_{org}$, and $\delta^{13}C_{org}$ data were 0.1 %, 0.2 ‰, and 0.3 ‰ or better, respectively. Following USGS recommendations (Coplen et al. 2006), raw carbon and nitrogen isotope values were normalized to the VPDB and AIR scales, respectively, using at least two internationally-certified reference materials with contrasting $\delta^{13}C$ and $\delta^{15}N$ values. C/N values were calculated from TOC derived from the LECO analysis and TN derived from elemental analysis; results are presented as atomic ratios. The results of TOC, TN, $\delta^{13}C$ from the other lakes were compiled from published literature using the program DigitizeIt (Bezerra and Mozetto 2008; McGlue et al. 2012; Bezerra et al. 2019; Rasbold et al. 2019). Elemental (C/N) and stable isotope ($\delta^{13}C_{org}$) geochemistry were used to identify the source of organic matter, which can be produced by lacustrine algae, C_3 land plants, and C_4 land plants (Meyers 1994).

Sponge spicules and phytoliths were extracted at the Paleoenvironmental Studies Laboratory (Lepafe) following a modified protocol of Volkmer-Ribeiro (1985). In brief, each sample (1 g) was oven-dried, crushed, and packed into a clean test tube, then acidified overnight with boiling HNO_3 (~5 ml) and washed with distilled water until a neutral pH was achieved. About 50 µL of acidified sample was dripped onto a clean microscope slide, dried on a hot plate, covered with Entellan® resin and a coverslip was used to fix the sample. Sponge spicule were counted microscopically and identified on three randomly selected transects on each slide, and three slides were prepared for each sample. Thus, nine transects per sample were assessed for the sponge spicule analysis, and an average of 720 spicules were counted per sample. Taxonomic identification was performed through systematic observations of the slides and distinguishing among the different sponge skeletal elements, including megascleres, gemmuloscleres, and microscleres (Rasbold et al. 2019). Identification of

different species followed the identification key of the Class Demospongiae Sollas, 1885, Order Spongillida Manconi and Pronzato, 2002 (Morrow and Cárdenas 2015). Sponge abundances were classified using the system described by Rasbold et al. (2019): 1-3 observations (very rare), 4-6 observations (rare), 7-10 observations (common), and >11 observations (abundant). Where sponge assemblages were characteristic of well-known aquatic sub-environments, we classified those intervals as spongiofacies as defined by Parolin et al. (2008). For internal consistency, a single analyst (GGR) completed the analysis. Plant phytoliths were counted microscopically and identified on three randomly selected transects on each slide, and three slides were prepared for each sample. Thus, nine transects per sample were assessed for the plant phytoliths analysis, and an average of 120 phytoliths were counted per sample. Morphological identification and quantification of plant phytoliths followed the International Code for Phytolith Nomenclature 1.0 (Madella et al. 2005). Photomicrographs of the sponge spicules (gemmuloscleres and microscleres), phytoliths, and of the other biological indicators were collected using an optical microscope (x640 magnification).

Sponge spicule assemblages and phytoliths were statistically sorted into units using a stratigraphically constrained cluster analysis in CONISS® in the Tilia® program (Grimm 1987). The units were separated according to a vertical cut in the dissimilarity dendrogram (~ 1 total sum of squares). The unconstrained cluster analysis was considered for merging stratigraphically adjacent clusters only. An analysis of depositional characteristics also complemented the division of units.

3.4 Results and interpretations

3.4.1 Modern characterization of Lake Cáceres

During the period of the survey (2016), Lake Cáceres had an open water area of ~31 km² and was characterized by an irregular shape. The lake had a maximum long axis length of ~7.7 km and a maximum width of ~5.2 km. The bathymetry is relatively simple, with a gentle lake floor slope and gradually increasing water depths towards the basin center that reach ~4.3 m when the Paraguay River is flooded in the austral summer (Fig. 2). The surface area of the lake has varied over the last 35 years, however that interval included several years that were relatively dry, and satellite images show that the surface area was a minimum of 14.71 km² in 2002, while a maximum of 102.20 km² occurred in 1984 (Fig. 3A and 3B).

Lake floor sedimentary TOC data show very high concentrations (maximum of ~27 wt. %) on the northwest and northeast side of the lake away from Tamengo channel and its

inputs. In most other areas of Lake Cáceres, TOC concentration is lower, with a mean of ~5.2 wt. % (Fig. 4). Geochemical analyses of OM from LCC indicate values of C/N and $\delta^{13}C_{org}$ that are typical lacustrine algae mixed with C_3 plant matter (Meyers 1994) (Fig. 4). Sedimentary OM in LCC exhibits C/N values that range from 10.9 to 21.9, and a mean $\delta^{13}C_{org}$ of -28.1‰.

The modern phytolith assemblage consists chiefly of Poaceae (short cells), Arecaceae (globular echinate), Dicotyledons (globular granulate), and Cyperaceae (papillae). The most abundant were short cell and bulliform grass phytoliths. The distribution of phytoliths was similar to the pattern of TOC concentration, with the densest concentrations on the northwest and northeast margin of the lake (Fig. 3). The highest concentration of sponge spicules is in the central and western side of Lake Cáceres, whereas intact megascleres were most abundant near the shorelines (Fig. 3). Gemmuloscleres were more abundant than microscleres, and thus it was possible to identify an assemblage of eight different species from three different families: Spongillidae Gray, 1867, Potamolepidae Brien, 1967, and Metaniidae Volkmer-Ribeiro, 1986. *Radiospongilla amazonensis* Volkmer-Ribeiro and Maciel 1983, is common in all of the lake floor sediments, although it is spatially concentrated on the west side of the lake and at sample sites close to connection points with the Tamengo channel. *R. amazonensis* is widely distributed in Brazil's lentic environments (Pinheiro, 2007), and it has been recorded on the roots of aquatic macrophytes, and on the branches or trunks of submerged trees (Volkmer-Ribeiro et al. 1999; Tavares et al. 2003; Oliveira et al. 2018). The sponge species *Tubella paulula* (Bowerbank, 1863), *Tubella variabilis* Bonetto & Ezcurra de Drago, 1973, *Corvospongilla seckti* Bonetto and Ezcurra de Drago, 1966, *Corvomeyenia* sp. Weltner, 1913, *Corvoheteromeyenia* sp. Ezcurra de Drago, 1979, *Metania spinata* (Carter, 1881), and *Oncosclera navicella* (Carter, 1881), occur in very rare frequency and low abundance in the lake.

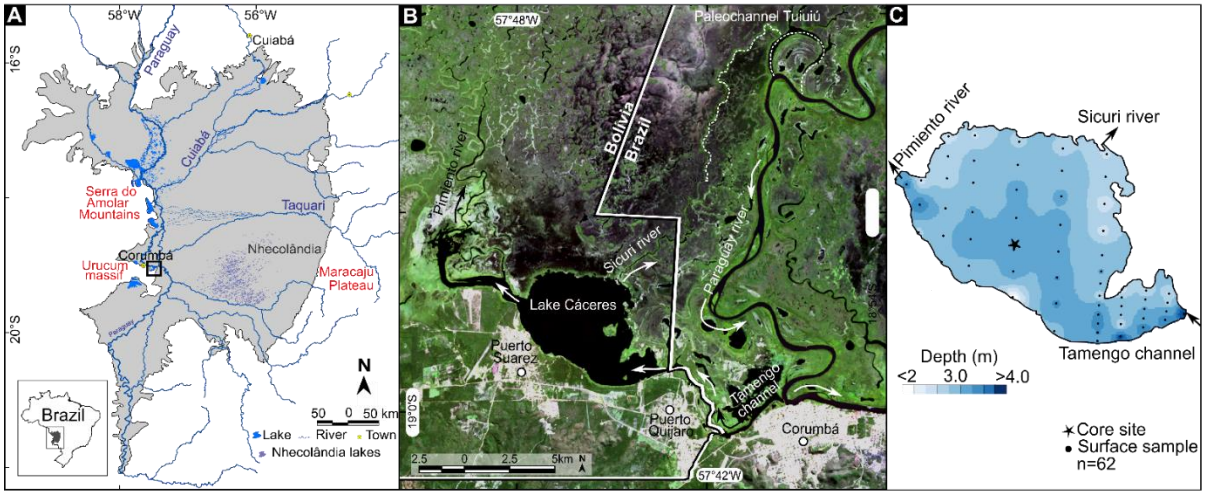

Figure 2. Study area location maps. A. Pantanal Basin (gray) in western tropical Brazil. B. Satellite image showing Lake Cáceres on the right side of the Paraguay River, near the cities of Corumbá (Brazil) and Porto Suarez (Bolivia). Landsat image, 2016/06/13, OLI-TIRS, orbit/point: 227/073. Landsat-8 image courtesy of the U.S. Geological Survey. C. Surface sediment sample grid for Lake Cáceres and bathymetry produced from the June 2016 survey. The location of sediment core LCC/16 is marked with star.

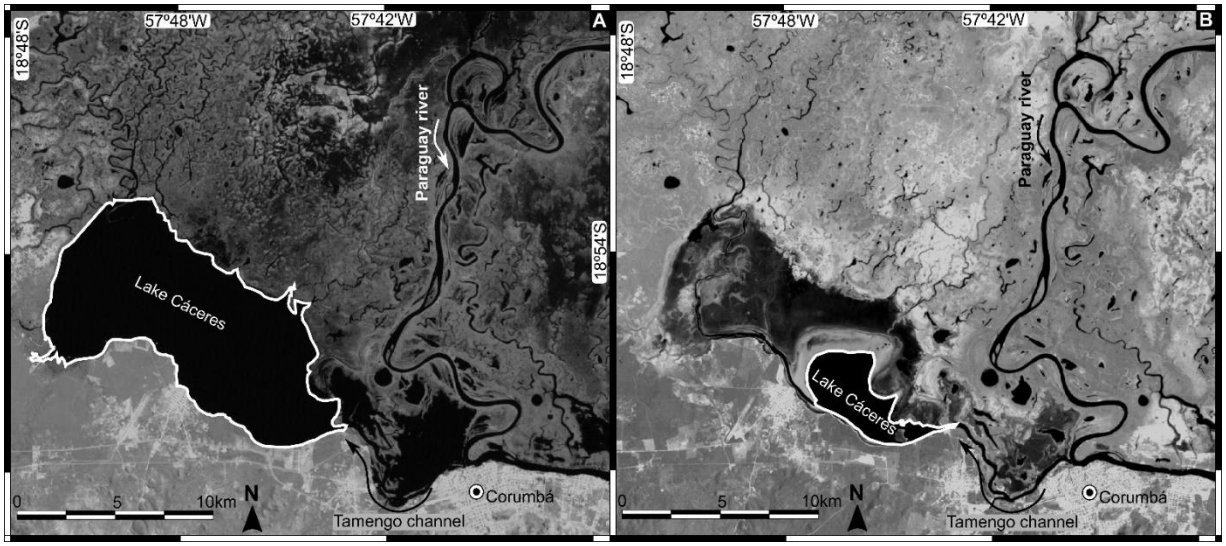

Figure 3. Satellite image showing surface area extremes from the past 35 years at Lake Cáceres. A. 102.20 km² (1984), Landsat 5 image, 1984/09/09, TM, orbit/point: 227/073. Landsat-5 image courtesy of the U.S. Geological Survey. B. 14.71 km² (2002), Landsat 5 image, 2002/03/01, TM, orbit/point: 227/073. Landsat-5 image courtesy of the U.S. Geological Survey.

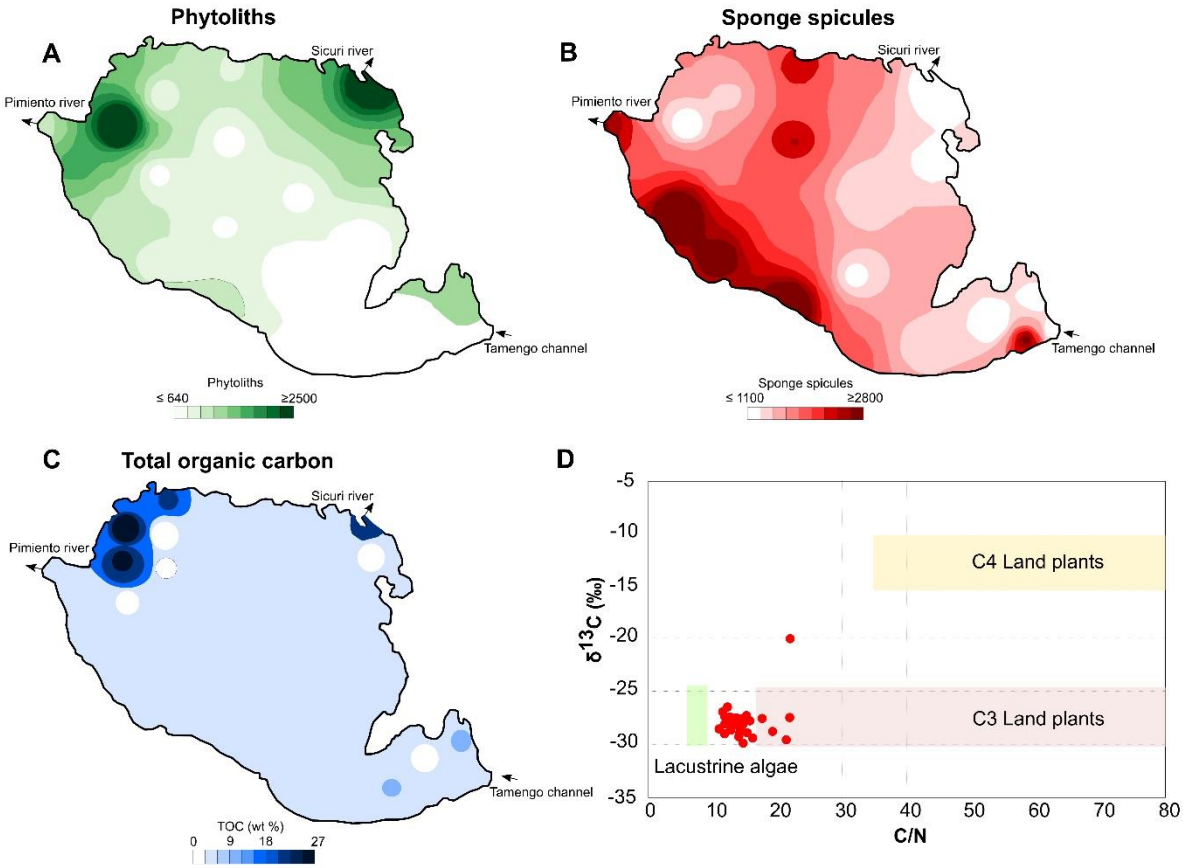

Figure 4. Bottom sediment concentration maps for Lake Cáceres (A-C). A. Phytoliths; B. Sponge spicules; C. Total organic carbon; D. Elemental (C/N) and isotopic ($\delta^{13}C$) crossplot, with fields for lacustrine algae, C_3 land plants, and C_4 land plants based on data from Meyers (1994).

3.4.2 Stratigraphy and geochronology of core LCC/16

Core LCC/16 chiefly consists of grey structureless silty clays and green-grey silty clays (Fig. 5), with a prominent black organic-rich sapropel unit between 25-8 cm below lake floor (cmblf). Most of the bedding contacts in the core are gradational.

Table 1. Radiocarbon dates used in the age-depth model from LCC/16 (Lake Cáceres).

Depth (cm)	Lab code	$\delta^{13}C$ (‰)	Age (^{14}C yr BP)	Error	2-σ range (cal yr BP)	Median Probability	Material
10	Beta-526327[a]	N/A	5760	40	6600-6440	6510	Plant and charcoal
20	Beta-479421[a]	-18.6	5690	30	6500-6320	6430	Organic sediment
27	Beta-519003[b]	-20.7	7060	40	7950-7740	7860	Plant
37	Beta-522796 [a]	-27.9	7920	30	8580-8970	8670	Plant
76	Beta-479422[a]	-23.0	9580	30	11080-10700	10900	Organic Sediment
102	Beta-479423[a]	-21.7	8870	30	10150-9700	9880	Organic Sediment

[a] Accelerator mass spectrometry (AMS);
[b] Micro-sample accelerator mass spectrometry analysis (MSAMS). See text for details.

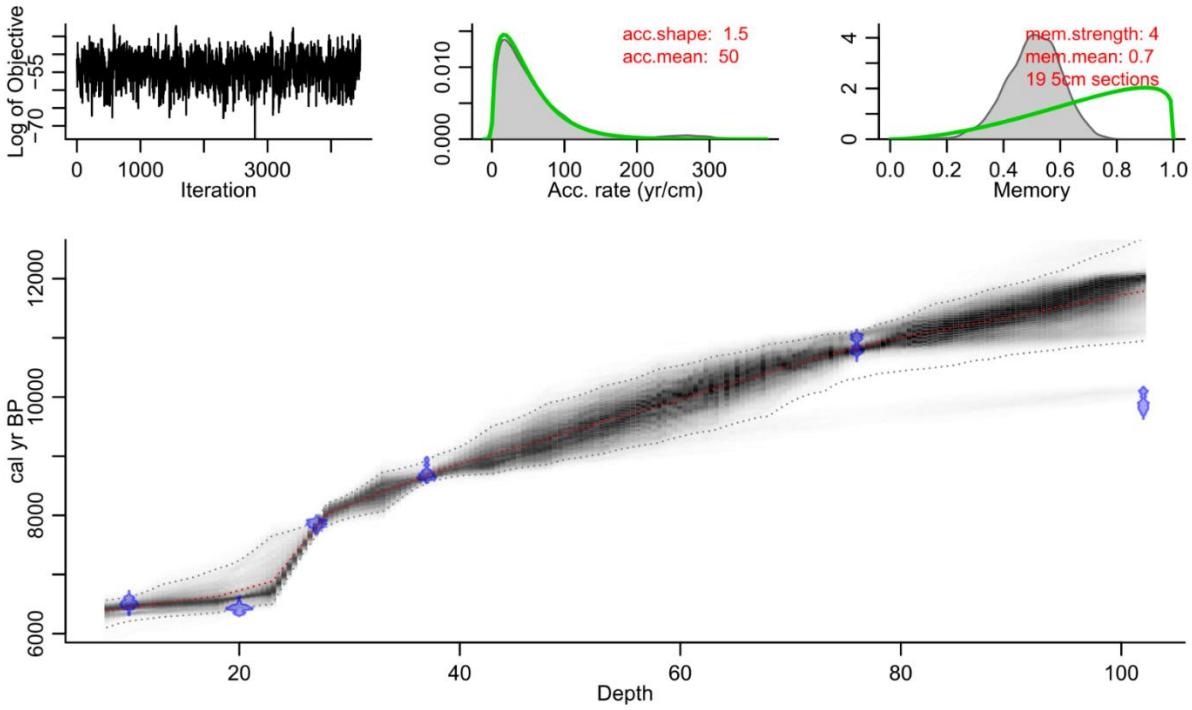

Figure 5. Bacon-derived age model for LCC/16 from Lake Cáceres. The age-depth model was calibrated using ^{14}C dates (Table 1), Bacon (Blaauw and Christen 2011), SHCal13 calibration curve (Hogg et al. 2013). Blue markers denote ^{14}C dates horizons (For interpretation of the references to color in this figure legend, the reader is referred to the web version of this article). One dated horizon was excluded by Bacon.

3.4.3 Unit I (12,000-10,000 cal yr BP)

Unit I consists of structureless mottled green clayey silt interbedded with structureless grey silty clay. The TOC concentrations were below the detection limit near the base of the unit (~12,000 cal yr BP at 102 cm blf) and increase to ~0.33 wt.% near the top. The sponge spicules were dominantly fragmented megascleres that were small (<50 µm) to

medium (50-100 µm) in size (Fig. 6). It was possible to identify *Radiospongilla amazonensis* Volkmer & Maciel, 1983 in the very rare gemmuloscleres present in the sediments. Phytoliths were present in low concentrations (average of ~ 80 phytoliths), and were dominated by cuneiform and parallepipedal bulliforms and elongate psilate forms (Fig. 6).

We interpret Unit I as a period characterized by an ephemeral wetland environment that received flood waters from the Paraguay River. The mottled, structureless sediment indicate a fluctuating water column and periodic changes in redox state that provided conditions necessary for bioturbation. Small and medium-sized sponge spicule fragments and the alternation of muds with high (~ 1000) and low concentrations (~ 70) of spicules (Fig. 6) suggest that the core site was influenced by riverine floods (Wilding and Dress 1968; Sifeddine et al. 2001; Kuerten et al., 2013). The preservation of only bulliforms and elongate psilate phytoliths indicates that grasses dominated the vegetation near the core site, and that these plants probability most likely experienced high evapotranspiration and hydric stresses (Parry and Smithson 1958; Sangster and Parry 1969; Bremond et al., 2005).

3.4.4 Unit II (10,000-9000 cal yr BP)

Unit II consists of structureless grey silty clay with relatively low TOC. The TOC concentrations were 0.33 wt.% at the base of the unit, and only slightly higher (~0.78 wt.%) in sediments near the unit top 9,000 cal yr BP. Sponge spicules exceeded 600 fossils and they were dominantly megascleres. However, a marked increase in gemmuloscleres was observed in this unit. Sponge spicules from *Oncosclera navicella* (Carter 1881) were common to abundant, whereas spicules from *R. amazonensis* were present but in rare to very rare amounts (Fig. 7). Phytoliths were present in low concentrations, and were dominated by bullifoms (cuneiform and parallepipedal) and elongate psilate morphologies.

We interpret that Unit II was deposited in an ephemeral shallow lake setting that was influenced by the Paraguay River, in evidence from the abundant gemmuloscleres of *O. navicella*, which commonly inhabits rocky river beds (Tavares-Frigo et al. 2015). The species has been found in several large South American rivers, including the Orinoco River (Volkmer-Ribeiro and Pauls 2000), Paraná River (Bonetto and Ezcurra de Drago 1967; 1970), Uruguay River (Bonetto and Ezcurra de Drago 1967; Ezcurra de Drago and Bonetto, 1969), and Araguaia River (Batista et al. 2003). In the southern Pantanal, *O. navicella* spicules were found in Holocene sediments from the Nabileque megafan, indicating inundation from riverine pulses (Kuerten et al. 2013). The preservation of phytoliths indicates grasses similar

to Unit I, suggesting that the lake margin vegetation did not change substantially between the units.

3.4.5 Unit III (9000-7560 cal yr BP)

Unit III consists of structureless, dark to very dark grey, silty clays. The TOC concentrations increase from the bottom to the top of the unit, reaching a maximum of ~4.1 wt.%. Unit III contained abundant and common whole gemmuloscleres and microscleres of *Corvoheteromeyenia heterosclera* (Ezcurra de Drago, 1974), *R. amazonensis*, and *O. navicella*, and very rare *Heteromeyenia barlettai* Pinheiro, Calheira & Hajdu, 2015, *Tubella variabilis* Bonetto & Ezcurra de Drago, 1973, *Tubella paulula* (Bowerbank, 1863), and *Tubella delicata* Bonetto & Ezcurra de Drago, 1967. (Fig. 7) Unit III is marked by an increase in phytoliths (>200), with higher concentrations of the robust forms (bulliforms and elongate psilate), and also increases in short cells, globular echinate, globular granulate, and papillae forms. Two phytoliths that correspond to the family Podostemaceae were encountered at 8450 cal yr BP in Unit III.

We interpret Unit III as evidence for a started perennial phase in Lake Cáceres's history. The increasing richness of lentic sponge species as well as higher concentrations of gemmuloscleres are consistent with a lacustrine environment (Volkmer-Ribeiro 1999; Volkmer-Ribeiro and Parolin 2010). The presence of abundant gemmuloscleres of *O. navicella* again indicates river influx, similar to the Unit II. Phytoliths should reflect changes in vegetation around the lake, and can be transported offshore by surface runoff or inflowing rivers (Piperno 2006). The presence of Podostomaceae phytoliths is another indicator of river inflow, because this family is composed of species adapted to lotic environments with swiftly moving water; most often, these plants adhere to rocks in tropical rivers (Philbrick et al 2010). Rasbold et al. (2020) suggesting the presence of this morphotype as evidence for allochthonous transport during the formation of channel islands in the Upper Paraná River. The increase of the short cells, globular echinate, globular granulate, and papillae forms indicate an increase in the diversity of vegetation growing on the margin of the lake, which were likely composed of Poaceae, Arecaceae, Bromeliaceae, Cyperaceae, and dicotyledons.

3.4.6 Unit IV (7560-6500 cal yr BP)

Unit IV consists of massive black sapropel. The TOC concentrations increase to peak values in the core, reaching 14.1 wt.% at ~6740 cal yr BP before decreasing to ~9.1 wt.% at the top of the unit. Preservation of sponge spicules is excellent in Unit IV, in evidence by abundant whole microscleres of *C. heterosclera* and *H. barlettai*. Spicules of *T. variabilis, R. amazonenses,* and *O. navicella* were also present, but in rare to very rare abundances. Unit IV is interpreted as a spongiofacies due to the abundance of spicules. Unit IV showed a decrease in the concentration of phytoliths relative to the underlying units.

We interpret Unit IV to reflect a stable shallow lake, with minimal riverine influence and high paleoproduction. The remarkable abundance of whole *C. heterosclera* and *H. barlettai* microscleres strongly argue in favor of a stable shallow lentic environment, as these structures are very fragile and their taphonomy indicates that the deposition was *in situ*. We interpret that extensive colonization of shallow areas by floating macrophyte mats acted as a wind barrier to reduce sediment remobilization, which aided in both the preservation of fragile microscleres and an increase in organic carbon content in the sediment. We interpret a hydrologically closed lake at this time, with minimal connectivity between the basin and adjacent rivers. In this interpretation, exportation of organic matter ceased, due to the absence of large flood pulses (Junk et al. 1989; Tockner et al. 1999).

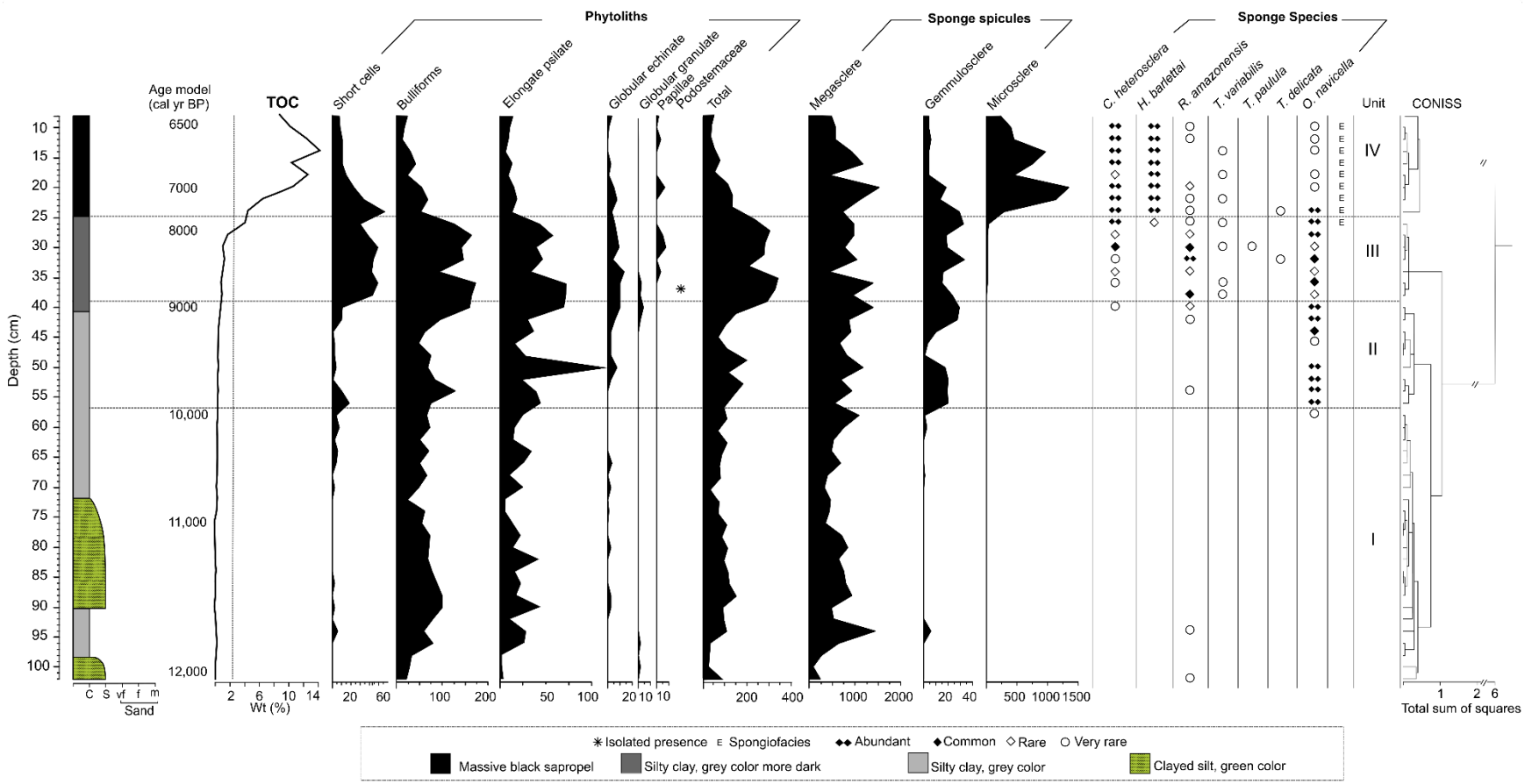

Figure 6. Sedimentary profile, age model, total organic carbon (TOC), phytoliths, sponge spicules, sponge species, and units for the core LCC/16 determined using a stratigraphically constrained cluster analysis in CONISS. Sponge species: very rare (white circles), rare (white diamonds), common occurrence (black diamonds), abundant occurrence (two black diamonds), Sponge-rich facies (E).

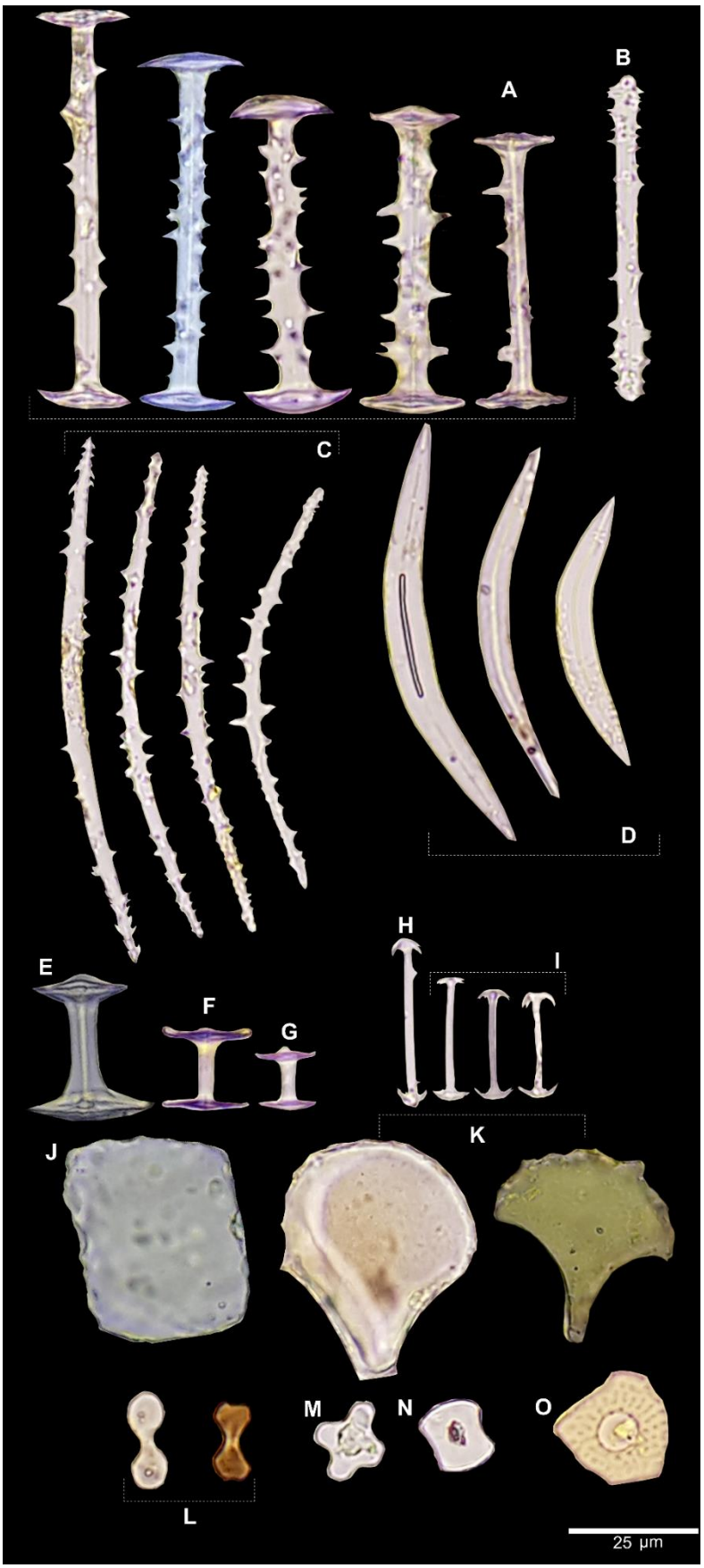

Figure 7. Scanning electron micrographs of freshwater sponge spicules (A–I) and phytoliths (J-O) from late Holocene sediments of Lake Cáceres. A. Gemmuloscleres birotule with a long spiny shaft. B. Gemmulosclere spiny strongyles of *Radiospongilla amazonensis*. C. Acanthoxea microsclere. D. Gemmulosclere oxea. E. Gemmulosclere birotule with a long spiny shaft of *Tubella paulula* F. Gemmulosclere birotule of *Tubella delicata.* G. Gemmulosclere birotule of *Tubella variabilis.* H. Pseudobirotule microsclere with pseudobirotules of long hooks. I. Pseudobirotule microsclere with pseudobirotules of short hooks. J. Parallepipedal bulliform. K. Cuneiform bulliform. L. Bilobate. M. Cross. N. Saddle. O. Pappilae. Scale bar = 25 µm.

3.5 Discussion

Our study seeks to understand the paleoenvironmental conditions of the central Pantanal and its lakes in the middle Holocene, with a special emphasis on the interactions among climate, vegetation, geomorphology, and hydrology that may have enabled higher carbon burial. Notably, four large Paraguay River-connected lakes show clear evidence for elevated TOC between 7.3 and 6.0 cal kyr BP. The maximum TOC values registered in this period were: ~15 wt. % at Lake Cáceres (this study), ~12 wt. % at Lake Castelo (Bezerra and Mozetto 2008), ~5 wt. % Lake Gaíva (McGlue et al. 2012), and ~7 wt. % at Lake Negra (Rasbold et al. 2019) (Figure 8). In general, during the terminal Pleistocene and the early Holocene, TOC concentrations are considerably lower in all of these lakes (mean of ~2 wt. %) (Figure 8).

Well-dated speleothem $\delta^{18}O$ records, interpreted to reflect the relative amount of precipitation, suggest that mid-western Brazil was relatively dry from ~11-5.5 kyr BP, in comparison to a wetter interval around the last glacial period (27.9-17.8 kyr BP) (Strikis et al. 2011; Novello et al. 2017; Novello et al. 2019). Those data suggest that the regional pattern of enhanced lacustrine carbon accumulation occurred during a low water period in the Pantanal. Some paleolimnological records from Pantanal arrived at a similar interpretation, for example in the work of Metcalfe et al. (2014). Those authors interpreted elevated Ca:Ti between 9-4 cal kyr BP to be consistent a lower water level in Lake Gaíva and a relatively dry climate. By contrast, Bezerra and Mozetto (2008) attributed the high TOC they measured in Lake Negra sediments to be associated with a Climatic Optimum at 6.5 cal kyr BP and a slightly wetter middle Holocene. McGlue et al. (2012) interpret the high TOC and lentic sponge spicules encountered between 8.9-5.3 cal kyr BP as a lowstand lake impacted by weak flood flows of Paraguay River, with water levels initially low, followed by lake expansion under the influence of increasingly strong floods by ~6.2 cal kyr BP.

The $\delta^{13}C$ and the C/N of organic matter between 8.5-5.5 cal kyr BP generally remained between -27.2‰ to -17.8 ‰ and 15 to 20 for Lakes Cáceres, Gaíva, Negra, and Castelo (Figure 8). This relationship indicates to us that part of the source of organic matter was aquatic macrophytes, since the values suggest contributions from C_3 land plants despite potential losses to oxidation. The C/N of particulate organic matter produced from aquatic macrophytes is lower than fresh material because carbon is lost by mineralization, however, N concentrations remain approximately the same (Fellerhoff et al. 2003). In terms of

preservation, organic matter is often more highly degraded in oxic and subaerially exposed environments versus anoxic subaqueous environments, but the research of Einsele et al. (2001) demonstrated that tropical and subtropical floodplain lakes have high preservation potential of OM even under oxic conditions. This is because the remineralization of organic matter is reduced in lakes with shallow bathymetry.

The sponge species *C. heterosclera*, *R. amazonensis*, *H. barlettai*, *T. paulula*, *T. variabilis*, and *C. australis* are most common between 7.3-6 cal kyr BP for the four lakes and these species typically reflect lentic environments (Bonetto and Ezcurra de Drago 1966; Bonetto and Ezcurra de Drago, 1973; Volkmer-Ribeiro 1999; Volkmer-Ribeiro et al. 1999) (Figure 9). Lakes Cáceres, Negra (Rasbold et al., 2019), and Gaíva (McGlue et al. 2012) had the same sponge fauna during this period, which suggests that the lakes may have had similar ecosystem characteristics. Species adapted to lotic environments, such as *C. seckti* and *O. navicella* (Bonetto and Ezcurra de Drago 1966; Volkmer-Ribeiro et al. 1975; Volkmer-Ribeiro and Hatanaka 1991; Ezcurra de Drago 1993; Batista and Volkmer-Ribeiro 2002; Pinheiro et al., 2003; Pinheiro, 2007), are generally observed earlier than 7.3 cal kyr BP, where possibly larger flood pulses occurred that allowed exchange between the lakes and the Paraguay River. The degree of fragmentation of sponge spicules can be an indicator of environmental energy and the presence of flowing water (Wilding and Drees 1968). The preservation of microscleres observed in Unit IV sediments indicates a tranquil aqueous environment, because those delicate structures often have a radial axis of ~ 10 µm, and they are easily broken when carried by intense flows. The abundance of microscleres are also interpreted to be a reflection of a larger population of sponges living in a habitat with dense macrophytes cover, which served as a fixation substrate (Volkmer-Ribeiro et al. 1975; Volkmer-Ribeiro and De Rosa-Barbosa 1985; Tavares et al. 2003).

Given the geochemistry and paleoecology of central Pantanal's lake sediments in the period between 7.3-6.0 cal kyr BP, we interpret that enhanced organic carbon accumulation occurred as the lakes contracted and became hydrologically closed. The decrease in open water (pelagic) area came as water levels declined and shallow waterlogged sediments were colonized by highly productive macrophytes, which included the formation of extensive green floating mats. Shallow lakes in the Pantanal are characterized by low bottom gradients, which during regressions generate large and relatively flat surfaces that can support highly productive macrophytes, whose population growth exceeds phytoplankton (Wetzel 1992). The data support longer dry seasons and less extreme or absent austral summer floods, and it is

plausible that connections to the Paraguay River were lost during this interval. The drying of tie channels between the lakes and the Paraguay River is significant, because it led to hydrological closure. Organic detritus and algal biomass can be exported from the floodplain and lakes to the river via the flood pulse (Tockner et al. 1999; Junk et al. 1989). This closure meant that floating macrophyte islands could not move out to the Paraguay River seasonally, effectively creating a local sink for macrophytes and associated algae following their life cycle. Therefore, we interpret that enhanced carbon accumulation is linked to the persistence of shallow lake levels and the drying of tie channels. If climatic conditions oscillate widely, it is likely that the macrophyte source is likely to be partially exported from the lake basin as water levels rise and seasonal outflows develop, thereby retaining less organic carbon in lake sediments. With less seasonality in a dry climate setting, the flood pulse influence and water level changes are muted. The persistent of a shallow water body in this setting favors carbon accumulation. In addition, the high productivity of macrophytes helps to consume oxygen during the decomposition process, which would help to promote the preservation of organic matrices in shallow waterlogged sediments (Sobeck et al., 2009).

Our interpretation regarding the Middle Holocene is also informed by sedimentation in extant Lake Cáceres, where the climatic conditions are directly observable. The TOC data from surface sediment samples show clearly that organic matter deposition is focused on the margins, not in the basin center (Fig. 10), which is best explained by the high density of aquatic macrophytes defining shallow water-shoreline wetlands (Wetzel, 1992). The expansion of the aquatic macrophytes colonies in seasonally and permanently flooded areas contribute to the formation of extensive green floating mats rich in organic matter derived from their decomposition (Coutinho et al. 2018; Lo et al. 2019). During the wet season, Lake Cáceres can have an open water area of up to ~102 km², however, this area retracts considerably (to ~14.71 km^2) in the dry season. This reduction suggests that 85% of Lake Cáceres can transition to an area of potential shallow coastal wetland (Fig. 10). Hydrodynamic conditions along the lake margins in the dry season are quiet, and the lack of strong waves or inflowing rivers is propitious for macrophyte colonization (Mourmul et al. 2013). Today, the shoreline wetlands register an average sedimentary TOC of ~7.1 wt %, and some points on the northwest margin can reach ~27.5 wt. %. In sharp contrast, the open water environments of deposition exhibit TOC with an average of ~3.1 wt %. We note that in the modern system, the C/N and $\delta^{13}C_{org}$ are similar for open water areas (average C/N and $\delta^{13}C_{org}$ of 13.4 and 28.3 wt.%, respectively) and coastal areas (average C/N and $\delta^{13}C_{org}$ of 14.0 and

28.0 wt.%, respectively). These C/N and $\delta^{13}C_{org}$ values are consistent with those observed for particulate organic matter (POM) originating from the most abundant aquatic macrophytes in the Pantanal (Fellerhoff et al. 2003), such as *Pontederia lanceolata*, *Salvinia auriculata*, *Eichhornia crassipes*, *Nymphaea amazonum*.

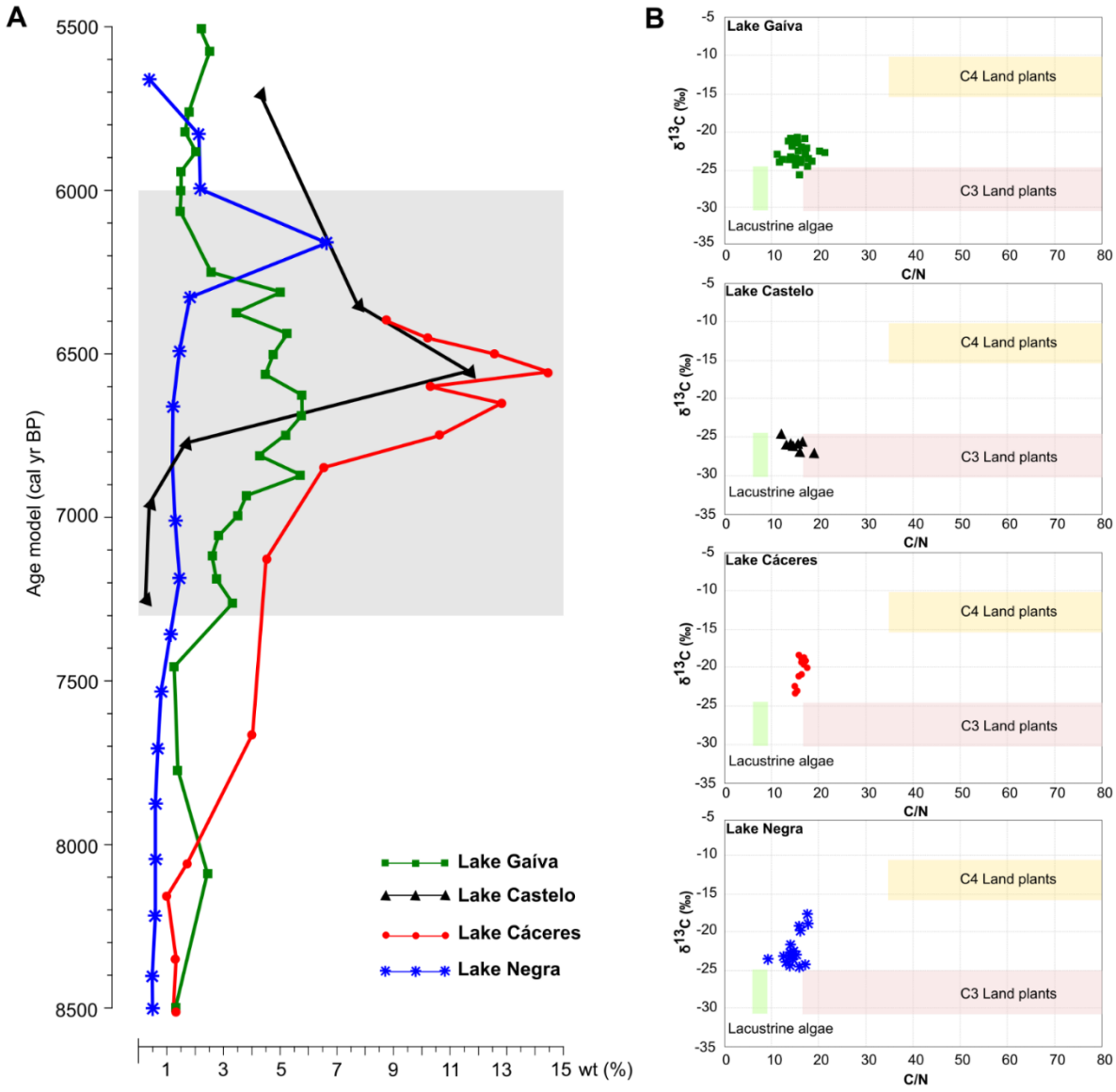

Figure 8. **A.** Total organic carbon (TOC) chemostratigraphies for Lake Negra (Rasbold et al. 2019), Lake Gaíva (McGlue et al. 2012), Lake Castelo (Bezerra and Mozetto 2008), and Lake Caceras (this study); **B.** Elemental (C/N) and isotopic ($\delta^{13}C$) crossplot for each lake, with fields for lacustrine algae, C_3 land plants, and C_4 land plants based on data from Meyers (1994).

The data suggest that the middle Holocene interval (7.3-6.0 kyr BP) of enhanced organic matter burial occurred as the pelagic area of the floodplain lakes contracted, allowing macrophytes to colonize waterlogged sediments within expanding marginal wetlands. Extreme drying was not likely during this phase. Stalagmite records indicate severe reductions in water availability between 3.8-2.1 kyr (Bertaux et al. 2002; Novello et al. 2016; Novello et al. 2019). Prolonged aridity of this kind appears to result in subaerial exposure and the development of hiatuses in even the largest floodplain lakes in the Pantanal, as has been reported for lakes Gaíva, Mandioré, and Negra (McGlue et al. 2012; Rasbold et al. 2019).

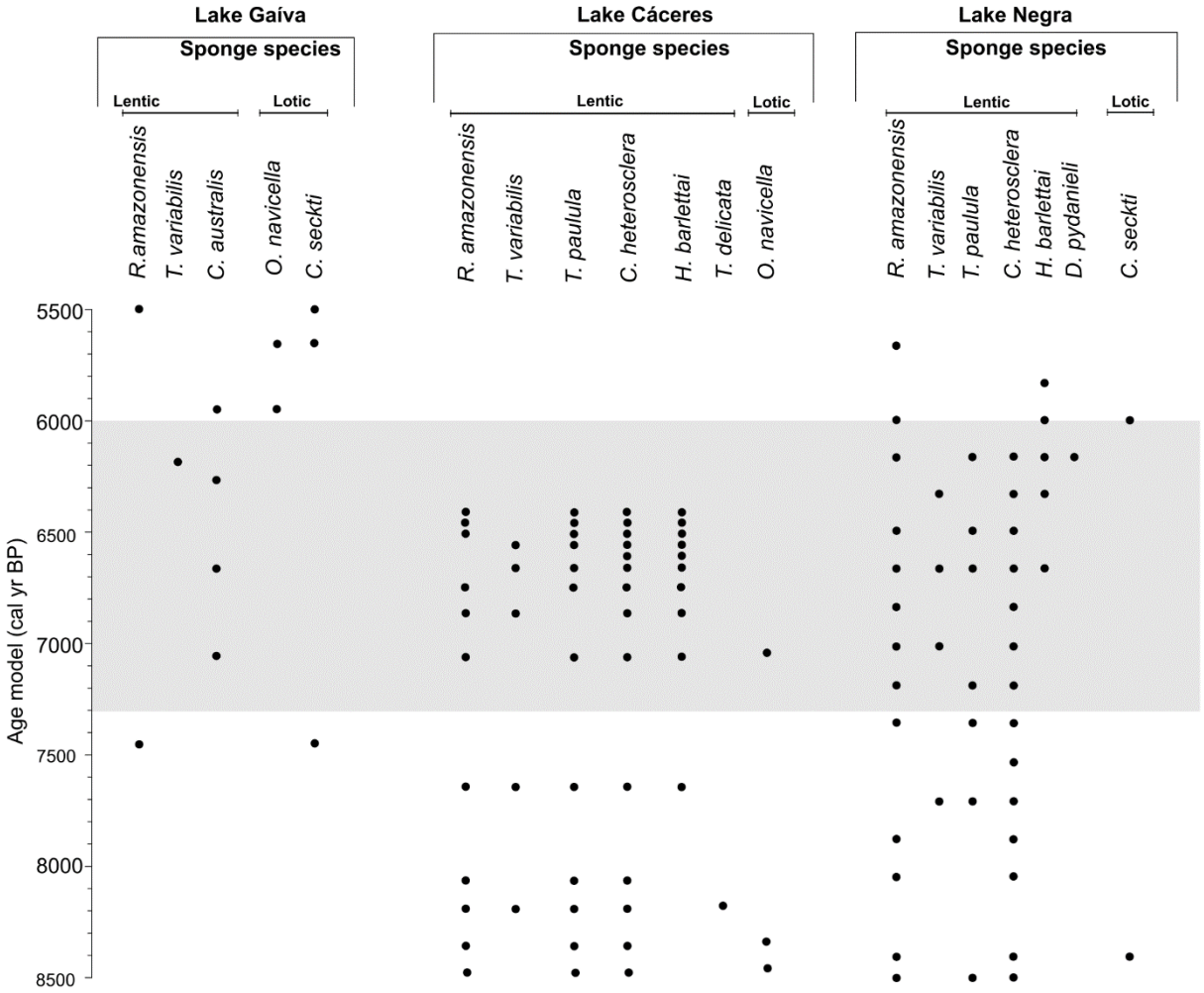

Figure 9. Age model and presence of freshwater sponge species for Lake Negra (Rasbold et al. 2019), Lake Gaíva (McGlue et al. 2012), and Lake Cáceres.

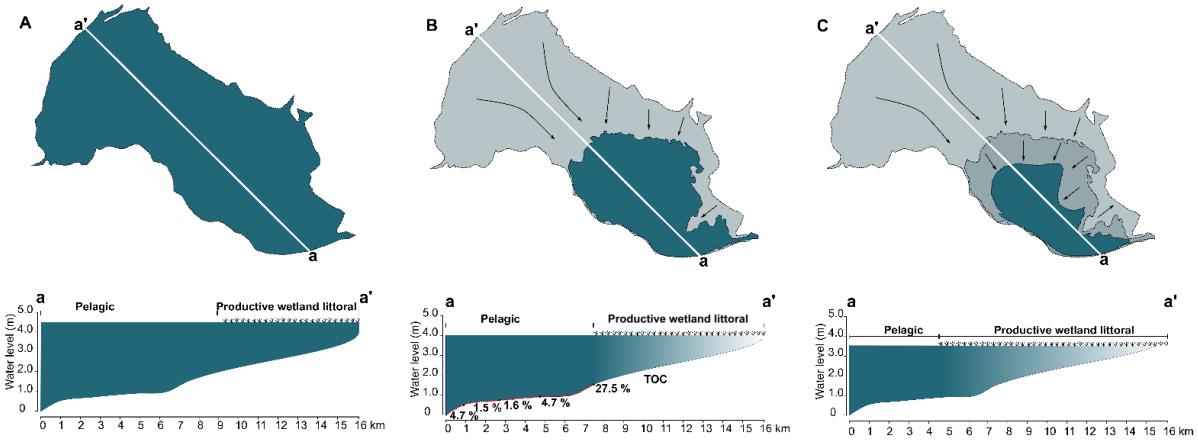

Figure 10. Expansion and retraction of pelagic and productive wetland littoral areas and the relationship with the OM production at the Lake Cáceres, Pantanal.

3.6 Conclusions

1. We analyzed modern Lake Cáceres (Bolivian Pantanal) surface sediments for TOC, C/N, $\delta^{13}C_{org}$, sponge spicules, and phytoliths, and studied satellite images of the lake that span the last 35 years. The images shows considerable changes in open water area through time that can be linked to seasonal changes in precipitation and flooding of the adjacent Paraguay River. The sediments illustrate spatial patterns in carbon accumulation, which increase towards the northern basin margin, where productive shoreline macrophytes are abundant. Even during seasonal dry periods, the low gradient margins appear to remain waterlogged and carpeted by macrophytes.

2. We recovered a short sediment core from Lake Cáceres that records 12-6.5 cal kyr BP. The core was analyzed similarly to the surface sediment samples, and was compared to both upstream and downstream floodplain lakes likewise connected to the Paraguay River. The primary objective was to more accurately resolve the environmental conditions that led to enhanced middle Holocene lacustrine carbon burial on the western border of the Pantanal wetlands.

3. Geochemical evidence from Lake Cáceres indicates that organic carbon burial reached a maximum between 7.3-6 cal kyr BP, similar to other lakes in the region. Sponge assemblages, phytoliths, and geochemistry suggest that enhanced carbon burial resulted under relatively dry conditions and diminished seasonal flooding that led to hydrological closure. These climatic conditions drove the lakes to become shallower and productive wetlands in the

littoral area expanded. Floating macrophyte mats colonizing these areas were locked in placed, and export of floating organic islands to Paraguay River ceased.

REFERENCES

Assine ML, Merino ER, Pupim FN, Warren LV, Guerreiro RL, McGlue MM (2015) Geology and Geomorphology of the Pantanal Basin. In: Bergier I, Assine ML (eds) Dynamics of the Pantanal Wetland in South America, The Handbook of Environmental Chemistry, Springer, Cham, pp. 23-50. https://doi.org/10.1007/698_2015_349

Batista TCA, Volkmer-Ribeiro C, Darwich A, Alves LF. 2003. Freshwater sponges as indicators of floodplain lake environments and of river rocky bottoms in Central Amazonia. Amazoniana XVII(3/4): 525-549

Batista TCA, Volkmer-Ribeiro C (2002) Comunidades de esponjas do curso superior dos rios Paraná (Goiás) e Paraguai (Mato Grosso), Brasil, com redescrição de Oncosclera schubarti (Bonetto & Ezcurra de Drago). Rev Bras Zool 19: 123–136. https://doi.org/10.1590/S0101-81752002000100010

Bergier I, Silva APS, Monteiro H, Guérin F, Macedo HA, Silva A, Krusche A, Sawakuchi HO, Bastviken D. Assine ML, Merino ER, Pupim FN, Warren LV, Guerreiro RL, McGlue MM (2015) Methane and Carbon Dioxide Dynamics in the Paraguay River Floodplain (Pantanal) in Episodic Anoxia Events. In: Bergier I, Assine ML (eds) Dynamics of the Pantanal Wetland in South America, The Handbook of Environmental Chemistry, Springer, Cham, pp. 163-178. https://doi.org/10.1007/698_2015_353

Bertaux J, Sondag F, Santos R, Soubies F, Casse C, Plagnes V, Le Cornec F, Seidel F (2002) Palaeoclimatic record of speleothems in a tropical region: study of laminated sequences from a Holocene stalagmite in central-west Brazil. Quaternary International 89: 3–16. https://doi.org/10.1016/S1040-6182(01)00077-5

Bezerra MAO, Mozeto AA (2008) Deposição de carbono orgânico na planície de inundação do Rio Paraguai durante o Holoceno médio. Oecologia Brasiliensis 12(1): 155-171

Bezerra MAO, Mozeto AA, Oliveira PE, Volkmer-Ribeiro C, Rodrigues VV, Aravena R (2019) Late Pleistocene/Holocene environmental history of the Southern Brazilian Pantanal wetlands. Oecologia Australis 23(4): 712-729. https://doi.org/ 10.4257/oeco.2019.2304.02

Blaauw M, Christen JA (2011) Flexible Paleoclimate Age-Depth Models Using an Autoregressive Gamma Process. Bayesian Analysis 6(3): 457-474. https://doi.org/10.1214/11-BA618

Bonetto AA, Ezcurra de Drago ID (1966) Nuevos aportes al conocimiento de las esponjas argentinas. Physis 26: 129–140

Bonetto AA, Ezcurra de Drago I (1967) Esponjas del noreste Argentino. Acta Zool Lilloana 23: 331-348

Bonetto AA, Ezcurra de Drago I (1970) Esponjas de los afluentes del Alto Parana em la província de Misiones. Acta Zool Lilloana 28: 37-68

Bonetto AA, Ezcurra de Drago I. 1973. Las esponjas del gênero Trochospongilla Vejdovsky en aguas argentinas. Physis 32: 13–18

Brasil. Ministério de Minas e Energia. Secretaria-Geral. Projeto RADAMBRASIL. Folha SE.21 Corumbá e parte da Folha SE.20; geologia, geomorfologia, pedologia, vegetação e uso potencial da terra. Rio de Janeiro, 1982. 452 p.

Bremond L, Alexandre A, Peyron O, Guiot J (2005) Grass water stress estimated from phytoliths in West Africa. J Biogeogr 32: 311–327. https://doi.org/10.1111/j.1365-2699.2004.01162.x

Carey CC, Doubek JP, McClure RP, Hanson P (2018) Oxygen dynamics control the burial of organic carbon in a eutrophic reservoir. Limnology and Oceanography Letters 3: 293-301. https://doi.org/10.1002/lol2.10057

Cohen AS, Gergurich EL, Kraemer BM, McGlue MM, McIntyre PB, Russell JM, Simmons JD, Swarzenski PW (2016) Climate warming reduces fish production and benthic habitat in Lake Tanganyika, one of the most biodiverse freshwater ecosystems. Proc Natl Acad Sci U S A 113(34): 9563-9568. https://doi.org/10.1073/pnas.1603237113

Cohen A, McGlue MM, Ellis GS, Zani H, Swarzenski PW, Assine ML, Silva A (2015) Lake formation, characteristics, and evolution in retroarc deposystems: A synthesis of the modern Andean orogen and its associated basins. Geodynamics of a Cordilleran Orogenic System: The Central Andes of Argentina and Northern Chile. Geological Society of America Memoir 212, pp.309-335

Cole JJ, Prairie YT, Caraco NF, McDowell WH, Tranvik LJ, Striegl RG, Duarte CM, Kortelainen P, Downing JA, Middelburg JJ, Melack J (2007) Plumbing the Global Carbon Cycle: Integrating Inland Waters into the Terrestrial Carbon Budget. Ecosystems 10: 171-184. https://doi.org/10.1007/s10021-006-9013-8

Coutinho BA, Pott VJ, Arrua BA, Aoki C, Pott A (2018) Ecological succession of aquatic macrophytes on floating meadows in the Pantanal wetland. Brazilian Journal of Botany 41(1): 65–75. https://doi.org/10.1007/s40415-017-0425-9

Coplen TB, Brand WA, Gehre M, Groning M, Meijer HAJ, Toman B, Verkouteren RM (2006) New Guidelines for $\delta^{13}C$ Measurements. Anal Chem 78: 2439-2441. https://doi.org/10.1021/ac052027c

Dalmagro HJ, Lathuillière MJ, Hawtrhorne I, Morais DD, Pinto Jr OB, Couto EG, Johnson MS (2018) Carbon biogeochemistry of a flooded Pantanal forest over three annual flood cycles. Biogeochemistry 139: 1–18. https://doi.org/10.1007/s10533-018-0450-1

Einsele G, Yan J, Hinderer M (2001) Atmospheric carbon burial in modern lake basins and its significance for the global carbon budget. Global and Planetary Change 30: 167–195. https://doi.org/10.1016/S0921-8181(01)00105-9

Ezcurra de Drago I, Bonetto AA (1969) Algunas características del bentos em los saltos del Rio Uruguay, com especial referencia a la ecologia de los poríferos. Physis XXVIII(7): 359-369

Ezcurra De Drago, I (1993) Distribución geográfica de las esponjas argentinas (Porifera: Spongillidae, Potamolepidae y Metaniidae). Relaciones zoogeográficas, vías de poblamiento. In: Boltovkoy A, López YH (eds.), Conferencias de Limnología. Instituto de Limnología "Dr. Raúl A. Ringuelet", La Plata, Buenos Aires, pp. 115–125.

Fellerhoff C, Voss M, Wantzen KM (2003) Stable carbon and nitrogen isotope signatures of decomposing tropical macrophytes. Aquat Ecol 37: 361–375. https://doi.org/10.1023/B:AECO.0000007049.25535.12

Frey R (1995) Flora and vegetation of "Las Piedritas" and the margin of Laguna Caceres, Puerto Suarez, Bolivian Pantanal. Bulletin of the Torrey Botanical Club, 122(4): 314-319. https://doi.org/10.2307/2996324

Garreaud RD, Vuille M, Compagnucci R, Marengo J (2009) Present-day South American climate. Palaeogeogr Palaeoclimatol Palaeoecol, 281: 180-195, https://doi.org/10.1016/j.palaeo.2007.10.032

Grimm EC (1987) CONISS: A Fortran 77 Program for Stratigraphically Constrained Cluster Analysis by the Method of Incremental Sum of Squares. Computers and Geosciences 13(1): 13-35. https://doi.org/10.1016/0098-3004(87)90022-7

Hogg AG, Hua Q, Blackwell PG, Niu M, Buck CE, Guilderson TP, Heaton TJ, Palmer JG, Reimer PJ, Reimer RW, Turney CSM, Zimmerman SRH (2013) SHCal13 Southern Hemisphere calibration, 0–50,000 Years cal BP. Radiocarbon 55(4): 1889–1903. https://doi.org/10.2458/azu_js_rc.55.16783

Ivory SJ, McGlue MM, Spera S, Silva A, Bergier I (2019) Vegetation, rainfall, and pulsing hydrology in the Pantanal, the world's largest tropical wetland. Environmental Research Letters 14: 124017. https://doi.org/10.1088/1748-9326/ab4ffe

Junk WJ, Bayley PB, Sparks RE (1989) The flood pulse concept in river-floodplain systems. Can Spec Publ Fish Aquat Sci 106: 110–127

Junk WJ, Piedade MTF, Lourival R, Wittmann F, Kandus P, Lacerda LD, Bozelli R, Esteves FA, Nunes da Cunha C, Maltchik L, Schöngart J, Schaeffer-Novelli Y, Agostinho AA (2014) Brazilian wetlands: their definition, delineation, and classification for research, sustainable management, and protection. Aquat Conserv: Marine and Freshwater Ecosystems 24: 5-22. https://doi.org/ 10.1002/aqc.2386

Junk WJ, An S, Finlayson CM, Gopal B, Kvě M, Stephen A, Mitsch WJ, Robarts RD (2013) Current state of knowledge regarding the world-s wetlands and their future under global climate change: a synthesis. Aquatic Sciences 75: 151-167. https://doi.org/10.1007/s00027-012-0278-z

Kuerten S, Parolin M, Assine M, McGlue MM (2013) Sponge spicules indicate Holocene environmental changes on the Nabileque River floodplain, southern Pantanal, Brazil. J Paleolimnol 49(2): 171–183. https://doi.org/10.1007/s10933-012-9652-z

Lacerda Filho JV, Silva MG, Hardy J (2006) Geologia e recursos minerais do Estado de Mato Grosso do Sul: texto explicativo dos mapas geológico e de recursos minerais do Estado de Mato Grosso do Sul : escala 1:1.000.000. Campo Grande: CPRM-Serviço Geológico do Brasil. 121 p

Lo EL, Silva A, Bergier I, Mcglue MM, Silva BLDP, Silva APS, Pereira LE, Macedo HDA, Assine ML, Silva ERDSD (2017) Spatiotemporal evolution of the margins of Lake Uberaba, Pantanal floodplain (Brazil). Geografia 42(3): 159-173

Lo EL, Mcglue MM, Silva A, Bergier I, Yeager KM, Macedo HÁ, Swallom M, Assine M (2019) Fluvio-lacustrine sedimentary processes and landforms on the distal Paraguay fluvial megafan (Brazil). Geomorphology, 342: 163-175. https://doi.org/10.1016/j.geomorph.2019.06.001

Madella M, Alexandre A, Ball T (2005) International code for phytolith nomenclature 1.0. Ann Bot (Lond) 96(2): 253-260. https://doi.org/10.1093/aob/mci172

McGlue MM, Silva A, Assine ML, Stevaux JC, Pupim FN (2015) Paleolimnology in the Pantanal: using lake sediments to track quaternary environmental change in the world's largest tropical wetland. In: Bergier I, Assine ML (eds) Dynamics of the Pantanal Wetland in South America. The Handbook of Environmental Chemistry, Springer, Cham, pp 51-81. https://doi.org/10.1007/698_2015_350

McGlue MM, Silva A, Corradini FA, Zani H, Tree MA, Ellis GE, Parolin M, Swarzenski PW, Cohen AS, Assine ML (2011) Limnogeology in Brazil's "forgotten wilderness": a synthesis from the large floodplain lakes of the Pantanal. J Paleolimnol 46: 273–289. https://doi.org/10.1007/s10933-011-9538-5

McGlue MM, Silva A, Zani H, Corradini FA, Parolin M, Abel EJ, Cohen AS, Assine ML, Ellis GS, Trees MA, Kuerten S, Gradella FS, Rasbold GG (2012) Lacustrine records of Holocene flood pulse dynamics in the Upper Paraguay River watershed (Pantanal wetlands, Brazil). Quat Res 78: 285-294. https://doi.org/10.1016/j.yqres.2012.05.015

Metcalfe SE, Whytney BS, Fitzpatrick KA, Mayle F, Loader NJ, Street-Perrot A, Mann DG (2014) Hydrology and climatology at Laguna La Gaiba, lowland Bolivia: complex responses to climatic forcings over the last 25 000 years. Journal of Quaternary Science 29(3): 289–300. https://doi.org/10.1002/jqs.2702

Meyers PA (1994) Preservation of source identification of sedimentary organic matter during and after deposition. Chemical Geology 144(3-4): 289–302. https://doi.org/10.1016/0009-2541(94)90059-0

Meyers PA (2003) Applications of organic geochemistry to paleolimnological reconstructions: a summary of examples from the Laurentian Great Lakes. Organic Geochemistry 34: 261–289. https://doi.org/10.1016/S0146-6380(02)00168-7

Mitsch WJ, Bernal B, Nahlik AM, Mander Ü, Zhang L, Anderson CJ, Jørgensen SE, Brix H (2013) Wetlands, carbon, and climate change. Landsc Ecol 28(4): 583-597. https://doi.org/10.1007/s10980-012-9758-8

Mitsch WJ, Nahlik A, Wolski P, Bernal B, Zhang L, Ramberg L (2010) Tropical wetlands: seasonal hydrologic pulsing, carbon sequestration, and methane emissions. Wetl Ecol Manag 18(5): 573-586. https://doi.org/10.1007/s11273-009-9164-4

Mitsch W, Gosselink JG (2015) Wetlands. Wiley, New Jersey

Morrow C, Cárdenas P (2015) Proposal for a revised classification of the Demospongiae (Porifera). Frontiers in Zoology 12(7): 1:27. https://doi.org/10.1186/s12983-015-0099-8

Mormul RP, Thomaz SM, Vieira LJS (2013) Richness and composition of macrophyte assemblages in four Amazonian lakes. Acta Scientiarum. Biological Sciences 35(3): 343-350. https://doi.org/10.4025/actascibiolsci.v35i3.11602

Neue HU, Gaunt JL, Wang ZP, Becker-Heidmann P, Quijano C (1997) Carbon in tropical wetlands. Geoderma 79: 163-185. https://doi.org/10.1016/S0016-7061(97)00041-4

Novello VF, Vuille M, Cruz FW, Stríkis NM, Paula MS, Edwards RL, Cheng H, Karmann I, Jaqueto PF, Trindade RIF, Hartmann GA, Moquet JS (2016) Centennial-scale solar forcing of the South American Monsoon System recorded in stalagmites. Sci Rep 6: 24762. https://doi.org/10.1038/srep24762

Novello VF, Cruz FW, Vuille M, Stríkis NM, Edwards RL, Cheng H, Emerick S, Saito de Paula M, Li X, Barreto ES, Karmann I, Santos RV (2017) A high-resolution history of the South American Monsoon from Last Glacial Maximum to the Holocene. Sci Rep 7: 44267. https://doi.org/10.1038/srep44267

Novello VF, Cruz FW, McGlue MM, Wong CI, Ward BM, Vuille M, Santos RA, Jaqueto P, Pessenda LC, Atorre T, Ribeiro LM (2019) Vegetation and environmental changes in tropical South America from the last glacial to the Holocene documented by multiple cave sediment proxies. Earth and Planetary Science Letters 524: 115717. https://doi.org/10.1016/j.epsl.2019.115717

Oliveira MRF, Melhado AFP, Oda FH, Melo SM, Parolin M, Benedito E (2018) Sponge species composition and habitat use in a small stream within the agricultural landscape in the lower Tietê River basin in southeastern Brazil, with the first record of Corvoheteromeyenia australis (Demospongiae: Spongillidae) in São Paulo state. North-Western Journal of Zoology 14(1): 30-36

Parolin M, Volkmer-Ribeiro C, Stevaux JC (2008) Use of Spongofacies as a proxy for River-Lake Paleohydrology in Quaternary Deposits of Central-Western Brazil. Revista Brasileira de Paleontologia 11(3): 187-198. https://doi.org/10.4072/rbp.2008.3.05

Parry WD, Smithson F (1958) Silicification of bulliform cells in grasses. Nature 181: 1549–1550. https://doi.org/10.1038/1811549b0

Philbrick CT, Bove CP, Stevens HI (2010) Endemism in neotropical Podostemaceae. Ann Mo Bot Gard 97: 425–456. https://doi.org/10.3417/2008087

Pinheiro US, Hajdu E, Caballero ME (2003) Três novos registros de esponjas (Porifera, Demospongiae): para águas continentais do Estado de São Paulo. 498. Boletim do Museu Nacional, Nova Série, Zoologia, pp. 1–14

Piperno DR (2006) Phytoliths: A Comprehensive Guide for Archaeologists and Paleoecologists. AltaMira Press, Lanham, pp. 248

Por FD (1995) The Pantanal of Mato Grosso (Brazil): World's Largest Wetlands. Kluwer Academic, Dordrecht. 125p. http://dx.doi.org/10.1007/978-94-011-0031-1

Pott A, da Silva JSV (2015) Terrestrial and Aquatic Vegetation Diversity of the Pantanal Wetland. In: Bergier I, Assine M (eds) Dynamics of the Pantanal Wetland in South America. The Handbook of Environmental Chemistry, Springer, Cham, pp. 111-131. https://doi.org/10.1007/698_2015_352

Rasbold GG, McGlue MM, Stevaux JC, Parolin M, Silva A, Bergier I (2019) Sponge spicule and phytolith evidence for Late Quaternary environmental changes in the tropical Pantanal wetlands of western Brazil. Palaeogeogr Palaeoclimatol Palaeoecol 518: 119-133. https://doi.org/10.1016/j.palaeo.2019.01.015

Rasbold GG, Stevaux JC, Parolin M, Leli IT, Luz LD, Brito HD (2020) Phytoliths indicate environmental changes correlated with facies analysis in a paleo island-lake, Upper Paraná River, Brazil. Journal of South American Earth Sciences 99: 102513. https://doi.org/10.1016/j.jsames.2020.102513

Sangster G, Parry WD (1969) Some factors in relation to bulliform cell silicification in the grass leaf. Ann Bot 33(2): 315–323. https://doi.org/10.1093/oxfordjournals.aob.a084285.

Sawakuchi AO, Hartmann GA, Sawakuchi HO, Pupim FN, Bertassoli DJ, Parra M, Antinao JL, Sousa LM, Pérez MHS, Oliveira PE, Santos RA, Savian JF, Grohmann CH, Medeiros VB, McGlue MM, Bucudo DC, Faustino SB (2015) The Volta Grande do Xingu: reconstruction of past environments and forecasting of future scenarios of a unique Amazonian fluvial landscape. Scientific Drilling, 20: 21-32. https://doi.org/10.5194/sd-20-21-2015

Schnurrenberger D, Russell JM, Kelts K (2003) Classification of lacustrine sediments based on sedimentary components. J Paleolimnol 29(2): 141-154. https://doi.org/10.1023/A:1023270324800

Sifeddine A, Martin L, Turcq B, Volkmer-Ribeiro C, Soubiès F, Cordeiro RC, Suguio K (2001) Variations of the Amazonian rainforest environment: a sedimentological record covering 30,000 years. Palaeogeogr Palaeoclimatol Palaeoecol 168: 221-235. https://doi.org/10.1016/S0031-0182(00)00256-X

Sobek S, Scherber C, Steffan-Dewenter I, Tscharntke T (2009) Sapling herbivory, invertebrate herbivores and predators across a natural tree diversity gradient in Germany's largest connected deciduous forest. Oecologia 160: 279–288. https://doi.org/10.1007/s00442-009-1304-2

Stríkis NM, Cruz FW, Cheng H, Karman I, Edwards L, Vuille M, Wang X, Paula MS, Novello VF, Auler AS (2011) Abrupt variations in South American monsoon rainfall during the Holocene based on a speleothem record from central-eastern Brazil. Geology 39(11): 1075–1078. https://doi.org/10.1130/G32098.1

Talbolt MR (1990) A review of the palaeohydrological interpretation of carbon and oxygen isotopic ratios in primary lacustrine carbonates. Chemical Geology: Isotope Geoscience section 80(4): 261-279. https://doi.org/10.1016/0168-9622(90)90009-2

Tavares MCM, Volkmer-Ribeiro C, De Rosa-Barbosa R (2003) Primeiro registro de Corvoheteromeyenia australis (Bonetto & Ezcurra de Drago) para o Brasil com chave taxonômica para os poríferos do Parque Estadual Delta do Jacuí, Rio Grande do Sul, Brasil. Revista Brasileira de Zoologia 20(2): 169-182. http://dx.doi.org/10.1590/S0101-81752003000200001

Tavares-Frigo MC, Volkmer-Ribeiro C, Oliveira AEZ, Machado VS (2015) Freshwater sponges from the Pampa Biome, Brazil, with description of a new species of Oncosclera. Neotropical Biology and Conservation 10(3): 110-122. https://doi.org/10.4013/nbc.2015.103.01

Tockner K, Pennetzdorfer D, Reiner K, Schimier F, Ward JV (1999) Hydrological connectivity, and the exchange of organic matter and nutrients in a dynamic river-floodplain system (Danube, Austria). Freshwater Biology 41: 521-535. https://doi.org/10.1046/j.1365-2427.1999.00399.x

Volkmer-Ribeiro C (1985) Esponjas de Água doce. Manuais Técnicos para a Preparação de Coleções Zoológicas, 3: 1-6

Volkmer-Ribeiro C (1999) Porifera. In: Ismael D, Valenti WC, Matsumura-Tundisi T, Rocha O (eds.) Biodiversidade do Estado de São Paulo: síntese do conhecimento ao final do século XX. Invertebrados de água doce. FAPESP, São Paulo, pp. 1–9

Volkmer-Ribeiro C, Grosser KM, Rosa-Barbosa R, Pauls SM (1975) Primeiro relato da ocorrência de Espongilideos (Porifera) na bacia do Guaíba, Estado do Rio Grande do Sul, Iheringia, Série Zoologia 46: 33-49

Volkmer-Ribeiro C, De Rosa-Barbosa R (1985) Redescription of the Freshwater Sponges *Trochospongilla repens* (Hinde, 1888) and *Trochospongilla amazonica* (Weltner, 1895) with an account of the South American species of *Trochospongilla* (Porifera, Spongillidae). Iheringia, Série Zoologia 65: 77-93

Volkmer-Ribeiro C, Hatanaka T (1991) Nota científica: composição específica e substrato da espongofauna (Porifera) no lago da Usina Hidroelétrica- Tucurui, Pará, Brasil. Iheringia, Série Zoologia 71: 177–178

Volkmer-Ribeiro C, Correia MF, Brenha SLA, Mendonça MA (1999) Freshwater sponges from a Neotropical sand dune area. Mem Queensl Mus 44: 643-649

Volkmer-Ribeiro C, Pauls SM (2000) Esponjas de agua Dulce (Porifera, Demospongiae) de Venezuela. Acta Biologica Venezuelica 20(1): 1-28

Volkmer-Ribeiro C, Parolin M (2010) As esponjas. In: Parolin M, Volkmer-Ribeiro C, Leandrini JA. (eds.) Abordagem ambiental interdisciplinar em bacias hidrográficas no Estado do Paraná. Editora da Fecilcam, Campo Mourão, pp. 105–130

Vuille M, Burns JS, Taylor BL, Cruz FW, Bird BW, Abbott MB, Kanner LC, Cheng H, Novello VF (2012) A review of the South American monsoon history as recorded in stable isotopic proxies over the past two millennia. Climate of the Past 8: 1309-1321. https://doi.org/10.5194/cpd-8-637-2012

Warren LV, Quaglio F, Simões MG, Freitas BT, Assine ML, Riccomini C (2015) Underneath the Pantanal Wetland: A Deep- Time History of Gondwana Assembly, Climate Change, and the Dawn of Metazoan Life. In: Bergier I, Assine M (eds) Dynamics of the Pantanal Wetland in South America. The Handbook of Environmental Chemistry, Springer, Cham, pp. 1-21. https://doi.org/ 10.1007/698_2014_326

Wetzel RG (1992) Gradient-dominated ecosystems: sources and regulatory functions of dissolved organic matter in freshwater ecosystems. Hydrobiologia 229: 181-198. https://doi.org/10.1007/BF00007000

Wilding LP, Drees LR (1968) Distribution and implications of sponge spicules In surficial deposits in Ohio. The Ohio Journal of Science 68(2): 92-99

APPENDIX A - Location and geochemistry of surface sediment samples from Lake Cáceres

Sample name	Lat **(°S)**	Long **(°S)**	Depth (m)	TOC (wt. %)	TN (wt. %)	C/N	$\delta^{15}N$ (‰)	$\delta^{13}C$ (‰)
LCC.01	18.979426	57.724926	4.11	1.51	0.08	22.01	3.14	-19.96
LCC.02	18.978744	57.729626	3.26	0.75	0.08	10.93	2.87	-28.56
LCC.03	18.98104	57.729969	3.51	1.79	0.17	12.28	2.99	-27.79
LCC.04	18.976506	57.72929	2.68	3.5	0.29	14.07	2.28	-29.17
LCC.05	18.974117	57.728917	2.53	13.34	1.25	12.45	1.3	-28.92
LCC.06	18.97332	57.735073	2.50	5.93	0.58	11.92	1.81	-27.71
LCC.07	18.975593	57.735273	2.90	2.85	0.25	13.29	2.57	-28.55
LCC.08	18.978121	57.735494	3.08	0.94	0.09	12.18	2.53	-28.71
LCC.09	18.98066	57.735751	3.26	1.77	0.17	12.14	2.99	-28.34
LCC.10	18.983049	57.735876	3.54	2.23	0.21	12.38	3.07	-27.67
LCC.11	18.985438	57.741965	3.93	4.7	0.46	11.92	3.19	-28.42
LCC.12	18.982138	57.741886	2.50	13.15	1.3	11.80	2.09	-28.49
LCC.13	18.979709	57.741791	2.77	1.21	0.09	15.68	1.88	-27.81
LCC.14	18.97739	57.741699	2.87	0.45	0.03	17.49	1.43	-27.65
LCC.15	18.975102	57.7416	2.80	1.05	0.08	15.31	2.2	-27.94
LCC.16	18.972987	57.741533	2.29	9.73	0.96	11.82	2.27	-29.02
LCC.17	18.986606	57.748134	3.08	2.49	0.23	12.62	2.29	-27.76
LCC.18	18.984378	57.748087	3.32	4.21	0.38	12.92	2.82	-28.3
LCC.19	18.981989	57.747993	3.51	3.47	0.32	12.65	2.96	-27.97
LCC.20	18.979641	57.747898	3.44	1.58	0.16	11.52	2.96	-28.48
LCC.21	18.977155	57.747758	3.26	2.2	0.21	12.22	2.55	-29.03
LCC.22	18.974685	57.747587	2.56	0.75	0.04	21.87	1.27	-27.49
LCC.23	18.971413	57.74732	2.90	0.5	0.04	14.58	1.2	-27.86
LCC.24	18.968193	57.747148	3.08	1.22	0.12	11.86	2.17	-28.9
LCC.25	18.963949	57.746866	2.90	1.75	0.17	12.00	2.23	-27.96
LCC.26	18.957491	57.746567	2.44	6.31	0.58	12.69	1.64	-28.07
LCC.27	18.950417	57.746218	2.35	3.03	0.23	15.36	1.39	-27.44
LCC.28	18.943218	57.745938	2.74	2.44	0.24	11.86	2.23	-26.84
LCC.29	18.937281	57.745595	2.50	26.55	1.6	19.35	1.08	-28.83
LCC.30	18.935742	57.757398	2.71	4.04	0.39	12.08	1.83	-27.45
LCC.31	18.941659	57.757663	2.96	3.63	0.33	12.83	1.93	-27.63
LCC.32	18.948433	57.757862	3.11	3.94	0.37	12.42	1.92	-28.56
LCC.33	18.955886	57.75809	3.23	2.92	0.25	13.62	1.85	-28.48
LCC.34	18.962993	57.758626	3.14	1.88	0.17	12.90	1.95	-28.69
LCC.35	18.969808	57.758955	3.32	1.64	0.14	13.66	2.51	-28.09
LCC.36	18.976662	57.759185	3.35	2.53	0.2	14.75	2.18	-27.96
LCC.37	18.984037	57.759729	2.99	3.24	0.3	12.59	2.33	-28.57
LCC.38	18.975014	57.77086	1.92	5.47	0.5	12.76	2.34	-28.34
LCC.39	18.968203	57.77072	3.23	3.6	0.33	12.72	2.26	-28.44
LCC.40	18.961155	57.770543	3.23	4.71	0.43	12.77	2.29	-28.08
LCC.41	18.954065	57.769971	3.14	4.4	0.41	12.51	2.22	-28.89

LCC.42	18.946659	57.769823	3.14	3.94	0.37	12.42	2.3	-28.27
LCC.43	18.940085	57.769474	3.05	3.37	0.31	12.68	1.96	-28.03
LCC.44	18.933965	57.769131	2.74	3.44	0.33	12.16	1.67	-27.81
LCC.45	18.932314	57.780984	2.53	19.08	1.04	21.39	0.21	-29.62
LCC.46	18.938929	57.781271	2.93	5.19	0.42	14.41	1.63	-29.14
LCC.47	18.944767	57.781467	3.02	3.74	0.33	13.22	2.01	-28.15
LCC.48	18.95258	57.781701	3.08	6.35	0.48	15.43	1.55	-29.09
LCC.49	18.959724	57.782158	3.29	4.06	0.35	13.53	2.13	-28.36
LCC.50	18.966732	57.782626	3.05	4.5	0.38	13.81	2.17	-27.81
LCC.51	18.965735	57.789915	2.99	3.41	0.3	13.26	2.43	-28.35
LCC.52	18.958826	57.789477	3.02	4.54	0.39	13.58	1.88	-28.43
LCC.53	18.951585	57.788924	3.05	4.41	0.38	13.53	1.69	-27.97
LCC.54	18.943649	57.788518	3.05	24.76	1.96	14.73	0.27	-29.92
LCC.55	18.937798	57.788226	2.56	27.5	1.98	16.20	0.35	-29.48
LCC.56	18.932542	57.788122	2.56	9.09	0.69	15.36	0.61	-28.89
LCC.57	18.944173	57.795456	2.41	3.6	0.34	12.35	1.76	-26.6
LCC.58	18.950556	57.795848	2.44	7.75	0.64	14.12	1.62	-28.94
LCC.59	18.957854	57.796099	3.57	4.05	0.32	14.76	2.49	-28.32
LCC.60	18.945252	57.799355	2.74	5.95	0.51	13.61	1.9	-27.59
LCC.61	18.943964	57.80225	3.41	5.75	0.51	13.15	1.94	-27.53

APPENDIX B - Quantification of phytoliths, sponge spicules of surface sediment samples from Lake Cáceres

	Phytoliths							Sponge spicules													
Sample	Short cells	Bulliforms	Other morphotypes	Globular echinate	Globular granulate	Conical echinate	Cone shape	Megasclere intact	Megasclere fragmented	Megasclere very fragmeted	Megasclere concentration	Gemmulosclere concentration	Microsclere concentration	*Radiospongilla amazonensis*	*Tubella variabilis*	*Tubella paulula*	*Metania spinata*	*Corvospongilla seckti*	*Corvoheteromeyenia sp.*	*Corvomeyenia*	*Oncosclera navicella*
LCC.1	8	87	41	4	3	0	0	74	80	186	340	11	0	1	1	0	1	0	0	1	1
LCC.3	24	84	49	7	0	0	2	126	365	954	1445	16	15	3	0	1	0	0	1	0	0
LCC.5	1264	210	488	12	0	0	20	57	78	303	438	57	37	23	3	2	0	0	0	2	0
LCC.8	49	73	88	1	1	5	0	56	97	122	275	22	2	1	1	1	0	5	0	0	0
LCC.19	161	88	167	7	0	0	0	32	113	420	565	22	3	2	1	0	0	0	1	1	0
LCC.25	79	102	165	7	0	0	2	155	218	398	771	26	6	6	2	0	0	5	1	1	0
LCC.27	994	258	238	2	0	0	0	48	110	284	442	37	9	8	5	2	0	6	0	2	0
LCC.29	3015	126	291	3	9	0	0	18	108	144	270	13	5	5	3	0	0	0	1	0	1
LCC.30	781	498	443	2	0	0	3	102	326	422	850	31	3	8	0	3	0	0	0	0	0
LCC.33	152	127	278	1	0	0	0	33	93	260	386	30	4	4	1	0	0	0	1	0	0
LCC.35	43	96	161	5	0	0	0	56	128	285	469	22	8	2	0	0	0	0	0	0	0
LCC.37	17	223	262	2	0	0	0	33	309	660	1002	30	0	2	0	2	0	0	0	0	0
LCC.38	18	603	468	2	0	0	5	90	563	1200	1853	16	3	2	0	0	0	0	0	0	0
LCC.40	55	183	325	14	2	0	11	39	231	691	961	53	0	9	0	2	0	0	0	5	0
LCC.42	14	159	305	2	0	0	0	60	291	836	1187	35	0	9	0	0	0	0	0	0	0
LCC.44	31	485	339	0	0	0	0	170	482	491	1143	24	2	6	0	0	2	0	0	0	0

LCC.46	185	226	241	6	0	0	0	50	210	340	600	32	4	14	0	0	0	0	0	0	0
LCC.48	43	218	230	2	0	0	0	60	261	573	894	43	2	11	0	0	0	0	0	0	0
LCC.50	65	380	430	2	0	0	0	100	585	827	1512	55	2	9	5	0	0	0	0	0	0
LCC.53	76	556	507	2	0	0	0	123	725	969	1817	63	2	21	0	0	0	0	0	1	0
LCC.55	2901	435	498	3	3	0	6	4	109	243	356	14	6	3	0	0	0	0	0	0	0
LCC.57	738	573	363	0	0	0	3	74	297	430	801	24	1	10	1	1	0	0	0	0	0
LCC.59	669	543	759	9	0	0	0	46	339	602	987	62	12	20	1	0	1	0	0	0	0
LCC.61	120	399	441	3	0	0	3	49	429	822	1300	31	8	12	2	0	0	0	0	0	0

APPENDIX C - Quantification of phytoliths, sponge spicules, total organic carbon (TOC), and total inorganic carbon (TIC), in the LCC/16 core from Lake Cáceres

			Phytoliths															Spoge spicules					Sponge species					
Depht (cm)	Total Organic Carbon (wt %)	Total Inorganic Carbon (wt %)	Bilobate	Cross	Sadlle	Rondel	Cuneiform	Paralelepipedl	Cylindrical traceid	Elongate echinate	Elongate psilate	Trapeziform polylobate	Globular echinate	Globular granulate	Acicular hair	Pappilae	Podostemaceae	Phytoliths concentration	Megasclere concentration	Gemmulosclere concentration	Microsclere concentration	Sponge spicules concentration	*Corvoheteromeyenia heterosclera*	*Heteromeyenia barlettai*	*Radiospongilla amazonensis*	*Tubella paulula*	*Tubella delicata*	*Tubella variabilis*	*Oncosclera navicella*
0	1.07	0.0031	0	0	0	0	0	2	0	0	2	0	0	0	0	0	0	4	6	2	0	8	0	1	0	0	0	0	0
2	1.16	0.0034	1	0	1	1	3	45	0	0	22	1	5	0	1	0	0	80	139	2	0	141	0	1	0	0	0	0	0
4	1.47	0.0021	4	0	1	1	4	24	2	0	27	1	2	0	0	1	0	67	303	8	112	423	5	3	0	0	0	0	2
6	1.32	0.0022	6	0	1	0	4	21	0	2	20	1	0	0	0	0	0	57	565	10	528	1103	6	6	2	0	0	1	2
8	1.12	0.0035	5	0	1	1	3	20	0	1	16	0	3	0	1	1	0	53	490	8	475	973	8	11	1	0	0	0	1
10	0.59	0.0017	8	0	0	0	4	14	0	0	12	3	1	0	0	0	0	42	574	8	806	1388	19	15	2	0	0	0	1
12	0.44	0.0008	8	0	1	2	1	11	0	0	11	0	0	0	0	3	0	38	565	12	970	1547	23	46	2	0	0	0	1
14	0.58	0.0000	7	1	1	2	6	25	1	0	8	1	0	0	1	0	0	54	918	8	2100	3026	54	128	0	0	0	1	1
16	0.54	0.0032	6	0	4	1	7	35	0	5	15	1	2	0	0	0	0	79	1161	8	1561	2730	16	60	0	0	0	0	0
18	0.50	0.0018	10	0	3	2	1	23	0	2	11	2	1	0	0	0	0	56	437	8	906	1351	5	18	0	0	0	1	2
20	0.49	0.0105	19	1	1	2	9	45	0	5	17	1	5	0	0	6	0	114	1528	36	2865	4429	35	161	4	0	0	0	3
22	0.23	0.0008	23	1	4	6	12	55	1	3	20	0	7	0	0	0	0	136	1110	26	2369	3505	11	117	3	0	0	1	0
24	0.27	0.0043	34	14	6	2	5	47	0	8	15	0	3	0	0	0	0	135	725	58	585	1368	36	17	3	0	1	0	12
26	0.32	0.0040	25	2	2	1	16	110	1	6	46	9	6	0	0	0	0	233	963	64	77	1104	24	5	1	0	0	1	18

28	0.25	0.0028	30	2	3	3	17	147	1	14	60	2	7	0	3	5	0	304	967	36	20	1023	4	0	4	0	0	0	11
30	0.28	0.0041	32	7	4	6	32	110	3	12	42	9	9	0	2	7	0	281	760	38	31	829	10	0	8	2	0	2	6
32	0.31	0.0024	24	5	5	10	21	125	0	10	49	8	4	0	0	0	2	276	1027	66	22	1115	3	0	12	0	1	0	10
34	0.27	0.0024	25	9	3	5	14	79	1	6	36	5	13	0	0	3	0	205	445	32	18	495	5	0	5	0	0	0	5
36	0.40	0.0057	20	8	13	8	31	141	1	10	75	9	10	2	2	0	0	342	1385	30	12	1427	2	0	0	0	0	1	7
38	0.41	0.0056	26	1	7	9	34	130	1	14	74	4	10	1	2	0	0	326	948	46	5	999	0	0	8	0	0	2	6
40	0.40	0.0079	6	0	3	2	34	125	0	7	72	13	10	4	3	0	0	290	1385	58	2	1445	1	0	4	0	0	0	15
42	2.13	0.0021	5	0	2	3	15	79	0	2	32	3	6	1	0	0	0	151	860	54	0	914	0	0	2	0	0	0	17
44	2.18	0.0018	1	0	0	0	11	51	0	0	39	0	2	0	0	0	0	105	897	20	0	917	0	0	0	0	0	0	10
46	6.65	0.0061	2	0	0	0	7	42	0	0	18	0	2	0	0	0	0	71	664	6	0	670	0	0	0	0	0	0	3
48	1.81	0.0025	1	0	0	1	11	64	0	0	30	1	2	0	0	0	0	110	818	2	0	820	0	0	0	0	0	0	0
50	1.44	0.0032	0	0	2	2	9	58	0	0	121	0	7	0	0	0	0	202	1174	34	0	1208	0	0	0	0	0	0	12
52	1.21	0.0039	1	0	0	0	16	67	0	0	26	2	2	0	0	0	0	114	690	40	0	730	0	0	0	0	0	0	15
54	1.19	0.0055	4	0	3	3	28	100	0	0	42	2	0	0	0	0	0	184	922	38	0	960	0	0	2	0	0	0	13
56	1.29	0.0054	4	0	12	2	20	54	0	0	46	0	0	0	0	0	0	138	550	40	0	590	0	0	0	0	0	0	20
58	1.45	0.0024	2	0	0	2	12	54	0	0	27	0	0	0	0	0	0	97	1084	2	0	1086	0	0	0	0	0	0	1
60	1.12	0.0088	4	0	3	0	19	54	0	0	18	7	0	0	2	0	0	107	742	4	0	746	0	0	0	0	0	0	0
62	0.79	0.0019	0	0	0	2	7	43	0	0	16	0	0	0	0	0	0	68	526	0	0	526	0	0	0	0	0	0	0
64	0.68	0.0045	2	0	4	0	4	66	0	0	36	0	0	0	0	0	0	112	478	0	0	478	0	0	0	0	0	0	0
66	0.59	0.0013	2	0	2	0	6	45	0	2	27	0	3	0	0	0	0	87	677	0	0	677	0	0	0	0	0	0	0
68	0.59	0.0017	0	0	0	0	4	61	0	0	12	0	0	0	0	0	0	77	399	2	0	401	0	0	0	0	0	0	0
70	0.59	0.0002	1	0	1	0	4	43	0	0	27	0	2	0	0	0	0	80	317	0	0	317	0	0	0	0	0	0	0
72	0.48	0.0031	0	0	0	0	4	19	0	0	7	0	0	0	0	0	0	34	465	0	0	465	0	0	0	0	0	0	0
74	0.50	0.0031	0	0	0	0	4	58	0	0	7	0	1	0	0	0	0	73	442	0	0	442	0	0	0	0	0	0	0
76	0.61	0.0040	0	0	0	0	12	43	0	0	15	0	0	0	0	0	0	72	359	0	0	359	0	0	0	0	0	0	0
78	0.85	0.0047	0	0	0	0	12	61	0	0	24	0	0	0	0	0	0	109	712	0	0	712	0	0	0	0	0	0	0
80	1.12	0.0015	0	0	0	0	9	61	0	0	16	0	2	0	0	0	0	88	843	0	0	843	0	0	0	0	0	0	0
82	1.37	0.0021	0	0	0	0	13	55	0	0	45	0	0	0	0	0	0	113	643	0	0	643	0	0	0	0	0	0	0

84	1.08	0.0002	0	0	0	0	16	60	0	0	18	0	0	0	0	0	0	97	755	0	0	755	0	0	0	0	0	0	0
86	1.17	0.0002	0	0	2	0	10	78	0	0	24	0	0	0	0	0	0	116	782	0	0	782	0	0	0	0	0	0	0
88	1.54	0.0002	0	0	0	0	9	90	0	0	19	0	2	0	0	0	0	122	932	0	0	932	0	0	0	0	0	0	0
90	1.27	0.0013	2	0	0	0	13	85	0	3	46	0	2	0	0	0	0	153	489	0	0	489	0	0	0	0	0	0	0
92	1.78	0.0032	0	0	0	0	4	76	0	0	12	0	0	0	0	0	0	92	536	0	0	536	0	0	0	0	0	0	0
94	1.67	0.0023	0	0	0	6	9	51	0	0	30	0	0	0	0	0	0	96	1446	12	0	1458	0	0	2	0	0	0	0
96	1.59	0.0026	0	0	0	0	6	73	0	0	28	0	0	1	0	0	0	109	634	0	0	634	0	0	0	0	0	0	0
98	1.31	0.0017	0	0	0	0	9	24	0	0	3	0	0	0	0	0	0	36	249	0	0	249	0	0	0	0	0	0	0
100	0.93	0.0029	0	0	0	0	6	21	0	0	3	0	0	1	0	0	0	31	75	0	0	75	0	0	0	0	0	0	0
102	0.72	0.0013	0	0	0	0	5	16	0	0	4	0	0	0	0	0	0	27	236	0	0	236	0	0	1	0	0	0	0

APPENDIX D - Age model of the LCC/16 core from Lake Cáceres

Depth (cm)	Age min	Age max	Age median	Agen mean	Depth (cm)	Age min	Age max	Age median	Agen mean
8	6102	6567.2	6398.9	6385.2	56	9165.7	10321.7	9747.2	9749
9	6168.3	6589.3	6423.4	6413.3	57	9196.9	10390.3	9806.9	9803.3
10	6207.9	6621.4	6449.5	6441.2	58	9224.3	10469.4	9863.2	9857.5
11	6233.5	6671.6	6471.7	6468.7	59	9286.5	10499.8	9921.5	9912.8
12	6258.9	6744.2	6491.3	6495.8	60	9330.3	10532.2	9979.1	9967.8
13	6282	6833	6508.1	6522.7	61	9375.1	10570.9	10036	10023.5
14	6295	6871.2	6525.1	6544.3	62	9410.5	10619.6	10094.3	10078.6
15	6309.6	6914.5	6540	6565.4	63	9433.3	10684.3	10150.7	10133.9
16	6324.2	6960.9	6553.7	6586.3	64	9499	10712.2	10206.2	10190.7
17	6339.3	7029.2	6565.7	6606.6	65	9556.4	10741.4	10262.9	10247.5
18	6350.9	7095.6	6579.2	6627.5	66	9602.8	10779.7	10323.4	10304.5
19	6391.3	7154.2	6613.5	6679.5	67	9654.3	10827.1	10384.7	10361.1
20	6425.3	7237.7	6650	6731.4	68	9677.1	10891.6	10448.1	10417.9
21	6454.6	7362.5	6691.8	6783.8	69	9806.4	10913.7	10498.5	10472.6
22	6480.1	7505.7	6736.7	6835.9	70	9916.6	10939.2	10549.3	10526.9
23	6496.9	7657.2	6778.6	6887.1	71	10003.2	10969	10601.7	10581.4
24	6816.9	7703.8	7035.1	7115.8	72	10062.9	11004.4	10654.2	10635.7
25	7121.5	7758.1	7294.9	7345	73	10089.9	11054.9	10710.3	10690
26	7405.2	7821.1	7556.4	7574.5	74	10209.3	11070.4	10748.8	10738.8
27	7660.1	7926.2	7806.6	7804.5	75	10284.3	11087.9	10787.7	10787.2
28	7822	8205.5	8036.8	8033.7	76	10309.9	11112.6	10829.5	10836
29	7901.9	8271.5	8109.9	8106.4	77	10351.2	11156.7	10876.6	10884.3
30	7957.1	8363.5	8184.1	8178.9	78	10395.6	11234.2	10930.2	10931.3
31	7997.2	8474.2	8256.3	8251.7	79	10417.7	11277.6	10969.9	10967.7
32	8030.5	8597.3	8326	8324.3	80	10437.6	11334.6	11012	11004.3
33	8058.1	8731	8397	8396.7	81	10462.1	11406.6	11049.3	11039.8
34	8196.9	8763	8464	8468.7	82	10474.3	11483.9	11082.5	11074.4
35	8331.8	8805.9	8532.5	8540.9	83	10496.2	11576	11114.8	11109.8
36	8452.4	8852.7	8598.5	8613.2	84	10519.1	11603.6	11156.7	11145.7
37	8541.3	8931	8666.1	8685.4	85	10540.8	11649.3	11193.5	11181.7
38	8596.1	9026.3	8737.8	8758.5	86	10591.3	11691.8	11231.4	11217.8
39	8640	9083.3	8794.7	8813.4	87	10624.4	11751	11266.2	11252.8
40	8667.9	9155.5	8848.3	8868.3	88	10636.9	11816.5	11301.5	11289
41	8684.1	9261.4	8899.5	8922.8	89	10677.3	11857.1	11342.6	11325.7
42	8694.4	9385.1	8948	8976.4	90	10718.2	11896.8	11382.8	11361.6

43	8703.6	9516.1	8995.6	9030.3	91	10736.1	11940.2	11423.1	11397.7
44	8750.2	9562.9	9053.4	9086.1	92	10756.2	11993.3	11461.5	11433.8
45	8790.7	9622.6	9114.5	9142.3	93	10777.6	12058.7	11495.5	11469.5
46	8816.8	9697.4	9170.1	9197.2	94	10795.8	12108.3	11536.3	11505.9
47	8841.2	9791.1	9225.1	9252.9	95	10825	12172.4	11578.8	11542.4
48	8860.4	9898.3	9276.8	9308.1	96	10846.7	12256.6	11622.4	11578.9
49	8917.4	9935.9	9336	9363.3	97	10870.2	12331.1	11661.3	11614.6
50	8954.5	9985	9394	9419.1	98	10874.7	12404.7	11698.6	11650.6
51	8981.2	10037.7	9456.2	9474.5	99	10897.5	12449.4	11742.4	11685.5
52	9013.4	10104.1	9516	9529.8	100	10913.7	12524.2	11789.9	11720.6
53	9039.6	10184.9	9569.2	9584.8	101	10930	12603.1	11839.2	11755.2
54	9092.3	10226.3	9626	9639.7	102	10947.4	12684.3	11888.2	11789.2
55	9132.2	10266.1	9685.3	9694.4					

.

APPENDIX E - Age model and geochemistry of LN95/L2 core from Lake Negra. We were compiled from published literature (Rasbold et al 2019) using the program DigitizeIt.

Depth (cm)	Age model (cal yr BP)	$\delta^{13}C$ (‰)	$\delta^{15}N$ (‰)	N (%)	C (%)	C/N
60	5663	-23.6	2.3	0.1	0.40	9.4
63	5831	-19.0	2.2	0.1	2.13	17.8
66	5997	-19.4	2.0	0.2	2.18	15.9
69	6162	-17.8	1.5	0.4	6.65	17.6
72	6328	-20.0	1.8	0.1	1.81	16.2
75	6493	-21.8	1.6	0.1	1.44	14.0
78	6663	-22.8	2.1	0.1	1.21	14.1
81	6836	-23.1	2.1	0.1	1.19	13.9
84	7012	-23.3	2.0	0.1	1.29	12.6
87	7186	-23.1	2.0	0.1	1.45	15.4
90	7357	-23.7	2.5	0.1	1.12	14.5
93	7534	-24.1	2.5	0.1	0.79	13.2
96	7708	-24.6	2.7	0.1	0.68	15.9
99	7878	-24.4	3.1	0.0	0.59	17.2
102	8047	-24.5	3.1	0.0	0.59	17.1
105	8220	-24.4	3.4	0.0	0.59	17.2
108	8405	-24.5	3.5	0.0	0.48	14.0
111	8583	-22.6	3.5	0.0	0.50	14.7

APPENDIX F - Age model and geochemistry of LG/2A core from Lake Gaíva. We were compiled from published literature (McGlue et al. 2012) using the program DigitizeIt.

Depth (cm)	Age model (cal yr BP)	$\delta^{13}C$ (‰)	C/N
58	5513	-24.4	17.7
60	5575	-25.6	16.0
62	5637	-24.0	16.1
64	5698	-24.3	15.2
66	5760	-23.9	11.7
68	5822	-23.4	15.2
70	5883	-23.7	18.6
72	5943	-23.5	13.9
74	6004	-23.5	17.9
76	6065	-23.6	12.3
78	6127	-23.3	14.2
80	6189	-23.6	16.4
82	6251	-22.1	16.4
84	6312	-21.8	14.4
86	6375	-20.7	15.4
88	6439	-20.9	17.1
90	6502	-21.0	15.2
92	6564	-21.0	14.1
94	6626	-21.0	14.2
96	6688	-21.2	15.3
98	6749	-21.4	15.7
100	6811	-21.3	13.8
102	6872	-20.9	15.2
104	6934	-22.2	16.4
106	6995	-22.4	15.8
108	7057	-22.6	17.0
110	7118	-22.8	17.2
112	7190	-22.3	17.4
114	7263	-22.4	17.3
116	7457	-22.9	11.4
118	7773	-22.5	20.4
120	8089	-22.5	17.2
122	8513	-22.7	21.2

APPENDIX G - Age model and geochemistry of LC95/L1 core from Lake Castelo. We were compiled from published literature (Bezerra and Mozeto, 2008; Bezerra et al. 2019) using the program DigitizeIt.

Depth (cm)	Age model (cal yr BP)	$\delta^{13}C$ (‰)	$\delta^{15}N$ (‰)	N (%)	C (%)	C/N
30	1090	-26	2.7	0.09	1.21	13.44
45	3310	-25.8	0.8	0.07	1.24	15.5
56	4370	-26.9	-0.55	0.15	2.74	16.12
66	4940	-25.8	0.61	0.2	3.32	15.81
79	5690	-26	1.1	0.27	4.35	15.54
90	6340	-25.9	1.8	0.53	7.74	14.33
96	6550	-24.5	1.1	0.96	11.64	12.09
100	6780	-25.6	2.75	0.09	1.64	16.4
110	6970	-26.1	-9.7	0.02	0.44	14.67
120	7250	-27.2	0.26	0.002	0.38	19

4 CONCLUSIONS

1. Sedimentary deposits from lakes on the western edge of the Pantanal have preserved important microfossils and isotopic records of paleoclimatic variations over the past thousands of years. The joint use of several proxy indicators (sponges spicules, phytoliths, $\delta^{13}C$, $\delta^{15}N$ and total organic carbon), refined yhe analysis since it minimized the individual limitations of each indicator.

2. The use of sediments and data from different lakes enabled a regional analysis of climate changes that occurred in the Pantanal from the Late Pleistocene to Holocene, which brought a better understanding of the responses of wetlands to climate change. The high chronological resolution obtained by multiple absolute dates and the standardized age models, was fundamental for the correlation of regional data, since the low chronological resolution in paleoenvironmental studies is one of the most critical problems in the characterization of the temporal and spatial patterns of climate change.

3. The Pantanal wetlands were strongly influenced by the variation of the SASM during the Late Pleistocene and in the transition to the Holocene, this climate system enhanced the intensity and frequency of the rains that contributed to the flood pulses of the Paraguay River and connection of the floodplain lakes. These influences were recorded by the characteristics of the sediments and composition of the assembly of freshwater sponges.

4. Sponge-rich facies were identified at sedimentary intervals dated to the Middle Holocene in cores recovered from the lakes Negra and Cáceres. The preservation and great abundance of sponges of the species *Corvoheteromeyenia heterosclera* and *Heteromeyenia barlettai* are indicative of perennial lacustrine paleoenvironments with minimal fluvial influence. The similarities in the records of spike assemblages of freshwater sponges in the studied lakes are evidence of similar ecosystem responses.

5. Sedimentary records of floodplain lakes showed a high deposition of organic carbon between 7.3-6 k cal yr BP. This pattern was identified for Lake Gaíva, Lake Castelo, Lake Cáceres and Lake Negra. The high rate of deposition of organic carbon in a period drier than the current one can be interpreted as the response of the disconnection of these lakes and the decrease of the pelagic area. Pantanal floodplain lakes have an indirect response to changes in precipitation. The geomorphological characteristics of these humid areas provide expansion of the shallow areas during dry periods, which increase primary production through the colonization of aquatic macrophytes.

6. The correlation of the high rates of organic deposition with the phases of retraction and expansion of the seasonal wetlands was based on the current connection mechanism of these lakes in the high-water and low-water levels of the Pantanal Basin. Historical series of satellite images, bathymetry and surface sediment analyses that included current patterns of deposition of organic carbon and biogenic silica, were fundamental for understanding this dynamic system, validating the hypotheses and calibrating the paleoenvironmental data.

7. Paleoenvironmental studies must be expanded to other environments in the Pantanal, to increase the spatial and temporal resolution of climate changes that have occurred in Pantanal ecosystems in the last thousands of years. This understanding is fundamental for the development of models and strategies for mitigating environmental impacts in response to climatic variations. The Pantanal is one of the world's "hotspots" for biodiversity, and it has significant economic and social importance for the communities that live and use this ecosystem for subsistence.